A tale of two hypotheses: Effect of the herpes simplex-1 virion host shutoff (vhs) protein on bicistronic reporters

by

Alexandra Ransom Rose

A thesis submitted in partial fulfillment of the requirements for the degree of

Master of Science

in

VIROLOGY

Department of Medical Microbiology and Immunology
University of Alberta

ABSTRACT

The herpes simplex virus virion host shutoff (vhs) protein acts as an mRNA specific endoribonuclease. Our lab has previously determined that vhs stimulates expression of the 3' CAT cistron of a bicistronic reporter plasmid while under the influence of the BiP IRES; however, the mechanism by which this occurs is unclear. Thus, different reporter constructs were assayed for CAT activity while under the influence of vhs. Vhs-induced CAT activation occurred not only in bicistronic reporter constructs containing the BiP IRES, but also in those containing truncated versions of the BiP IRES or an exonuclease blocking RNA element. The unrelated viral host shutoff nucleases EBV BGLF5, KHSV SOX and SARS coronavirus Nsp1 were also capable of stimulating CAT activity. Finally, a loss of mRNA was detected using northern blot after addition of vhs. Thus, it appears as if vhs activates 3' cistron expression by degrading the 5' cistron of the bicistronic mRNA instead of activating cap-independent translation.

ACKNOWLEDGMENTS

First and foremost, I'd like to extend a sincere thank you to my supervisor Dr. Jim Smiley for his support and mentorship throughout the course of this degree. Additionally, I would like to thank all members of the Smiley lab for their assistance and advice with both science and life. A special thank you goes to Holly Saffran, without whom this degree would not have been possible! Also thanks to the staff of the former Avenue Pizza for much needed weekly alcoholic and comedic reprieve. I would also like to thank Dr. Ryan Mercer for his endless assistance and support. Lastly, thanks to Jinx and Oz for their "help" with my writing; I could always count on you to climb on top of my laptop and distract me!

TABLE OF CONTENTS

LIST OF FIGURES

LIST OF TABLES

LIST OF ABBREVIATIONS

aa	Amino acid
Aly/REF	Ally of AML-1 and LEF-1
ApaF1	Apoptotic protease activating factor 1
AREs	Adenylate-uridylate (AU)-rich elements
ATP	Adenosine triphosphate
ATRX	Alpha-thalassemia mental retardation protein (X-linked)
β-gal	β-galactosidase
BiP	Binding immunoglobulin protein
C	Carboxy
CAT	Chloramphenicol acetyltransferase
cdc25C	Cell division cycle 25 homolog C
cdk1	Cyclin-dependent kinase cdc2
CrPV	Cricket paralysis virus
CSPG	Chondroitin sulfate cell surface proteoglycans
DAP5	Death associated protein 5
Daxx	Death domain-associated protein
DNA	Deoxyribonucleic acid
DNA-PKcs	DNA-dependent protein kinase, catalytic subunit
E, β	Early
E2FBP1	E2 factor binding protein 1

EBV	Epstein-Barr virus
eIF	Eukaryotic initiation factor
EMCV	Encephalomyocarditis virus
FEN-1	Flap structure specific endonuclease 1
g	Glycoprotein
GABP	GA-binding protein
GDP	Guanosine diphosphate
GTP	Guanosine triphosphate
HCF-1	Host cell factor 1
HCMV	Human cytomegalovirus (HCMV)
HHV-6	Human herpesvirus 6
HHV-7	Human herpesvirus 7
HLA	Human leukocyte antigen
HSPG	Heparin sulfate surface proteoglycans
HSV-1	Herpes simplex virus 1
HSV-2	Herpes simplex virus 2
HVEM	Herpesvirus entry mediator
ICP	Infected cell protein
IE, α	Immediate-early
IL	Interleukin
IRES	Internal ribosome entry site
kbp	Kilo base pairs
kDa	Kiladalton

KHSV	Karposi's sarcoma-associated herpesvirus
L, γ	Late
Met	Methionine
MHC	Major histocompatibility complex
MIP	Macrophage Inflammatory Protein
MEK	Mitogen extracellular signal regulated kinase
mRNA	Messenger ribonucleic acid
N	Amino
ND10	Nuclear domain 10
NEC	Nuclear envelopment complex
NF-κB	Nuclear factor kappa-light-chain-enhancer of activated B cells
nm	Nanometer
Nsp1	Nonstructural protein 1
Nup62	Nucleoporin 62kD
NXF1	Nuclear RNA Export Factor 1
Oct-1	Octamer 1 transcription factor
PKR	Protein kinase R
PM	Plasma membrane
PML	Promyelocytic leukemia (nuclear bodies)
RING	Really interesting new gene
RNA	Ribonucleic acid
RNAP	RNA polymerase

RNF8	RING finger protein 8
RNF168	RING finger protein 168
SAGA	Spt–Ada–Gcn5–acetyltransferase
SAP145	Spliceosome-associated protein 145kDa
SARS	Severe acute respiratory syndrome
SCoV	SARS coronavirus
Sp1	Specificity protein 1
SP100	Speckled protein of 100kDa
SRK1	Serine rich kinase 1
SRPK1	Serine/arginine-Rich protein-specific kinase
SWI/SNF2	SWItch/sucrose non-fermenting protein
TAF	TATA box binding protein (TBP)-associated factor
TAP	Transporter associated with antigen processing protein
TBP	TATA-binding protein
TFIIB	Transcription factor II B
TFIIH	Transcription factor II H
TGN	Trans-Golgi network
TPC	Tripartite complex
TTP	Tristetraprolin
Tyr	Tyrosine
UL/U_L	Unique long

U_S	Unique short
US	UnitedStates
UV	Ultra-violet
VICE	Virus-induced, chaperone-enriched
Vhs	Virion host shutoff
VP	Virion protein
VZV	Human varicella zoster virus

CHAPTER 1: INTRODUCTION

1.1 INTRODUCTION TO HERPESVIRUSES

Herpesviruses are some of the most ubiquitous viral pathogens in existence, infecting both humans and a wide variety of animals. The order *Herpesviriales* consists of three families, including the *Herpesviridae*. The family *Herpesviridae* encompasses most members of this large, enveloped, double stranded group of DNA viruses (http://www.ictvonline.org/virusTaxonomy.asp). All members of this family share common characteristics, both architecturally and biologically.

All herpesvirus virions share four architectural similarities: a core containing a linear double stranded DNA genome, an icosadeltahedral capsid, an amorphous, proteinacious layer surrounding the capsid called the tegument, and an envelope containing embedded viral glycoprotein spikes. Biologically speaking, four similarities are also noted. First, all members encode a large number of enzymes involved in nucleic acid synthesis and DNA metabolism, as well as a protease and protein kinases. Also, synthesis of DNA and capsid assembly occurs in the nucleus. Production of infectious progeny results in destruction of the host cell, and lastly, all are capable of establishing latent infections in their natural hosts (Roizmann *et al,* 1992).

Members of the family *Herpesviridae* are divided into three subfamilies: *Alphaherpesvirinae*, *Betaherpesvirinae* and *Gammaherpesvirinae.* These classifications are based primarily on

differences in biological properties. For example, members of *alphaherpesvirinae* have a variable host range, rapid replication and dissemination, and the ability to establish latency in sensory ganglia. This subfamily contains the prototypical member of the *Herpesviridae,* herpes simplex virus 1 (HSV-1), as well as (the common) herpes simplex virus 2 (HSV-2) and human varicella zoster virus (VZV). Members of the *betaherpesvirinae* have a restricted host range, slow replication and spread in cell culture and often cause their host cells to become enlarged. Latency is established in lymphoreticular cells, secretory glands, kidneys and possibly other tissues. This subfamily includes human cytomegalovirus (HCMV) as well as human herpesvirus 6 (HHV-6) and 7 (HHV-7). Members of the *gammaherpesvirinae* have a narrow host range and can replicate in lymphoblastoid, epitheiloid and fibroblastic cells. Either T or B lymphocytes can be infected, with latency being established in these lymphoid tissues. This subfamily contains both Epstein-Barr virus (EBV) and Karposi's sarcoma-associated herpesvirus (KHSV) (Roizmann *et al,* 1992).

1.2 INTRODUCTION TO HERPES SIMPLEX VIRUSES

Herpes simplex virus 1 (HSV-1) and its close relative herpes simplex virus 2 (HSV-2) [*already defined]* are two of the most ancient and well-documented human viral illnesses. The characteristic inflamed skin lesions have been recorded as far back as ancient Greece (Wildly, 1973).

Today, HSV infections are ubiquitous and widespread, affecting 60% to 95% of human adults (Ohana *et al,* 2000).

1.2.1 PATHOGENESIS

Both types of HSV infect skin and mucous membranes, with oral infections being caused primarily by HSV-1 and genital infections by HSV-2 (Whitley and Roizman, 2001 and Fatahzadeh *et al*, 2007). Primary infection involves the invasion of epithelial cells either at mucosal surfaces or at a site of broken skin, followed by replication of the virus. Progeny virus particles can then infect nearby sensory neurons and migrate to trigeminal (HSV-1) or cervical (HSV-2) ganglia. Viral replication then continues (temporarily) and eventually life-long latency is established.

During latency, the viral genome exists as a circular episome and no viral proteins are produced (Whitley, 2001). After primary infection and establishment of latency, HSV can reactivate by migrating along the sensory neurons to the site of primary infection. At this point, a recurrent outbreak characterized by infectious lesions may occur. Reactivation without clinical manifestation is also possible. In this case, asymptomatic shedding of virus particles occurs. In both cases, transmission of infectious virus to a new host can occur (Turner *et al,* 1982 and Whitley and Roizman, 2001). An individual's susceptibility to reactivation depends on a myriad of factors: for example, age, stress, exposure to heat/cold/UV

light, genetic susceptibility, immune status, sexual intercourse or tissue trauma (Whitley and Roizman, 2001).

1.2.2. EPIDEMIOLOGY

Herpes simplex viruses are amongst the most ubiquitous human infections on earth, with 45-98% of the world's population testing seropositive for HSV-1, depending on the region. Rates of HSV-2 are less dramatic, with 20-25% of US citizens testing seropositive (Fatahzadeh *et al*, 2007). However, considering the stigma attached to herpes simplex infections (especially HSV-2) it is possible that these numbers are under-estimations. A number of factors play a role in the prevalence of HSV infections, including age, gender, race, geographic location, socioeconomic status, education, prior sexually transmitted infections, age of first sexual intercourse and number of sexual partners; the latter four primarily in relation to HSV-2 alone (Fatahzadeh *et al*, 2007).

1.2.3. CLINICAL MANIFESTATIONS

Although both HSV types infect skin and mucous membranes, the clinical manifestations of infection depend on how the virus entered the body, host immune status, and whether the infection is primary or recurrent. Most commonly, HSV infection results in gingivostomatitis (lesions in or around the oral cavity), orolabial disease (lesions on the lips), ocular disease, and genital infections. Both gingivostomatitis and

orolabial disease are relatively mild, with symptoms resolving after 10-14 days (Sciubba, 2003). With anti-viral treatment, symptoms may resolve more quickly (2-6 days) and be less severe (Brady and Bernstein, 2003). Despite resolution of symptoms, contagious virus continues to be shed for several weeks (Sciubba, 2003). Recurrent episodes of oral lesions are usually milder and shorter (Lynch, 2000). HSV-induced ocular disease is more serious; it is the most common cause of corneal blindness in the US. Rapid diagnosis and treatment with anti-virals is essential. Both HSV-1 and HSV-2 can cause genital lesions; however, the vast majority are caused by HSV-2. Genital lesions are treated with oral anti-virals, which help to reduce healing time and viral shedding. If reoccurring outbreaks are frequent, more aggressive treatment regimes are available (Brady and Bernstein, 2003).

Rarely, other skin infections such as herpetic whitlow, eczema herpeticum and herpes gladiatorum can occur. In immune-compromised individuals, neonatal infection, encephalitis, and disseminated infections can occur, all which are potentially fatal (Brady and Bernstein, 2003).

1.3. HSV VIRION

HSV virions are 125–130 nm in diameter and contain four main structural elements: the nucleocapsid, DNA core, tegument and envelope (Steven and Spear, 1997).

1.3.1. THE NUCLEOCAPSID

The nucleocapsid is composed of 162 penton or hexon structured capsomeres, seven viral proteins [VP5 (UL19), VP19C (UL38), VP21 (UL26), VP22a (UL26.5), VP23 (UL18), VP24 (UL26), and VP26 (UL35)] and the products of the UL6 and UL25 genes. Together, they form a highly ordered, icosadeltahedral (T = 16) structure (Zhou *at el*, 1998 and Vittone *et al*, 2005). Four of the aforementioned proteins (VP5, VP26, VP23 and VP19C) are present on the surface and are therefore involved in forming the penton/hexon capsid shell. The penton structures are formed by five monomers of the major capsid protein VP5 (149kDa) and are located at the icosahedral 5-fold vertices. The hexon structures are formed by six copies of both VP5 and VP26 (12 kDa) and form the faces and edges of the capsid structure (Zhou *at el*, 1995). The final two viral proteins [VP23 (34 kDa) and VP19C (50 kDa)] assemble together in a 2:1 ratio (respectively) to form a complex known as the triplex. The triplex functions like a scaffold to connect the capsomere units and form the structured capsid shell (Spencer *at el*, 1998)

1.3.2. THE DNA CORE

The DNA core is located inside the nucelocapsid structure and consists of a single linear molecule of double stranded DNA – the viral genome (Knipe, 2007). The genome is both large (152 kbp) and structurally complex. It consists of two covalently linked segments: a long

(L) and a short (S), making up 82% and 18% of the genome, respectively. These segments each contain unique regions (U_L and U_S) which are flanked by inverted repeat sequences referred to as “b” and “c”. A third inverted repeat sequence referred to as “a” flanks the entire structure, giving a final arrangement of ab – U_L – b′a′c′ – U_S – ca (Ward and Weller, 2011 and Mahiet, 2012). The genome also contains two classes of closely related origins of replication, OriS and OriL. OriS is present in the inverted repeat sequence flanking the U_S region and is thus present twice. OriL is located near the middle of the U_L region (Challberg, 1996). Both OriL and OriS contain recognition sites for UL9, the origin-binding protein (Aslani *et al*, 2002).

1.3.3. THE TEGUMENT

Surrounding the nucleocapsid is an amorphous, proteinaceous layer called the tegument. The tegument contains at least 20 proteins, including VP1/2 (UL36), VP11/12 (UL46), VP13/14 (UL47), VP16 (UL48), VP22 (UL49), ICP0, ICP4, vhs, and the gene products of US2, US3, US10, US11, UL13, UL14, UL16, UL17, UL21, UL37, UL51, and UL56 (Roizman and Sears, 1996 and Vittone *et al*, 2005).

Some of these, termed outer tegument proteins, are immediately delivered into the cytoplasm of the infected cell, allowing them to act before gene expression occurs (Steven and Spear, 1997 and Wolfstein *et al*, 2006). Others, termed inner tegument proteins, remain associated with

the capsid. Notable outer tegument proteins include VP16 (transcriptional activator of immediate-early genes and structural component) and vhs (mRNA specific nuclease). Notable inner tegument proteins include VP1/2 (essential for viral replication) and gene products of UL37 (activates NF-κB signaling) and US3 (protein kinase) (Goldmacher *et al*, 1999, Munger and Chee, 2001, Liu and Hong Zhou, 2007, Liu *et al* 2008, Abaitua, 2009 and Cardone *et al*, 2012).

Tegument proteins are involved in almost every viral process, including capsid transport, transcriptional regulation, translation, apoptosis, DNA replication, immune modulation, cytoskeletal assembly, viral assembly and egress (Kelly *et al*, 2009).

1.3.4. THE ENVELOPE

Surrounding the tegument is a host-cell derived lipid envelope containing multiple copies of viral glycoproteins gB, gC, gD, gE, gG, gH, gI, gJ, gK, gL, and gM (Roizman and Sears, 1996 and Knipe, 2007). These glycoproteins, specifically gB, gH and gL, play crucial roles in viral entry and attachment (Knipe, 2007 and Eisenberg *et al*, 2012). These three proteins form what is referred to as the “core fusion machinery”, consisting of gB and gH/gL which function as a heterodimer. Accessory membrane fusion proteins are also utilized; in the case of HSV, that protein is gD. gD is responsible for binding the cellular HSV receptors

HVEM, nectin-1 and 3-O-sulphated heparin sulfate and thus determines tropism of the virus (Eisenberg *et al*, 2012).

1.4. HSV LYTIC INFECTION

HSV-1 lytic infection involves the processes of attachment and entry into the host cell, temporally regulated gene expression, DNA replication, assembly and egress. All are discussed in detail below.

1.4.1. ATTACHMENT AND ENTRY

Attachment and entry of the HSV-1 virion into the host cell occurs in a three step process involving fusion between the viral envelope and the host cell membrane. Five viral glycoproteins present on the viral envelope are utilized in viral attachment, gC, gB, gD, gH and gL (Spear, 1993). Initial attachment is mediated by binding of either gC or gB viral glycoproteins to heparan sulfate and chondroitin sulfate cell surface proteoglycans (HSPG and CSPG) (Herold *et al*, 1991 and Shieh *et al*, 1992). Although gC is the primary mediator of this interaction, it is actually not an essential binding protein. In its absence, gB can perform this role. However, if both gC and gB are non-functional, binding to the host cell membrane is severely impaired (Herold *et al*, 1991 and Herold *et al*, 1994).

The primary function of this initial attachment is to concentrate HSV virions on the surface of the host cell (reviewed in Hadigal and Shukla,

2013). Following the initial interaction, bundles of actin filaments termed filopodia aid the virion in “surfing” along the host cell surface towards the location of the viral glycoprotein gD receptors (Svitkina *et al,* 2003). gD glycoproteins contain both receptor and glycoprotein binding sites, located on the N-terminus and C-terminus, respectively (Cairns *et al,* 2005). At least three cellular receptors have been identified as gD N-terminal binding partners, HVEM, Nectin-1 and 3-O-sulfated heparin sulfate (Montgomery *et al*, 1996, Shukla *et al,* 1999 and Spear *et al,* 2000). HVEM is a member of the tumor necrosis factor-receptor family (Montgomery *et al*, 1996). Residues within the first and second cysteine rich domains of HVEM are responsible for attachment to gD (Whitbeck *et al*, 2001 and Connolly *et al*, 2002). Nectin-1 is a cell adhesion molecule with a binding site disctinct from that of HVEM. An exposed tyrosine residue (Tyr38) has been identified as the most critical binding residue (Connolly *et al,* 2005).

Non-protein interactions also play a role in gD-mediated entry. For example, modifications made to heparin sulfate molecules by 3-O-sulfotransferases create specific sulfate patterns which can be recognized by gD glycoproteins (Shukla *et al,* 1999 and O’Donnell *et al,* 2006). Binding of gD to its receptors causes a conformational change in which the glycoprotein binding C- terminus is released from its folded, closed confirmation. This binding leads to the exposure of the glycoprotein binding sites and an open conformation which favours membrane fusion (Fusco *et al,* 2005). The newly exposed C-terminus can now interact with

the core fusion machinery, consisting of the gH/gL glycoprotein heterodimer and the gB fusion protein (Turner *et al*, 1998, Lazear *et al,* 2008 Stampfer and Heldwein, 2013). These interactions between the core fusion proteins help form the fusion pore (Atanasiu *et al,* 2010) which completes the fusion process.

Depending on the cell type, fusion can occur either with the cellular plasma membrane or with the membrane of an endosomal vesicle (Nicola *et al,* 2003 and Smith and Helenius, 2004). After fusion occurs, the nucleocapsid and certain outer tegument proteins are released into the cytoplasm of the newly infected cell. Some of the inner tegument proteins remain associated with the nucleocapsid as it is transported along the microtubular network to the nucleus (Sodeik *et al,* 1997).

1.4.2. IMMEDIATE-EARLY (IE) GENE EXPRESSION

As previously mentioned, HSV gene expression occurs in a temporally regulated fashion. During infection, approximately 80 genes are sequentially expressed in three major kinetic groups: immediate-early (IE, α), early (E, β), and late (L, γ) genes (Honess and Roizmann, 1974). Regulation of HSV gene transcription is primarily determined by promoter structure (Wagner *et al,* 1995). Each of the HSV genes has its own promoter and accompanying TATA box, which are recognized by host RNA polymerase II (RNAP II) transcription machinery. This host RNA polymerase is responsible for transcription of all HSV gene classes

(Constanzo *et al,* 1977 and Wagner *et al,* 1995). Both the IE and E gene promoters contain several *cis*-acting elements upstream of the TATA box (Wagner *et al,* 1995 and Wagner *et al,* 1998). Transcription is initiated when these elements are recognized by various cellular and viral proteins to be discussed below (Gelman and Silverstein, 1987 and Wagner *et al,* 1995).

IE genes are the first to be transcribed – approximately 3 to 4 hours post-infection, before any *de novo* protein synthesis occurs. Their transcription is also responsible for stimulation of early (E) and late (L) gene expression (Honess and Roizmann, 1974). HSV IE regulatory domains contain specific binding sites for cellular transcription factors such as Sp1 and GABP. These transcription factors work in tandem with members of the enhancer core complex (Oct-1, VP16 and HCF-1) to promote IE gene expression (reviewed in Kristie, 2007). Another key component of the IE regulatory domain is the TAATGARAT enhancer core element. This sequence is present in multiple copies and flanked by the Sp1 and GABP binding sites (Fields *et al,* 1996). Assembly of the enhancer core complex involves the association of the cellular DNA binding protein Oct-1 with a DNA sequence directly adjacent to and including part of the TAATGARAT enhancer core element –ATGCTAAT (Sturm *et al,* 1988 and reviewed in Kristie, 2007). VP16 acts as the viral component of the enhancer core complex, binding to both the TAATGARAT DNA element and Oct-1 (Kristie and Sharp, 1990). Its

recognition and association with the TAATGARAT element and Oct-1 (respectively) determines the specificity of the core complex, making VP16 a critical component (Kristie and Sharp, 1990 and reviewed in Kristie, 2007). The final protein constituent of the complex is the cellular co-activator and key cell cycle component HCF-1. Rather than directly binding DNA, HCF-1 plays the role of complex assembly coordinator and stabilizer by interacting with the other protein components of the complex: VP16, Oct-1, Sp1 and GABP (Vogel and Kristie, 2000). Additionally, HCF-1 is essential for transport of VP16 to the nucleus, as VP16 itself does not contain a nuclear localization sequence (Boissiere *et al,* 1999). Because of its essential role in VP16 transport, complex assembly and stabilization, HCF-1 is required for maximum transcription of IE genes (Luciano and Wilson, 2002).

VP16 is one of the most critical and multifunctional HSV-1 proteins. Approximately 900 copies of this tegument protein are delivered into the cytoplasm of a host cell immediately following infection (reviewed in Kristie *et al,* 2007). Following its release, VP16 is transported to the nucleus, aided by HCF-1, to participate in the core enhancer complex discussed above (Boissiere *et al,* 1999 and Kristie and Sharp, 1990). The VP16 protein itself consists of 490 amino acids, with a conserved structural core (aa 49–403). The core contains interaction domains for Oct-1, HCF-1 and DNA which are located at the N-terminus (Kristie and Sharp, 1990 and Lai and Herr, 1997). At the C-terminus of the core, an acidic transcription

activation domain (aa 412–490) is present. This activation domain interacts with basal transcription factors (TFIIB, TFIIH, TBP), chromatin remodeling proteins (SAGA), nucleosome modification factors (SWI 2/SNF2) and the RNAP II holoenzyme (Gold *et al*, 1996, Hall and Struhl, 2002, Herrmann *et al*, 1996, Herrera and Triezenberg, 2004, Memedula and Belmont, 2003, Vignali *et al*, 2000, Hengartner *et al,* 1995). The activation domain of VP16 is involved in a myriad of early transcriptional processes, such as chromatin remodeling and histone modifications, assembly of the preinitiation complex, RNAP II positioning and open complex formation, RNAP II promoter escape, mRNA splicing efficiency, and reinitiation scaffold stabilization (reviewed in Kristie, 2007). Six IE proteins are produced via VP16 induced transcriptional activation – ICP0, ICP4, ICP22, ICP27, US1.5 and ICP47. All except the latter aid in the stimulation of E gene expression (Roizman and Knipe, 2001).

1.4.2.1. ICP0

ICP0 is a multifunctional RING-finger E3 ubiquitin ligase which plays a role in both early stages of lytic infection and reactivation from latency. During early lytic infection, ICP0 helps enable efficient viral replication by enhancing localization of key proteins to nuclear replication compartments and aiding in immune evasion by inhibiting host IRF3 activation and thus interferon production (Boutell *et al,* 2005 and Paladino *et al,* 2010). ICPO also mediates the ubiquitination and proteasome-

dependent degradation of several cellular proteins via its E3 ubiquitin ligase activity. Amongst these proteins are major ND10 constituent proteins (PML, SP100, Daxx and ATRX), DNA repair proteins (DNA-PKcs, RNF8 and RNF168) and transcriptional regulator E2FBP1. The degradation of these proteins aids the virus in a myriad of ways. By degrading ND10 constituent proteins, DNA repair proteins and E2FBP1, intrinsic antiviral immunity is inhibited and transcriptional repression is achieved. Ultimately, reactivation of latent viral genomes occurs (reviewed in Boutell and Everett, 2013). These (and other) interactions mediate ICP0's ability to indirectly stimulate expression of IE, E and L genes and generally enhance viral infectivity.

1.4.2.2. ICP4

ICP4 is the major regulator of viral transcription; it is capable of acting as both a transcriptional activator and repressor, and is thus essential for replication (DeLuca and Schaffer, 1985 and Godowski and Knipe, 1986). ICP4 is a nuclear phosphoprotein that acts as a homodimer and interacts with several proteins (Metzler and Wilcox, 1985 and Pereira *et al,* 1977). Firstly, direct interactions with TBP and TAF1 of the TFIID complex help stabilize the preinitiation complex on viral promoters (Gu and DeLuca, 1994, Carrozza and DeLuca, 1996 and Grondin and DeLuca, 2000). Additionally, ICP4 can suppress activated transcription at promoters containing the ICP4 binding site by forming a stable, tripartite

complex (TPC) on DNA at promoters containing the ICP4 binding site. The TPC is formed by the cooperative binding of ICP4, TBP and TFIIB (Smith *et al,* 1993). ICP4 also interacts with viral gene regulator proteins ICP0 and ICP27 (Yao and Schaffer, 1994 and Panagiotidis *et al,* 1997).

1.4.2.3. ICP22

ICP22 is the least well characterized of the IE proteins. After its synthesis, ICP22 is transported to the nucleus where it remains diffuse or specifically localizes to small nuclear bodies (Leopardi *et al,* 1997 and Jahedi *et al,* 1999). At later times during infection, the L protein UL4 may colocalize with ICP0 (Jahedi *et al,* 1999). ICP22 has also been shown to associate with, and be essential in the formation of, VICE (virus-induced, chaperone-enriched) domains (Bastian *et al,* 2010). ICP22 has been shown to both promote and repress gene expression. Although the exact mechanism is currently unclear, ICP22 acts to decrease phosphorylation of serine 2 of the RNA polymerase II C-terminal domain (RNAPII Ser-2), which is vital for transcription elongation (Fraser and Rice, 2007).

ICP22 also acts to enhance transcription of certain L genes in a UL13 dependent manner (Purves *et al,* 1993). An interaction between ICP22, UL13 and the cyclin-dependent kinase cdc2 (cdk1) is likely involved in the enhancement of L genes (Advani *et al,* 2000a). During HSV-1 infection, ICP22 and US13 work together to alter cdk1 in several ways: increasing intracellular levels by replacing cdk1's normal cyclin

partners with a HSV-1 equivalent (UL47) (Advani *et al,* 2000b), and maintaining cdk1 activity via an interaction with host cell phosphatase cdc25C. This results in a removal of inhibitory phosphate groups (Smith-Donald and Roizman, 2008). As shown by Advani *et al* (2000b), cdk1 is required for efficient expression of the L gene US11, indicating that the ICP22/US13/cdk1 interaction is central to ICP22's role in promoting transcription of L genes.

1.4.2.4. ICP27

ICP27 is an essential, multifunctional regulator of viral gene expression that associates with a variety of cellular proteins in different cellular locations. Early in infection, ICP27 localizes to the nucleus where it plays a role in host protein shutoff and viral replication. The former is achieved by inhibiting host cell splicing, resulting in the accumulation of unspliced pre-mRNAs in the nucleus and the early cessation of cellular protein synthesis (Hardwicke and Sandri-Goldin, 1994 and Sandri-Goldin, 1998). The latter is mediated by an association with cellular RNA polymerase II, resulting in its recruitment to viral replication sites (Dai-Ju *et al*, 2006).

About five hours after infection, ICP27 relocates to viral transcription/replication compartments alongside the cellular mRNA export factor Aly/REF (Chen *et al,* 2002). Here, it proceeds to bind viral

intronless mRNA transcripts and facilitates their nuclear export via its shuttling activity (Mears and Rice, 1998 and Sandri-Goldin, 1998). This is mediated by an interaction with the cellular mRNA export receptor TAP/NXF1 (Hernandez and Sandri-Goldin, 2010). The interaction with Aly/REF also helps direct RNA towards TAP/NXF1 (Chen *et al,* 2002). An association with core nucleoporin Nup62 may also aid in ICP27-mediated RNA shuttling by increasing the number of binding sites at the nuclear pore (Malik *et al,* 2012). Once in the cytoplasm, ICP27 stimulates translation of certain viral transcripts via interactions with translation initiation factors (Fontaine-Rodriguez *et al*, 2004, Ellison *et al,* 2005 and Fontaine-Rodriguez and Knipe, 2008). Notably, ICP27 is required for transcription of gC and UL47 (Jean *et al,* 2001), and it enhances translation of VP16 (Ellison *et al,* 2005).

ICP27 also works to prevent apoptosis both by translocating NF-κB to the nucleus (Goodkin *et al,* 2003) and by blocking the cell cycle at the G1 phase (Song *et al,* 2001).

1.4.2.5. ICP47

ICP47 is the only IE protein which does not play a role in the regulation of gene expression; instead, it is involved in host immune evasion. ICP47 works to inhibit HLA class-I antigen presentation by binding to and blocking the TAP transporter (York *et al,* 1994, Früh *et al,* 1995, Hill *et al,* 1995 and Beinert *et al,* 1997). This inhibition disrupts

antigen loading and cell surface presentation, resulting in the failure of $CD8^+$ T cells to recognize infected cells (Früh *et al,* 1995).

1.4.3. EARLY GENE EXPRESSION AND DNA REPLICATION

Following expression of the IE genes, the E genes are expressed. Expression of these genes occurs before the onset of DNA replication, as some of the E proteins are required for replication to occur. Expression peaks approximately 5 to 7 hours post-infection, and decreases thereafter (Honess and Roizman, 1974). Functional ICP4 is required (Honess and Roizman, 1975). E genes are expressed in two groups: the β1 genes, which are expressed almost simultaneously with IE genes, and the β2 genes, which are expressed second (Knipe *et al,* 2001).

HSV-1 encodes seven essential replication proteins: the single-strand DNA-binding protein ICP8 (β1 gene UL29), an origin-binding protein (UL9), a 3-subunit helicase/primase complex (UL5, contains helicase motifs; UL8, interacts with other proteins; UL52, contains primase motifs) and a 2-subunit DNA polymerase (β2 gene UL30, catalytic subunit; UL42, processivity subunit) (reviewed in Ward and Weller, 2011). Other non-essential HSV encoded genes also play a role in DNA replication. For example, the uracil-DNA glycosylase UL2 may play a role for base excision repair during DNA replication (Bogani *et al,* 2010). Replication itself begins at one of the three origins of replication, with both ICP8 and UL9 present to induce replication-conducive conformational changes in

the surrounding DNA (Makhov *et al,* 2003). The helicase/primase complex is then recruited, where it is proposed to initiate DNA replication by unwinding the duplexed DNA and synthesizing short RNA primers (Chen, 2011). Lastly, the DNA polymerase holoenzyme is recruited to the replication fork, possibly though interactions with the US8 subunit of the helicase/primase complex (Marsden *et al,* 1996). The polymerase is hypothesized to then catalyse DNA synthesis via a leading and lagging strand mechanism (Falkenberg *et al,* 2000 and Stengel *et al,* 2011). Final replication products are concatemeric molecules that are later cleaved at the genomic termini to the appropriate size (reviewed in Boehmer & Lehman, 1997).

1.4.4. LATE GENE EXPRESSION, VIRION ASSEMBLY AND EGRESS

L gene expression occurs last, up to 12 hours post-infection, with rates of expression increasing up until that point (Honess and Roizman, 1974). Their expression is greatly influenced by DNA replication; L genes are actually subdivided into two groups: those that can be expressed without DNA replication [leaky-late (γ_1)] and those that cannot [true-late (γ_2)] (Honess and Roizman, 1974 and Holland *et al,* 1980). Unlike IE and E gene promoters, L gene promoters do not have upstream *cis*-acting elements. Instead, regions downstream of the TATA box have been implicated in transcriptional regulation (Homa *et al,* 1986, Kibler *et al,* 1991, Steffy and Weir, 1991 and Huang *et al*, 1993). Additionally, several

IE and E proteins are required for stimulation (ICP8) and expression of the L γ_1 (ICP0, ICP4, ICP27, ICP22 and γ_2 (ICP22) genes (Gai and Knipe, 1991, Chen and Knipe, 1996 and Roizman and Knipe, 2001). After L gene products are synthesized, capsid assembly can occur.

Both capsid formation and encapsidation of replicated viral DNA occur in the nucleus. The capsid itself consists of five proteins: VP5, VP19C and VP23, VP26, and UL6 (Steven and Spear, 1997). VP5 is the major capsid protein; approximately 955 copies form the virion shell. They are organized in a highly structured fashion; 11 pentons, each containing five copies of VP5, and 150 hexons, each containing six copies of VP5. Linking the pentons and hexons together are VP19C and VP23, which function together as a tripartite complex consisting of two copies of VP23 and one copy of VP19C (Newcomb *et al*, 1993a). VP26 forms the tips of the hexons and is non-essential. Lastly, UL6 forms what is referred to as the portal vertex. At one of the vertices, 12 copies of the UL6 protein form the channel through which DNA is both packaged into the capsid and expelled after infection of a new host cell (Newcomb *et al*, 1993b and B.L. Trus *et al*, 2004). Capsid assembly itself likely begins with the formation of this critical portal structure, around which all the other capsid proteins assemble (Newcomb *et al*, 1993c). Additional proteins ICP35/VP22a and the gene products of UL26 (cleaved autoproteolytically into VP21 and VP24) form the inner scaffold of the capsid structure, with ICP35/VP22a acting as the major scaffolding protein and VP21 as the minor scaffolding

protein. (Liu and Roizman, 1991 and Preston *et al,* 1994). VP24 acts as a protease, which is essential for capsid maturation. Its activity causes the spherical capsid to adopt its characteristic icosahedral conformation, which is much more stable and less porous than its spherical counterpart (Trus *et al*, 1996 and J.B. Heymann *et al*, 2003).

Encapsidation of viral DNA also takes place in the nucleus, specifically, in replication compartments (Lamberti and Weller, 1998). As previously mentioned, DNA produced during replication exist as concatemeric molecules that must be cleaved into genome-sized fragments prior to packaging into mature capsids (reviewed in Boehmer & Lehman, 1997). This task is executed by a highly specialized, multi-protein ATPase called the terminase (Booy *et al*, 1991 and Yu and Weller, 1998). Consisting of HSV proteins UL15, UL28 and UL33, this complex scans the DNA for cleavage sites designated by *cis*-acting packaging signals (pac1/2), cleaves the DNA and pumps it into the capsid via the portal structure (Adelman *et al*, 2001).

Acquisition of the viral envelope is thought to occur via an envelopment, deenvelopment and reenvelopment process (reviewed in Farnsworth *et al*, 2003). Primary envelopment occurs as the mature capsid buds through the inner nuclear membrane into the perinuclear space (Farnsworth *et al*, 2003). This requires the nuclear envelopment complex (NEC), which consists of viral proteins UL31 and UL34 (Reynolds *et al*, 2001). The NEC likely functions via indirect or direct interactions

between the NEC proteins and the mature capsid proteins, as the NEC proteins have been shown to associate with the capsid in the perinuclear space (Reynolds *et al*, 2002).

Deenvelopment occurs as enveloped particles in the perinuclear space fuse with the outer nuclear membrane, delivering the now naked capsids into the cytoplasm. NEC proteins remain in the outer nuclear membrane (Reynolds *et al*, 2002). Viral protein US3 plays a role in promoting deenvelopment during fusion of the virion envelope and outer nuclear membrane (Wisner *et al*, 2009 and Mou *et al*, 2009). Acquisition of the tegument proteins (including VP1-2, VP16, vhs, VP22, ICP0, ICP4, US3, US11, UL36 and UL37) occurs in several locations during egress. VP1-2, UL37, vhs, VP22 and VP16 are all initially acquired in the nucleus, with additional copies added in the cytoplasm after deenvelopment (Mettenleiter *et al*, 2009). Other tegument proteins are exclusively added in the cytoplasm. Here, VP16, vhs and VP22 assemble into a complex that coats the viral capsid and associates with the trans-Golgi network (TGN) membranes. The TGN membranes contain viral glycoproteins (including gE–gI, gD, gB, gH–gL) which interact with the tegument proteins on the surface of the capsid. These associations not only affect the assembly of tegument proteins into the virion, but help promote secondary envelopment (reviewed in Johnson and Baines, 2011).

Interactions between HSV proteins UL11, UL16 and UL21 also help promote secondary envelopment by connecting the envelope to the capsid

(Meckes *et al,* 2010). Once coated in tegument proteins, the virion envelope is acquired by budding into cytoplasmic membranes including the *cis*-Golgi, the medial Golgi, the TGN and endosomes (reviewed in Johnson and Baines, 2011). Once the envelope is acquired, the virion is transported to the plasma membrane (PM) and eventually released into the extracellular space. This movement is facilitated by disruption of TGN trafficking. As suggested by Wisner *et al* (2004), blocking backward transport from endosomes to the TGN may favor forward transport of the HSV virions to the PM.

1.5. VIRION HOST SHUTOFF

Infection with HSV results in the rapid and irreversible shutoff of host protein synthesis (Kwong *et al*, 1988). This phenomenon was first noticed decades ago (Roizman *et al*, 1965 and Sydiskis and Roizman, 1966, 1968), but the underlying mechanism was not yet clear. Early reports from Fenwick and Clark (1982) describe the shutoff of host protein synthesis occurring in two stages: an 'early shutoff' stage that occurs early in infection, prior to any viral gene expression and a 'delayed shutoff' later in infection, after gene expression has occurred. Several viral proteins are thought to contribute to the observed 'delayed shutoff' of host protein synthesis, mediated through transcriptional repression (Spencer *et al,* 1997) and inhibition of pre-mRNA splicing (Hardy and Sandri-Goldin, 1997).

The former is mediated by alterations to the RNAP II holoenzyme complex, causing it to favour transcription of viral genes by changing phosphorylation status (Rice *et al*, 1994). The IE protein ICP22 and the UL13 kinase are implicated in these RNAP II alterations (Rice *et al*, 1995 and Long *et al,* 1999). Additionally, viral proteins including ICP4, ICP27, and ICP8 have been shown to interact with the RNAP II (Jenkins and Spencer, 2001 and Zhou and Knipe, 2002). This interaction has been proposed to alter its preference for cellular transcripts and instead favour transcription of the viral genome (Jenkins and Spencer, 2001).

The latter is mediated by the IE protein ICP27, which is both necessary and sufficient to impair pre-mRNA splicing (reviewed in Sandri-Goldin, 1998). ICP27 binds splicing factors such as SAP145 (Bryant *et al,* 2001) and SR proteins such as SRPK1 and well as the SR kinase SRK1 – interactions which result in inhibition of splicing due to impaired spliceosome assembly and sequestration of splicing factors (Sciabica *et al*, 2003).

'Early shutoff' has been defined as that which occurs prior to any *de novo* gene expression (Fenwick and Clark, 1982). This shutoff is characterized by the disruption of preexisting polysomes, the degradation of host mRNAs and the shutoff of host protein synthesis (reviewed in Smiley, 2004). Early studies indicated that a viral component, specifically the product of the UL41 gene, was responsible (Strom and Frenkel, 1987

and Kwong *et al*, 1988). This UL41 gene product was referred to as the virion host shutoff protein, or vhs.

1.5.1. HSV-1 VIRION HOST SHUTOFF (VHS) PROTEIN

Vhs is a 58 kDa phosphoprotein which is synthesized late during infection and then packaged into the tegument, ready to be immediately released into the infected host cell cytoplasm following infection (Fenwick and Clark, 1982 and Read *et al,* 1993). Although vhs is not essential for viral replication, vhs-null mutants are attenuated both in tissue culture and *in vivo,* showing a 5-10 fold reduction in virus yield in tissue culture (Read and Frenkel, 1983, Smibert and Smiley, 1990 and Read *et al,* 1993). This attenuation may be explained by vhs's role as a *bona fide* virulence factor, capable of disrupting both innate and adaptive host immune responses. The former include the suppression of proinflammatory cytokine and chemokine production, including interleukin 1β (IL-1β), IL-8, MIP-1α (in U937 cells) and IL-8 (in HEL cells) (Suzutani *et al,* 2000), the reduction of the type I interferon system effectiveness (Duerst and Morrison, 2004 and Pasieka *et al,* 2008), blocked activation of dendritic cells (Samady *et al,* 2003) and blocked activation of PKR in cooperation with MEK (Sciortino *et al,* 2013). The latter include increased resistance to cytotoxic T lymphocyte-mediated lysis by contributing to the loss of cell surface MHC-I (Koppers-Lalic *et al,* 2001) and impaired antigen presentation via reduction of MHC-II molecules (Trgovcich *et al,* 2002).

Early investigations into vhs uncovered evidence that it was acting as a RNA specific nuclease (reviewed in Smiley, 2004). Firstly, functionally critical similarities in amino acid sequence between vhs and the cellular endo/exonuclease FEN-1 were discovered (Everly *et al*, 2002, reviewed in Smiley, 2004). Additionally, several vhs mutations (in some cases in the nuclease domain) were shown to eliminate its RNase activity *in vitro* (Zelus *et al,* 1996, Elgadi *et al,* 1999 and Everly *et al*, 2002). More specifically, vhs was determined to be highly specific to mRNA *in vivo*, targeting mRNA specifically and ignoring other types of cytoplasmic RNA (Kwong and Frenkel, 1987 and Zelus *et al,* 1996).

Early attempts to elucidate how vhs specifically targets mRNA found that although no interaction between vhs and the 5′ cap or 3′ poly(A) tail structure could be found, evidence suggested specific areas of RNA transcripts were indeed targeted (Zelus *et al,* 1996, Elgadi *et al,* 1999 and Karr and Read, 1999). For example, areas directly downstream of an encephalomyocarditis virus and a poliovirus internal ribosome entry site (IRES, see below section for further detail) were targeted by vhs (Elgadi and Smiley, 1999). Additionally, Karr and Read (1999) show that the 5' end of HSV thymidine kinase mRNA transcripts were preferentially targeted over the 3' end *in vivo.* The proposed mechanism involved a vhs-mediated removal of the 5' cap structure, followed by a directed 5′ to 3′ degradation of the mRNA transcript (Perez-Parada *et al,* 2004).

Given the common theme of vhs-mediated targeting of areas of translational initiation, it is not surprising that later research determined that vhs binds to the translation initiation factors eIF4B and eIF4H as well as a component of the cap-binding complex, eIF4A (Feng *et al,* 2001/2005 Doepker *et al,* 2004 and Page and Read, 2010). These associations between vhs and the cap-binding complex are currently proposed as the best model for mRNA-specific targeting by vhs.

Although it is clear that vhs preferentially targets mRNA, its preference for different subsets of mRNA is currently unclear. Initial reports suggest that vhs equally targets both cellular and viral mRNA for destabilization and degradation (Kwong and Frenkel, 1987 and Oroskar and Read, 1987). This indiscriminate targeting would result in a global reduction in mRNA stability in HSV infected cells. Biologically speaking, reduced mRNA stability is highly beneficial to a rapidly replicating virus, especially one that expresses its genes in a tightly temporally-regulated fashion such as HSV. In terms of the viral mRNA, the instability results in a high turnover rate, which allows for efficient use of translation machinery and a sharpening of transitions between gene classes. In terms of the cellular mRNA, a striking decline in cellular mRNA levels and subsequent shutoff of host protein synthesis helps alleviate competition for cellular translation machinery, allowing the virus to utilize these components for its own processes (Kwong and Frenkel, 1987 and Oroskar and Read, 1987).

Despite this longstanding proposal, contrasting evidence suggesting more specific targeting by vhs has been reported. Esclatine *et al* (2004a/b) found that some stable host mRNAs are more rapidly degraded than others. They noted that certain stress response mRNAs carrying adenylate-uridylate (AU)-rich elements (AREs) in their 3′ UTR – such as tristetraprolin (TTP) – were resistant to vhs-mediated degradation (Esclatine *et al*, 2004b). More recently, Taddeo *et al* (2013) report that vhs preferentially targets IE mRNAs, sparing its E and L mRNA counterparts, and allows them to accumulate during infection. How this activity and specificity is being regulated is currently unclear. Nevertheless, vhs activity has been shown to be altered by interactions with several viral proteins. For example, during late stages of viral replication, L gene products VP16 and VP22 block or neutralize vhs-mediated RNase activity (Lam *et al*, 1996 and Taddeo *et al,* 2007). Recently, Shu *et al* (2013) show that VP13/14 binds vhs, resulting in the attenuation of vhs-induced viral and stable host mRNA degradation. Interestingly, they found this interaction had no effect on the stability of the stress response mRNAs carrying AREs in their 3′ UTR (Esclatine *et al*, 2004b).

Originally, it was proposed that an interaction with ICP27 helped stabilize these ARE-containing RNAs, rendering them immune to the effects of vhs (Corcoran *et al,* 2006). However a more recent report discounted this hypothesis, instead suggesting that the binding of ICP27 to vhs at the cap structure of certain mRNAs prevents vhs from cleaving the

transported mRNAs (recall ICP27 section: ICP27 is responsible for shuttling certain mRNAs late in infection).

Furthermore, it is currently unclear whether the observed vhs-dependent mRNA degradation is mediated solely by vhs or requires other viral or cellular nucleases. Vhs-mediated degradation proceeds in an overall 5′-to-3′ direction (Elgadi and Smiley, 1999, Elgadi *et al,* 1999, Karr and Reid, 1999 and Perez-Parada *et al,* 2004); however, it is unclear whether vhs itself is solely responsible.

A recent report from Gaglia *et al* (2012) suggests a mechanism in which vhs makes an initial endonucleolytic cleavage close to the 5' end of the mRNA transcript, and the cellular exonuclease XrnI completes the degradation, proceeding in a 5'-to-3' direction. Interestingly, this report suggested a similar mechanism of action for several unrelated (to vhs) viral host shutoff nucleases, including three gammaherpesvirus alkaline exonuclease homologs, Kaposi's sarcoma-associated herpesvirus (KSHV) SOX, Epstein Barr virus (EBV) BGLF5 and murine herpesvirus muSOX. Also included was the betacoronavirus SARS coronavirus Nsp1 protein, which has no known homology to any cellular or viral nucleases. Further analysis of the similarities and differences between these nucleases and vhs will be part of the body of this thesis. As evidenced by the above literature, further investigation into the specificity and activity of vhs is needed to better understand its mechanism of action.

Another function of vhs was recently proposed, that of a translational regulator. The connection between vhs and translation was established early; as discussed above, vhs is recruited to regions of translation initiation, either to the 5' cap structure (by binding components of the cap-binding complex) or to regions of internal initiation (by selective recruitment to areas directly downstream of viral IRES sequences putatively via interactions with eIF4 factors). However, a more recent report suggest that vhs may be able to activate cap-independent translation through specific *cis*-acting elements, such as certain IRES's (a mutant EMCV IRES and the cellular ApaF1, BiP, and DAP5 IRES's) in a cell-type dependent manner (Saffran *et al,* 2010). More detail on this report will follow. Dauber *et al* (2011) also found that during lytic infections, translation of certain viral true late RNAs (such as gC and US11) were stimulated by vhs in a cell-type dependent manner. Most recently, Shiflett and Read (2013) show that mutations in mRNA that affect its translation also affect the location of the vhs cut sites.

It is clear that despite the wealth of research on vhs, many mysteries still remain about how it is targeted to mRNA, what features of mRNAs determine their sensitivities to vhs degradation, and the mechanism by which vhs-mediated degradation occurs. What is clear is that vhs is obviously not exclusively a host shutoff factor; instead, it is a multifunctional protein capable of affecting both translation and degradation of many mRNAs (Shiflett and Read, 2013).

1.6. TRANSLATION INITIATION

Eukaryotic translation can occur in one of two ways. The majority of cellular mRNAs are translated via cap-dependent translation. A second, cap-independent mode of translation initiation is mediated by *cis*-acting regulatory elements called internal ribosome entry sites (IRESs). Both modes of initiation are discussed in more detail below.

1.6.1. CAP-DEPENDENT TRANSLATION

Cap-dependent translation is the canonical mode of translation initiation. The current pathway can be divided into eight stages (see Figure #1), with at least nine eukaryotic initiation factors (eIFs) required for the process to occur.

Stage 1 involves the formation of 43S preinitiation complexes. As translation is a cyclical process, ribosomal subunits must be recycled from post-termination ribosomal complexes to be used in subsequent rounds of initiation. During this recycling process, the 40S small ribosomal subunit interacts with translation initiation factors eIF3, eIF1, and eIF1A. At the same time, the ternary complex (eIF2–GTP–Met-tRNA^{Met}) assembles and attaches to the newly recycled 40S subunits already bound to eIF3, eIF1 and eIF1A. This new complex is referred to as the 43S complex (reviewed in Jackson *et al,* 2010).

Next, the 43S complexes must attach to the mRNA. Through the cooperative action of the cap-binding complex eIF4F and eIF4B/eIF4H, the significant secondary structure often located at regions of translational initiation (5' UTRs) can be unwound and the mRNA prepared for 43S complex attachment. The cap-binding complex eIF4F is composed of initiation factors eIF4E, eIF4G and eIF4A (Pestova *et al*, 2007 and reviewed in Jackson *et al,* 2010). eIF4E functions as the cap-binding protein. Binding of eIF4E to mRNA is enhanced by the scaffolding protein eIF4G, which wraps around eIF4E and also binds eIF4A, the poly(A)-binding protein (PABP) and eIF3 of the 43S complex (Gross *et al,* 2003 and Volpon *et al,* 2006). eIF4A is an RNA helicase RNA/ATPase capable of unwinding secondary structure due to its DEAD-box motif. However, initiation factors eIF4G and eIF4B/eIF4H strongly enhance the inherently weak helicase activity of eIF4A (Rogers *et al,* 2001 and reviewed in Jackson *et al,* 2010). Once unwound, the RNA is prepared for attachment of the 43S complex and subsequent ribosomal scanning (reviewed in Jackson *et al,* 2010).

Once the 43S complex is assembled at the 5' cap, it travels downstream along the mRNA transcript until it reaches a start codon (AUG) in the appropriate context. Both eIF1 and eIF1A are critical; they maintain the mRNA in an open conformation conducive to ribosomal scanning (Pestova *et al*, 2002 and Passmore, *et al*, 2007). eIF4A, eIF4G, eIF4B and ATP are also required, even if the mRNA in question does not

possess significant secondary structure (Pestova *et al*, 2002). The placement of eIF4G, eIF4A, and eIF4B/H in relation to the ribosome and the occurrence of any conformational changes to the complex during scanning are currently unclear (reviewed in Jackson *et al,* 2010).

Scanning proceeds until a start codon (AUG) is encountered in the appropriate context; that is, GCC(A/G)CC**AUG**G (if the A of AUG is +1: a purine is at the −3 and a G at the +4 position) (Kozak, 1991). eIF1 plays a imperative role in this process. It not only discriminates between AUG and non–AUG sequences, but also ensure the AUG codon is in the appropriate context and not too close to the 5' end of the transcript (Pestova *et al,* 1998, Pestova *et al*, 2002 and Pisarev *et al*, 2006). Additionally, eIF1 mediates conformational changes in the 43S complex which allows for binding of the Met-tRNA^{Met} anticodon to the AUG codon. This anticodon/codon interaction leads to tighter binding of eIF4AI to 40S, dissociation of eIF1 from the 40S P-site, and a closing of the complex's conformation, causing it to 'lock' around the mRNA transcript (Lomakin *et al*, 2003, Unbehaun *et al*, 2004, Maag *et al*, 2005 and Maag *et al*, 2006). At this point, the 48S complex is formed.

Once the AUG codon has been selected, ribosomes must commit to that codon. This step is mediated by the eIF2-specific GTPase-activating protein (GAP) eIF5 (Pestova *et al*, 2007). eIF1's displacement allows for GTP hydrolysis of eIF2–GTP–Met-tRNA^{Met} complexes that are bound to 40S subunits (Paulin *et al,* 2001). GTP hydrolysis leads to partial

dissociation of eIF2–GDP from 40S subunits by reducing eIF2's affinity for Met-tRNA^{Met} (Kapp and Lorsch, 2004 and Pisarev *et al*, 2006).

Joining of the ribosomal 60S subunit is mediated by the ribosome-dependent GTPase eIF5B and eIF1A. An interaction between the C-terminal domains of eIF5B and eIF1A is required for efficient joining of the large 60S ribosomal subunit. Once this interaction has occurred, GTP hydrolysis by eIF5B is permitted and subsequent dissociation of eIF1, eIF1A, eIF3 and residual eIF2–GDP from assembled 80S ribosomes can occur (Olsen *et al*, 2003 and Marintchev *et al*, 2003).

Once the 80S ribosomal subunit has been assembled, translation of the mRNA and polypeptide synthesis can occur (reviewed in Jackson *et al,* 2010).

1.6.2. CAP-INDEPENDENT TRANSLATION

Another method of translational initiation occurs independently of the 5' cap structure, aptly named cap-independent initiation. In this case, the ribosome is recruited to areas of mRNA containing *cis*-acting regulatory elements termed internal ribosome entry sites (IRES's). IRES's are highly structured RNA elements that are present in the 5' UTRs of certain viral and cellular mRNAs. They were first discovered in encephalomyocarditis virus (EMCV) and poliovirus several decades ago (Jang *et al,* 1988 and Pelletier and Sonenberg, 1988).

Viral IRES's have been well characterized and classified into 4 groups: Type 1, Type 2, Type 3 and Type 4 (see Figure #2), each defined by how initiation occurs. For type 1 and type 2 IRES's, such as the poliovirus IRES and encephalomyocarditis virus (EMCV) IRES, respectively, the p50 domain of eIF4G binds directly to the IRES. This binding is enhanced by eIF4A (Pestova *et al,* 1996a/b and de Breyne *et al,* 2009). eIF4E is not required for recruitment of 43S complex (Wilson *et al,* 2007 and reviewed in Jackson *et al,* 2010). In type 3 IRES's, such as the hepatitis C virus IRES, the 43S complex is directly recruited to the AUG start codon without the use of eIF4F, eIF4B, eIF1 or eIF1A. This process is mediated through an interaction between the IRES, eIF3 and the small 40S ribosomal subunit (Pestova *et al,* 1998 and Siridechadilok *et al,* 2005). Type 4 IRES's, such as the cricket paralysis virus (CrPV) IRES, do not requires any eIFs or $tRNA_i^{Met}$; instead, the mRNA transcript forms a pseudo-tRNA structure and the small ribosomal subunit is directly recruited to the IRES (Schuler *et al*, 2006 and Wilson *et al,* 2007). In some cases, additional RNA-binding proteins known as IRES trans-acting factors (ITAFs) are required, likely for structural stabilization (Jackson, 2005)

Cellular IRES's are much more cryptic and poorly characterized. The first cellular IRES to be documented was the BiP IRES (Sarnow, 1989). The BiP IRES is located in the 5' untranslated region (UTR) of the mRNA encoding the BiP protein, also known as glucose-regulated protein

78 (GRP78). BiP is an immunoglobulin heavy-chain-binding protein and a member of the heat shock protein 70 family. It is proposed to be involved with of mediation of proper protein folding, assembly of nascent proteins, and scavenging of misfolded proteins in the ER (Bole *et al,* 1986 and Pelham *et al,* 1986). Although the BiP IRES has been shown to be capable of facilitating translation of BiP mRNA even when cap-dependent translation is inhibited (Sarnow, 1989) little is known about the molecular mechanism governing this phenomenon.

Although at least 85 other cellular IRESs have been described following the discovery of the BiP IRES (Baird *et al,* 2006), their very existence is a topic of debate and controversy in the field (Schneider *et al*, 2001 and Kozak, 2001/2005). The main criticisms in these reviews stem from the experimental design and subsequent interpretation of the results. In these experiments, putative IRES sequences are placed in between 2 reporter genes. Their ability to activate expression of the downstream reporter gene is generally accepted as evidence for IRES activity (see Chapter 2 for a detailed description of a bicistronic reporter system). However, a positive result in a bicistronic reporter system may not indicate the presence of a cellular IRES. Rather, generation of monocistronic RNAs or splicing due to the presence of a 3′ splice site (ss) or a cryptic promoter in the IRES sequence may explain the expression of the seemingly IRES-controlled reporter gene (Kozak, 2001/2005 and Van Eden *et al,* 2004). Perhaps not surprisingly, these alternate explanations

have lead to the discounting of many putative cellular IRES sequences (Kozak, 2001/2005, Van Eden *et al,* 2004 and Baranick *et al,* 2008). This contentious issue will be discussed further in Chapter 4.

1.7. THESIS RATIONALE

As a follow-up to the initial report from Elgadi and Smiley (1999) suggesting that certain IRES's could selectively target vhs to 3' flanking sequences, Saffran *et al* (2010) designed a series of experiments to determine if certain viral and cellular IRES elements were capable of modifying the susceptibility of mRNAs to vhs *in vivo*. To test this hypothesis, Saffran *et al* used bicistronic reporter constructs containing a 5' β-galactosidase (β-gal) cistron and a 3' chloramphenicol acetyltransferase (CAT) cistron driven from a common upstream HCMV IE promoter (pβgal/CAT). Different IRES sequences were inserted between these cistrons, including the cellular ApaF1, BiP, Dap5 IRES's and the viral EMCV IRES (wild-type) as well as mutant versions. As expected, vhs strongly inhibited expression of the 5' (cap-dependent) β-gal cistron. More surprisingly, vhs was found to be capable of strongly stimulating expression of the 3' (cap-independent) CAT cistron while under the influence of certain cellular IRES's, a mutant EMCV IRES and HSV 5′ UTR sequences (Saffran and Smiley, 2010).

The most striking activation in response to vhs was that which was driven from the putative cellular BiP IRES. The BiP IRES is located in the

5’ UTR of the mRNA encoding the BiP protein. BiP is a chaperone protein located in the endoplasmic reticulum, and is involved with stress response, specifically, the unfolded protein response (Kleizen and Braakman, 2004).

Saffran *et* al (2010) proposed that the observed vhs-dependent activation of 3’ CAT cistron activity while under the influence of the BiP IRES could be explained by one of two hypotheses: (1) vhs is promoting cap-independent translation by activating the BiP IRES, or (2) vhs is truncating the bicistronic mRNA, rendering it monocistronic. Initially, the former was favoured, as no change in RNA levels or structure could be detected in transient-transfection assays performed in HeLa cells (Saffran and Smiley, 2010). However, this observation does not rule out the latter hypothesis, especially given the uncertain nature of cellular IRES’s. Therefore, my project sought to determine which hypothesis is most correct.

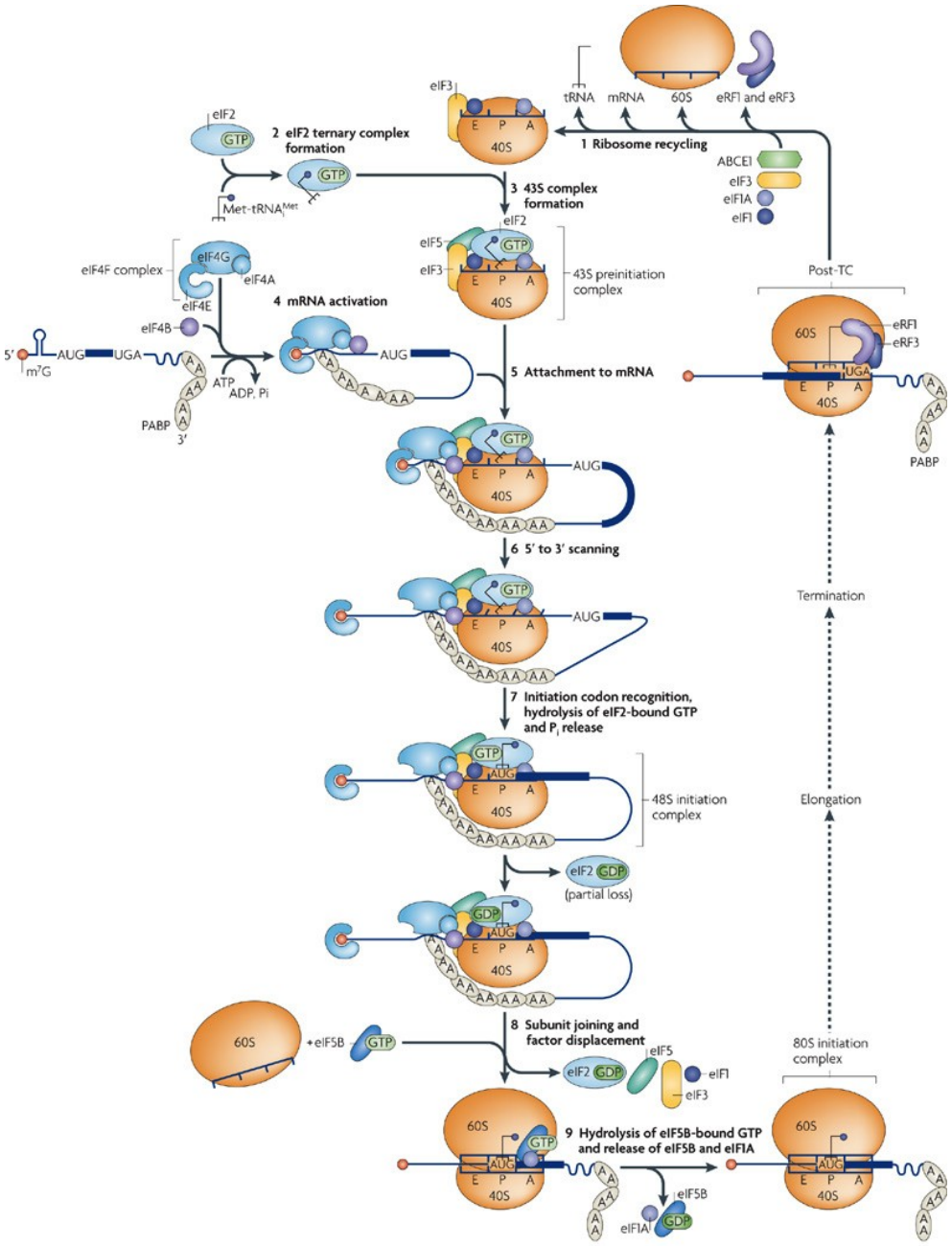

Figure 1: **Cap-dependent translation initiation**. Starting at top right: Ribosomal subunits are recruited from post translation complexes. The 43S complex is formed from the small 40S ribosomal subunit and initiation factors. The 43S complex is recruited to the 5' cap to bind the eIF4F cap-binding complex. The complex scans the length of the transcript until it reaches an start codon in the appropriate context, then, the Met-tRNA^{Met} anticodon binds the AUG start codon. The large 60S ribosomal subunit is then recruited, the 80S ribosomal subunit is formed and polypeptide synthesis can begin.

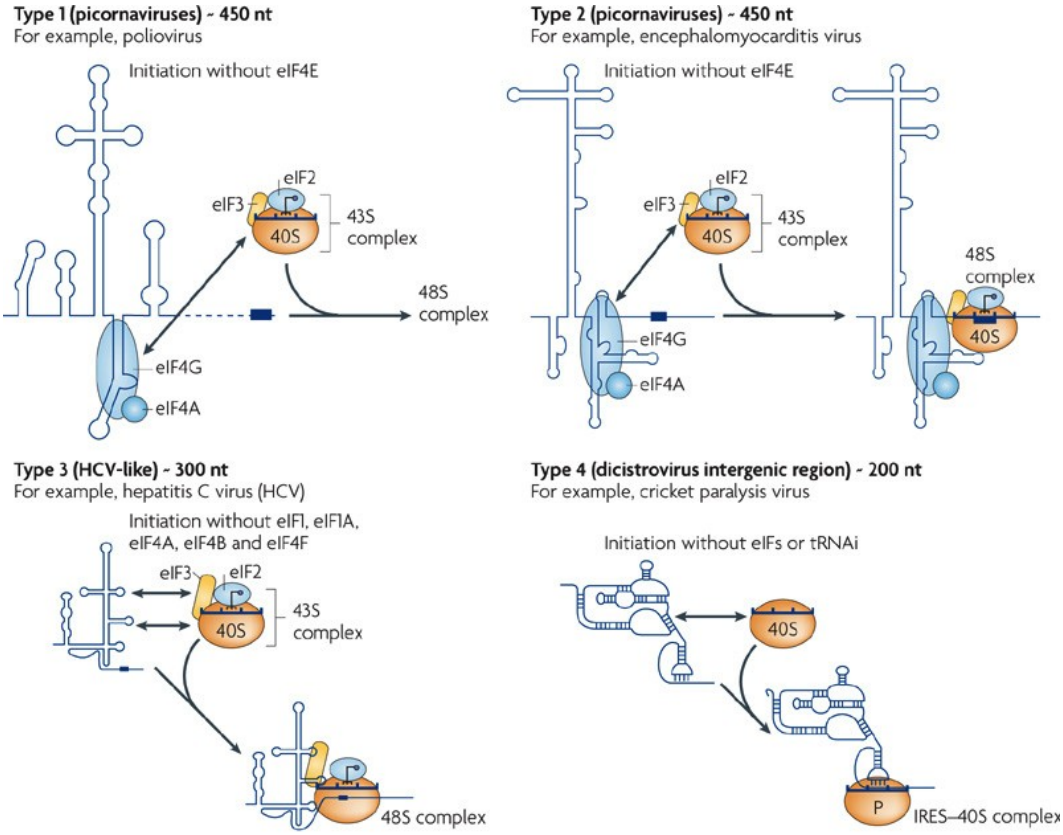

Figure 2: **Cap-independent translation initiation**. Shown are the 4 types of **viral** IRES's. Type 1 and 2 IRES's require the canonical initiation factors, but do not require the cap-binding eIF4E. Type 3 IRES's recruit the 40S ribosomal subunit through an association with eIF3 and other translation initiation factors. They do not require any proteins of the eIF4F cap-binding complex. Type 4 IRES's recruit the 40S ribosomal subunit directly without the need for translation initiation factors or $tRNAi^{Met}$.

The mechanism of initiation for the cellular BiP IRES is unknown.

CHAPTER 2: MATERIALS AND METHODS

2.1. PLASMIDS

See Table 1 for a complete list and description of all plasmid constructs used in this study. See Table 2 for oligonucleotide and primer sequences.

Bicistronic reporter plasmid constructs (pβgal/CAT and pβgal/BiP/CAT) and monocistronic reporter plasmid constructs (pCAT and pBiP/CAT) were obtained from Martin Holcik, University of Ottawa (Holcik *et al*, 1999). pβgal/CAT (10546 base pairs (bp) total) contains two independent reporter cistrons downstream of a common CMV promoter. The 3088 bp β-galactosidase (βgal) reporter cistron is located immediately downstream of the promoter and is therefore denoted the 5' cistron. In contrast, the 660 bp chloramphenicol acetyltransferase (CAT) cistron is located downstream of the 5' βgal cistron, and thus is denoted the 3' cistron. 310 bp separate the two cistrons. pβgal/BiP/CAT (10773 bp total) is virtually identical to pβgal/CAT with the exception of the intercistronic region. In the case of pβgal/BiP/CAT, 545 bp separate the two cistrons, and contains the BiP IRES sequence (221 base pairs). Both plasmids have multiple poly-adenylation (poly-A) signals following the 3' CAT cistron.

BiP IRES fragment mutants were fashioned from 2 complementary oligonucleotides (purchased from Integrated DNA Technologies (IDT, see Table 2). These oligonucleotides contain a portion of the BiP IRES

sequence and were annealed by combining complementary oligonucleotides at equimolar concentration in a buffer containing 10 mM Tris (pH 7.5–8.0) 50 mM NaCl, 1 mM EDTA. The mixture was immersed in boiling water and allowed to cool to room temperature. The annealed oligonucleotides were then digested with XhoI [New England Biolabs (NEB)] according to the manufacturer's instructions, to create a 5' overhang and ligated using T4 ligase (NEB; according to the manufacturer's instructions) into pβgal/CAT that had previously been digested with XhoI and treated with antarctic phophatase (NEB; according to the manufacturer's instructions). The BiP IRES fragment 1-88 was made by excision of a XbaI/PspXI fragment from pβgal/BiP/CAT by double digestion with XbaI/PspXI (NEB; according to the manufacturer's instructions). Open plasmid was then treated with DNA Polymerase I, Large (Klenow) Fragment (NEB; according to the manufacturer's instructions) to blunt the ends and re-ligated using T4 ligase (NEB; according to the manufacturer's instructions). The BiP IRES fragment 1/3 fusion was made by ligating (using T4 ligase, according to the manufacturer's instructions) the BiP fragment 3 oligonucleotides that had been previously annealed (as previously described) and digested with XhoI into pβgal/BiP1/CAT that had previously been digested with PspXI and treated with antarctic phosphatase (all as previously described).

The RNA aptamer pβgal/SC/CAT plasmid constructed using the highly structured sequence (referred to here as SC) described in Paige *et*

al (2011). In the context of the 2011 study by Paige *et al,* the SC RNA sequence (referred to as “Spinach” by the authors) was used to bind fluorophores, creating RNA-fluorophore complexes capable of emitting visible green fluorescence and subsequently used to image living cells. In the context of my experiments, this RNA sequence served as an ideal candidate to determine the contribution of structure to the observed increase in CAT activity, as it is highly structured (similar to the BiP IRES sequence) and not known to have any IRES activity. The pβgal/SC/CAT plasmid was constructed from 2 complementary oligonucleotides (IDT) containing the SC sequence were annealed and digested with XhoI (as previously described). They were then ligated into pβgal/CAT that had previously been digested with XhoI and treated with antarctic phosphatase (as previously described).

Hairpin (HP) constucts were constructed using the stem-loop sequence described by Attal *et al* (2000). The bicistronic HP construct pβgal/HP/CAT and the monocistronic construct pHP/CAT were made from 2 complementary oligonucleotides (IDT) containing the stem-loop sequence were annealed and digested with XhoI (as previously described). They were then ligated into pβgal/CAT or pCAT (respectively) that had previously been digested with XhoI and treated with antarctic phosphatase (NEB; according to the manufacturer’s instructions). The bicistronic HP construct pβgal/HP/BiP/CAT was generated by excising a portion of double stranded DNA containing the stem-loop sequence

followed by the BiP IRES sequence (HP/BiP, separated by a SexAI restriction site) from the pGOV4 plasmid vector (GeneOracle) using XhoI (NEB; according to the manufacturer's instructions). This fragment was then ligated into pβgal/CAT that had previously been digested with XhoI and treated with antarctic phosphatase (NEB; according to the manufacturer's instructions). The monocistronic pHP/BiP/CAT was made from 2 complementary oligonucleotides (IDT) containing the stem-loop sequence that were annealed and digested with either KpnI and HindIII (NEB; according to the manufacturer's instructions). They were then ligated into pBiP/CAT that had previously been digested with KpnI/HindIII and treated with antarctic phosphatase (NEB; according to the manufacturer's instructions).

The plasmid containing the SLII element (pD2EGFP-N1_3'SLII) was obtained from Brett Glaunsinger, University of California, Berkeley (Pijlman *et al*, 2008). To make the pβgal/SLII/BiP/CAT plasmid, a PmeI restriction site was introduced into pβgal/BiP/CAT via site-directed mutagenesis using the ©ClonTech In-Fusion® HD Cloning Kit (according to the manufacturer's instructions). The vector was then cut with PmeI to blunt the ends and treated with antarctic phosphatase (NEB; according to the manufacturer's instructions). The SLII element was then excised from pD2EGFP-N1_3'SLII using NotI, treated with DNA Polymerase I, Large (Klenow) Fragment to blunt the ends and ligated into the mutated pβgal/BiP/CAT plasmid using T4 ligase (NEB; according to the

manufacturer's instructions). pβgal/SLII/CAT was fashioned by excising the BiP IRES fragment from pβgal/SLII/BiP/CAT using XhoI restriction digestion (NEB; according to the manufacturer's instructions).

The Nsp1 effector plasmid (pcAGGGS_Nsp1-myc) was obtained from Dr. Shinji Makino, University of Texas Medical Branch (Makino *et al,* 2006).

The pMZS3F BGLF5-SPA effector plasmid was generated by Brett Duguay, by PCR of total cell DNA from B95-8 cells (Miller and Lipman, 1975) which are latently infected with EBV.

The pMZS3F SOX-SPA effector plasmid was generated by Shayla Duley by PCR from pCDEF3 SOX, which was donated by Brett Glaunsinger, University of California, Berkeley (Glaunsinger and Ganem, 2004).

Table 1: List and description of all plasmid constructs used in this study

Plasmid Name	**Description**	**Insert size (base pairs)**
pβgal/CAT (biCAT)	Bicistronic no IRES control	No insert
pβgal/BiP/CAT (biBiP)	Bicistronic with full length BiP IRES between cistrons	221
pβgal/EMCV/CAT (biEMCV)	Bicistronic with EMCV IRES between cistrons	502
pβgal/SC/CAT (biSC)	Bicistronic with RNA aptamer (SC) between cistrons	98
pβgal/BiP1/CAT (biBiP1)	Bicistronic with BiP IRES fragment 1 between cistrons	69
pβgal/BiP2/CAT (biBiP2)	Bicistronic with BiP IRES fragment 2 between cistrons	70
pβgal/BiP3/CAT (biBiP3)	Bicistronic with BiP IRES fragment 3 between cistrons	82

pβgal/BiP4/CAT (biBiP4)	Bicistronic with BiP IRES fragment 4 between cistrons	70
pβgal/BiP4/BiP4/BiP4/ CAT (biBiP4x3)	Bicistronic with BiP IRES fragment 4 (triplicated) between cistrons	222
pβgal/BiP4.1/CAT (biBiP4.1)	Bicistronic with BiP IRES fragment 4.1 between cistrons	34
pβgal/BiP5/CAT (biBiP5)	Bicistronic with BiP IRES fragment 5 between cistrons	70
pβgal/BiP5/BiP5/CAT (biBiP5x2)	Bicistronic with BiP IRES fragment 5 (duplicated) between cistrons	146
pβgal/BiP1-88/CAT (biBiP 1-88)	Bicistronic with first 88 basepairs of BiP IRES between cistrons	88
pβgal/BiP1_3/CAT (biBiP1/3)	Bicistronic with BiP IRES fragments 1 and 3 fused	157

pβgal/HP/CAT	Bicistronic with hairpin between cistrons	24
pβgal/HP/BiP/CAT (HP.BiP in biCAT)	Bicistronic with hairpin upstream of BiP IRES	24
pD2EGFP-N1_3'SLII	GFP reporter plasmid containing SLII element	81
pβgal/SLII/BiP/CAT (biSLII with BiP IRES or SLII with BiP IRES)	Bicistronic with SLII element upstream of BiP IRES fragment	81
pβgal/SLII/CAT (biSLII or SLII)	Bicistronic with SLII element between cistrons (no BiP IRES)	81
pCAT (monoCAT)	Monocistronic no IRES control	No insert
pBiP/CAT (monoBiP)	Monocistronic with BiP IRES between promoter and CAT cistron	221
pHP/CAT (HP in monoCAT)	Monocistronic with HP between promoter and CAT cistron	24
pHP/BiP/CAT (HP in	Monocistronic with HP	24

monoBIP)	upstream of BiP IRES	
pGOV4	Gene oracle cloning plasmid	258
pCDNA3.1	pCMV DNA “filler” plasmid for transfection	No insert
pUC19	Non-pCMV DNA “filler” plasmid for transfection	No insert
pCMVvhs (vhs)	Vhs effector plasmid	No insert
pcAGGGS_Nsp1-myc (Nsp1)	Nsp1 effector plasmid	No insert
pMZS3F BGLF5-SPA (BGLF5)	BGLF5 effector plasmid	No insert
pMZS3F SOX-SPA (SOX)	SOX effector plasmid	No insert

Table 2: List and sequence of all DNA oligonucleotides and primers used in this study. Embedded restriction sites used for cloning (see Materials and Methods for details) are shown in **bold**.

BiP1 (F)	GGG**CTCGAG**AGGTCGACGCCG GCCAAGACAGCACAGACAGATT GACCTATTGGGGTGTTTCGCGA GTGTGAGAGGGAA**CTCGAG**GGG
BiP1 (R)	CCC**CTCGAG**TTCCCTCTCACACT CGCGAAACACCCCAATAGGTCA ATCTGTCTGTGCTGTCTTGGCCG GCGTCGACCT**CTCGAG**CCC
BiP2 (F)	GGG**CTCGAG**GCGCCGCGGCCT GTATTTCTAGACCTGCCCTTCGC CTGGTTCGTGGCGCCTTGTGAC CCCGGGCCCCTGC**CTCGAG**GG G
BiP2 (R)	CCC**CTCGAG**GCAGGGGCCCGG GGTCACAAGGCGCCACGAACCA GGCGAAGGGCAGGTCTAGAAAT ACAGGCCGCGGCGC**CTCGAG**C CC
BiP3 (F)	GGG**CTCGAG**CGCCTGCAAGTCG AAATTGCGCTGTGCTCCTGTGCT ACGGCCTGTGGCTGGACTGCCT GCTGCTGCCCAACTGGCTGGCA AG**CTCGAG**GGG
BiP3 (R)	CCC**CTCGAG**CTTGCCAGCCAGT TGGGCAGCAGCAGGCAGTCCAG CCACAGGCCGTAGCACAGGAGC ACAGCGCAATTTCGACTTGCAGG CG**CTCGAG**CCC
BiP4 (F)	GGG**CTCGAG**GACCTATTGGGGT GTTTCGCGAGTGTGAGAGGGAA GCGCCGCGGCCTGTATTTCTAG ACCTGCCCTTCGC**CTCGAG**GGG
BiP4 (R)	CCC**CTCGAG**GCGAAGGGCAGGT CTAGAAATACAGGCCGCGGCGC TTCCCTCTCACACTCGCGAAACA CCCCAATAGGTC**CTCGAG**CCC
BiP5 (F)	GGG**CTCGAG**TCGTGGCGCCTTG TGACCCCGGGCCCCTGCCGCCT GCAAGTCGAAATTGCGCTGTGCT CCTGTGCTACGG**CTCGAG**GGG
BiP5 (R)	CCC**CTCGAG**CCGTAGCACAGGA GCACAGCGCAATTTCGACTTGCA GGCGGCAGGGGCCCGGGGTCA

	CAAGGCGCCACGA**CTCGAG**CCC
Hairpin (XhoI)	GGG**CTCGAG**GGCCGGGCGCGG CCGCGCCCGGCC**CTCGAG**GGG
Hairpin (XhoI) (RC)	CCC**CTCGAG**GGCCGGGCGCGG CCGCGCCCGGCC**CTCGAG**CCC
HP (KpnI/HindIII) F	**AGCTT**GGCCGGGCGCGGCCGC GCCCGGCC**GGTAC**
HP (KpnI/HindIII) R	**C**GGCCGGGCGCGGCCGCGCCC GGCC**A**
BiP4.1 (F)	GGG**CTCGAG**GCGAGTGTGAGAG GGAAGCGCCGCGGCCTGTATT**C TCGAG**GGG
BiP4.1 (R)	CCC**CTCGAG**AATACAGGCCGCG GCGCTTCCCTCTCACACTCGC**CT CGAG**CCC
HP.BiP	GGG**CTCGAG**GGCCGGGCGCGG CCGCGCCCGGCCACCAGGTAGG TCGACGCCGGCCAAGACAGCAC AGACAGATTGACCTATTGGGGTG TTTCGCGAGTGTGAGAGGGAAG CGCCGCGGCCTGTATTTCTAGA CCTGCCCTTCGCCTGGTTCGTG GCGCCTTGTGACCCCGGGCCCC TGCCGCCTGCAAGTCGAAATTG CGCTGTGCTCCTGTGCTACGGC CTGTGGCTGGACTGCCTGCTGC TGCCCAACTGGCTGGCAAG**CTC GAG**GGG
Mutagenic primer F	CGGGTATTATTTTTGCCGGTTTA AACCTATTTCTCTGTTCTCGC
Mutagenic primer R	GCGAGAACAGAGAAATAGGTTTA AACCGGCAAAAATAATACCCG
In-fusioncloning primer F	TATTTTTGCCGGTTTAAACAGAA AGTCAGGCCGGGAAG
In-fusioncloning primer R	CAGAGAAATAGGTTTAAACACCC AGTCCTCCTGGGGTT
CAT probe PCR primer F	CTTGCCCGCCTGATGAA
CAT probe PCR primer R	CACAAACGGCATGATGAACC
CATbac sequencing primer	GCTTCCTTAGCTCCTGAA
CATbac2 sequencing primer	AGCTGAACGGTCTGGTTA

2.2. BACTERIAL STRAINS AND GROWTH CONDITIONS

All plasmids were maintained and amplified in the electrocompetent *Escherichia coli* strain DH5α (Invitrogen). Unless otherwise indicated, all strains transformed with recombinant plasmids were cultured at 37°C in Luria-Bertani medium (LB; 1.0% Bacto Tryptone, 0.5% yeast extract, 1.0% NaCl, pH 7.0) containing 100µg ampicillin per mL in a shaker incubator set to 225rpm. The pD2EGFP-N1_3'SLII plasmid was cultured at 37°C in Luria-Bertani medium (LB; 1.0% Bacto Tryptone, 0.5% yeast extract, 1.0% NaCl, pH 7.0) containing 50µg kanomycin per mL in a shaker incubator set to 225rpm.

2.3. TRANSFECTIONS

HeLa cells in 24-well plates were transfected with specified bicistronic or monocistronic reporter plasmid, 'filler' plasmids pUC19 and pCDNA3.1, and effector plasmid of interest (pCMVvhs (50 ng), pMZS3F BGLF5-SPA (200 ng), pMZS3F SOX-SPA (200 ng) or pcAGGGS_Nsp1-myc (50 ng)) using Lipofectamine 2000 (Invitrogen; according to manufacturer's instructions). After 48 hours, cells were washed 2X with Phosphate buffered saline (PBS) (137mM NaCl, 2.7mM KCl, 8.1mM Na_2HPO_4, and 1.47mM KH_2PO_4, pH 7.4). Lysates were prepared using 200µL of 1X reporter lysis buffer (Promega).

β-Galactosidase and chloramphenicol acetyltransferase (CAT) assays (protocols detailed below) were then performed on portions of the lysates.

To perform RNA analyses, 6-well plates were again transfected with bicistronic reporter plasmids along with effector plasmid of interest (pCMVvhs, pMZS3F BGLF5-SPA, pMZS3F SOX-SPA or pcAGGGS_Nsp1-myc) using Lipofectamine 2000. After 48 hours, cells were washed 1X with PBS and treated with 1mL of TRIzol (Invitrogen). RNA extraction protocol is outlined below. Purification of poly(A)+ RNA was accomplished using an Oligotex mRNA mini kit (Qiagen) according to the manufacturer's instructions.

2.4. β-GALACTOSIDASE ASSAY

The protocol was performed as outlined by ProMega, available online at www.promega.com/tbs. In short, after treatment with 1X reporter lysis buffer, cells were scraped into 1.5mL microcentrifuge tubes. 50μL of this lysate was used. 100 μL of 1X reporter lysis buffer was added to bring volume up to 150μL. An equal volume (150μL) of 2X β-Galactosidase Assay Buffer [200mM sodium phosphate buffer (pH 7.3), 2mM MgCl2, 100mM β-mercaptoethanol and 1.33mg/ml ONPG (o-nitrophenyl-β-D-galactopyranoside, acts as substrate)] was added, and samples were incubated for 1 hour 30 minutes. After incubation, 500μL of sodium carbonate was added to terminate the reaction. The amount of yellow

product (β-Galactosidase hydrolyses colorless ONPG substrate, forming nitrophenol – a yellow product) was then quantified via spectrophotometer (Thermo Fisher) at 420nm.

2.5. CHLORAMPHENICOL ACETYLTRANSFERASE (CAT) ASSAY

Protocol was performed as outlined by ProMega, available online at www.promega.com/tbs. In short, after 50μL aliquot of lysate was removed for use in β-Galactosidase Assay, remaining lysate was heated to 65^{o}C for 10 minutes to inactivate any endogenous deacetylase activity. Heated lysates were spun at maximum speed in a microcentrifuge for 3 minutes, and supernatant collected. 1.5μL of [^{14}C]chloramphenicol (at 0.10mCi), 5 μL of n-Butyryl CoA, 50μL of supernatant (bicistronic) or 15μL of supernatant (monocistronic) and enough distilled water to reach a final volume of 125μL was added. Samples were incubated at 37^{o}C for 30 minutes (monocistronic) or 3 hours (bicistronic). To terminate the reaction, 300μL of mixed xylenes (Sigma Aldrich Cat.# 247642) was added. Samples were then vortexed thoroughly and spun at maximum speed in a microfuge for 3 minutes to ensure optimal phase separation. 280μL of the upper phase was transferred in 2 aliquots (140μL X 2) to a fresh 1.5mL microfuge tube. 100μl of 0.25M Tris-HCl (pH 8.0) was then added. Again, samples were vortexed thoroughly and spun at maximum speed in a microfuge for 3 minutes to ensure optimal phase separation. 200μl of the upper phase was transferred to a scintillation vial containing 5mL of

scintillation fluid (Ready-Safe™ scintillant, Promega). The amount of radioactive, butyrylated chloramphenicol product was then measured in a liquid scintillation counter as counts per minute (CPM).

2.6. RNA EXTRACTION AND PURIFICATION

After harvesting cell lystaes with TRIzol, total RNA was purified as follows. 200μL of chloroform was added, tubes were shaken vigorously by hand for 2-3 minutes, and spun at 12,000 × g in a microfuge for 10 minutes at 4°C. The colorless upper aqueous phase (containing the RNA) was then transferred to a fresh 1.5mL microfuge tube. Extraction was repeated with 600μL of chloroform, and aqueous phase again transferred to a fresh 1.5mL microfuge tube. Samples were then treated with 2μL of DNase I (Sigma-Aldrich) and incubated at 37°C for 30 minutes. 600μL of Isopropanol was then added, and samples were incubated at room temperature for 10 minutes to allow RNA to precipitate. Samples were then spun at 12,000 × g in a microfuge for 15 minutes at 4°C to allow for RNA pellet formation. The supernatant was then carefully aspirated using a pipette. RNA pellet was then washed with 1mL of 70% ethanol and spun at 4500 × g in a microfuge for 5 minutes. The supernatant was then again carefully aspirated using a pipette and the pellet left to air dry until no traces of ethanol remained, approximately 10-15 minutes. 50μL of DEPC-treated distilled water was added and pellet was resuspended by freezing at -80°C, heating to 60°C for 10 minutes and vortexing vigorously. The

amount of RNA was then quantified using a NanoDrop spectrophotometer (Thermo Fisher).

2.7. NORTHERN BLOT ANALYSIS

Appropriate amounts of purified RNA samples were combined with formamide, formaldehyde, RNA loading buffer (50% glycerol, 1mM EDTA, 10mg of xylene cyanol/mL and 10mg of bromophenol blue/mL) and 1X MOPS, then incubated at 60^{o}C for 15 minutes, placed on ice and spun briefly in a microfuge. Samples were then electrophoresed through a 1.2% agarose-formaldehyde gel in 10% 1X MOPS buffer at 100V for approximately 2 hours. RNA was then transferred overnight to a GeneScreen membrane (NEN Life Sciences Products) in 10X Saline-Sodium Citrate (SSC; 1.5M sodium chloride and 150mM sodium citrate) buffer. The membrane was then UV-cross linked (2X).

The GFP probe was made by gel extraction of a Not1/AflII fragment cut from the pD2EGFP-N1_3'SLII plasmid (NEB; digest according to the manufacturer's instructions). The probe was then radiolabeled with ^{32}P by random priming. Briefly, 250ng of the CAT gene amplicon was added to 2µg of random DNA hexamer and adjusted to a volume of 35µL with distilled water. The mixture was heated to 98°C for 4 minutes, then placed on ice for 2 minutes and spun briefly in a microfuge. Next, 7µL of Oligo Labeling Buffer (250µL 2M Tris (pH 8), 50µL 1M $MgCl_2$, 7.2µL 2-mercaptoethanol, 2µL 100 mM dGTP, 2µL 100 mM dATP, 2µL 100 mM

dTTP, 10282μL 2M HEPES (pH 6.6) and 248μL distilled water), 2μL of 100X BSA, 1μL Klenow (NEB) and an appropriate amount of α-^{32}P dCTP (either 5μL or 10μL, depending on age of radioactivity) was added and the mixture incubated at 37°C for 30 minutes. The volume was then adjusted to 100μL using TE buffer (10mM Tris and 1mM EDTA, ph 8). A phenol/chloroform extraction was then performed by adding 100μL of phenol:chloroform:isoamyl alcohol (25:24:1) saturated with 10mM Tris (ph 8) and 1mM EDTA (Sigma), mixing thoroughly and spinning for 5 minutes at room temperature. A GE Heathcare illusta™ NICK™ column (Sephadex™ G-50 DNA Grade) was equilibrated with 3mL TE buffer, then 100μL of the upper phase of the sample was added. The column was washed with 400μL of TE buffer and sample was eluted in 500μL of TE buffer.

Hybridizations were done using ExpressHyb (Clontech) according to the user's manual. Briefly, ExpressHyb Solution was warmed to 68°C to dissolve any precipitate. Prehybridization was performed using 5mL of warmed ExpressHyb solution for 30 min at 68°C on a rotational shaker. The CAT probe was incubated at 95°C for 15 minutes in a heat block to denature, added to the prehybridization solution at a concentration of 10^7 CPM/mL, and then incubated for 1 hour at 68°C on a rotational shaker. The membrane was then washed with Wash Solution 1 (2X SSC and 0.05% SDS) with several changes for 30-40 minutes at room temperature on a rotational shaker. The membrane was then washed with Wash

Solution 2 (0.1X SSC and 0.1% SDS) with 1 change for 40 min at 50°C on a rotational shaker. The membrane was then exposed to Kodak BioMax MS film at room temperature overnight. The data were then evaluated using a Phosphoimager.

2.8. WESTERN BLOT ANALYSIS

Levels of the 26 kilodalton CAT protein were assessed by western blot. HeLa cells were transiently transfected with appropriate reporter plasmid (bicistronic pβgal/BiP/CAT or monocistronic pBiP/CAT) and effector plasmid (pCMV vhs). Cell lysates were harvested using 1X reporter lysis buffer as described above. A 15% SDS-PAGE polyacrylamide gel was prepared as follows; *stacking gel*: 0.72mL water, 0.125mL 40% acrylamide, 0.13mL 1M Tris (pH 6.8), 0.01mL 10% SDS, and 0.01mL 10% APS and 0.001mL TEMED and *separating gel*: 2.8mL water, 0.75mL 40% acrylamide, 1.3mL 1M Tris (pH 8.8), 0.05mL 10% SDS, and 0.05mL 10% APS and 0.004mL TEMED. 5X protein sample buffer (200 mM Tris-HCl [pH 6.8], 5% SDS, 50% glycerol, 1.43 M β-mercaptoethanol) was added to lysate and 10μL was loaded into stacking gel.

The gel was run in 25 mM Tris base, 190 mM glycine and 0.1% SDS running buffer at 100V until the sample entered the separating gel. The voltage was then increased to 150V until the bromophenol blue had run to the bottom of the separating gel (1-1.5 hours). The samples were

then transferred to a nitrocellulose membrane (Hybond ECL; GE Healthcare) using a semi-dry transfer apparatus (Tyler Instruments) using a transfer buffer consisting of 48mM Tris, 39mM glycine, 20% methanol and 0.04% SDS. The semi-dry transfer apparatus was run for 45 minutes at 0.45 A. Membrane was then blocked in Odyssey blocking buffer (Li-COR) and TBST buffer (Tris-buffered saline (1:1) containing 0.1% Tween 20) for 1 hour at room temperature. Primary antibodies (rabbit polyclonal anti-chloramphenicol acetyltransferase (10µg/mL; abcam) and mouse anti-actin (1:5000 dilution; Sigma) were incubated with membrane in 1:1 Odyssey buffer:TBST at 4°C overnight. The membranes were then washed in TBST 3 times for 5 minutes each wash. Secondary antibodies (Alexa Fluor 680 goat anti-rabbit (Invitrogen) and Anti-mouse IgG IRDye800 (Rockland); both at 1:10000) were incubated with membrane in 1:1 Odyssey buffer:TBST at room temperature for 1 hour. The membranes were again washed in TBST buffer 3 times for 5 minutes each wash. Levels of CAT protein were then detected using an Odyssey infrared imaging system (Li-COR).

CHAPTER 3: RESULTS

3.1 VHS REPRESSES 5’ β-GALACTOSIDASE ACTIVITY AND STIMULATES 3’ CAT CISTRON ACTIVITY IN A BICISTRONIC REPORTER

As mentioned in Chapter 1, this laboratory has previously reported that in transiently transfected HeLa cells, a vhs expression plasmid has opposing effects on a bicistronic reporter plasmid bearing a intercistronic BiP IRES sequence (Saffran *et al*, 2010). In this report, Holly Saffran noted that the addition of vhs caused a marked decrease in 5’ β-galactosidase (β-gal) cistron activity. Given the known shutoff activity of vhs, this observation is not surprising. However, Holly also observed a substantial increase in 3’ chloramphenicol acetyltransferase (CAT) cistron activity after addition of vhs, which was unprecedented (Saffran *et al*, 2010).

Holly proposed that this effect could be attributed to at least two distinct hypotheses; (1) IRES activation or (2) RNase activity. More specifically, the IRES activation hypothesis (1) predicts that vhs stimulates the ability of the BiP IRES to promote internal initiation of translation from the intact bicistronic mRNA, resulting in expression of the CAT cistron. The RNase activity hypothesis (2) predicts that vhs activates the 3' CAT cistron by cleaving near the 5' end of the RNA (as previously described) upstream of the lacZ gene, followed by 5' to 3' degradation mediated by vhs and/or cellular exoribonucleases, leading to transient production of

uncapped monocistronic mRNA encompassing the 3' CAT cistron. Evidence for both of these processes has been previously published (Gaglia *et al*, 2010). According to this model, the BiP IRES enhances 3' cistron expression by (1) enhancing cap-independent translation of the 3' degradation product, or (2) by hindering its 5' → 3' decay, or (3) by a combination of both mechanisms. In an attempt to determine which was most likely, Holly analyzed a series of shutoff-null vhs mutants, as well as attempted to detect any monocistronic RNA generated by removal of the preceding 5' cistron. Holly was able to correlate the shutoff activity of vhs with its ability to activate the 3' CAT cistron; however, monocistronic RNA could not be detected. The absence of any detectable monocistronic RNA lends support for the IRES activation hypothesis. Moreover, no substantial loss of intact bicistronic RNA was found, despite the decrease in β-gal expression following addition of vhs. This lead Holly to speculate that vhs was inhibiting cap-dependent translation of the 5' cistron, thus stimulating 3' cistron activation by freeing up translation initiation factors and allowing them to be recruited to the IRES. Thus, Holly concluded that vhs was somehow provoking IRES activity and subsequent translation of the CAT RNA.

Although this conclusion was tentative at best, the link between vhs and translation is evident; subsequent studies have found that during lytic infections, vhs stimulates translation of certain viral true late RNAs (Dauber *et al*, 2011) and that mutations in mRNA that affect its translation

also affect the location of vhs cut sites (Shiflett and Read, 2013). Despite this obvious link, it is still unclear whether or not vhs-dependent IRES stimulation is responsible for the CAT activation. A lack of evidence for the generation of monocistronic RNA containing the CAT ORF (generated by degradation of the 5' cistron) does not confirm the IRES activity hypothesis.

My project began with an attempt to replicate and confirm the results obtained by Holly (Saffran *et al,* 2010); specifically, show a vhs-induced repression of the 5' β-gal cistron and activation of the 3' CAT cistron. To do this, HeLa cells were transiently transfected with a fixed amount of the appropriate bicistronic reporter plasmid (biBiP; described in Chapter 2) and increasing amounts of a vhs effector plasmid (pCMVvhs; Figure 3, described in Chapter 2). After 48 hours, the lysates were harvested and portions were assayed for β-gal and CAT activity by analyzing enzymatic activity as described in Chapter 2. In agreement with the results of Saffran *et al* (2010) the addition of vhs strongly reduced β-gal activity, and this effect was dose-dependent (Figure 4); as the amount of vhs increased, the amount of β-gal activity decreased. One interpretation of these data is that the 5' β-gal cistron is degraded by vhs, another that vhs represses translation of the 5' cistron. These two possibilities will be discussed further in subsequent sections. Also in agreement with the results of Saffran *et al* (2010), I saw a substantial increase in 3' CAT activity after the addition of vhs. As shown in Figure 5,

CAT activity increases as the amount of vhs increases, up until a point (in this case > 50 ng of vhs expression plasmid). It is possible that at low-to-moderate concentrations, vhs acts as an activator, but in high concentrations vhs instead functions as an inhibitor. However, in all subsequent experiments, 50 ng of vhs expression plasmid was added; this amount was determined from the dose curves (Figure 4 and Figure 5) to be effective at reducing β-gal activity. Note, the data used to generate Figures 4 and 5 were obtained from separate experiments; each is a representative of multiple repetitions (20+) performed over the course of my study.

I also tested additional bicistronic reporter constructs for β-gal activity as described above; including constructs with no IRES between cistrons (biCAT), an EMCV IRES or non-IRES RNA aptamer in between cistrons (biEMCV or biSC respectively), a variety of BiP IRES fragments and constructs containing hairpins and nuclease blocking elements in the intercistronic region. A complete list of all constructs tested is shown in Table 1. With all constructs tested, the addition of vhs repressed β-gal activity. A representative experiment showing the effect of vhs on β-gal activity on the no IRES control (biCAT), wild-type BiP IRES (biBiP) and 5' BiP IRES fragment (biBiP1) is depicted in Figure 6. With all three constructs, the β-gal cistron was effectively translated in the absence of vhs, as evidenced by the high levels of β-gal activity. After the addition of vhs, levels of β-gal were markedly decreased. As mentioned, this effect

was consistent in all constructs tested and confirmed the results reported in Saffran *et al* (2010). Due to the consistency of this vhs-induced β-gal repression, only the effect on the 3' CAT cistron will be discussed for the majority of the subsequent experiments.

3.2 CAT ACTIVITY IS MOST STRONGLY STIMULATED BY VHS IN BICISTRONIC REPORTER CONSTRUCTS CONTAINING THE BIP IRES

As mentioned above, the effect of vhs on the 5' β-gal cistron was not surprising considering the shutoff activity of vhs. The surprising result described in Saffran *et al* (2010) and confirmed in my study was the effect of vhs on the 3' CAT cistron. Specifically, CAT activity is stimulated by the addition of vhs when the BiP IRES is located in the intercistronic region of the reporter plasmid. When the BiP IRES was not present, this substantial increase in CAT activity did not occur. This experiment was repeatedly replicated in my study by transiently transfecting HeLa cells with either biCAT (no IRES control) or biBiP (BiP IRES in between cistrons) in the presence and absence of 50 ng of the vhs expression plasmid. The lysates were then harvested and CAT activation was assessed as described in Chapter 2. Consistent with the results obtained in Saffran *et al* (2010), the addition of vhs resulted in a substantial increase in CAT activity in the biBiP reporter (Figure 7). Specifically, an average 10 fold increase in CAT activity was seen after addition of the vhs expression plasmid while under the influence of the BiP IRES. This effect was both

highly reproducible and statistically significant as determined by a 2-tailed, paired t-test assuming normal distribution ($p = 2.7 \times 10^{-12}$). In the absence of the BiP IRES (biCAT), an average 2.6 fold increase in CAT activity is observed after addition of vhs. Although much less substantial, this increase was also highly reproducible and statistically significant ($p = 2.7 \times 10^{-5}$). This vhs-induced CAT activation in the no IRES control (biCAT) was noted in the original report by Saffran *et al* (2010), however its relevance was not apparent. Due to the large number of replicates performed in my study, I am sufficiently confident that this increase is relevant. This will be further discussed in subsequent sections.

In the absence of vhs, the presence of the BiP IRES increased CAT activity by approximately 1.6 fold relative to the biCAT control. This effect was highly reproducible and also determined to be statistically significant ($p = 3.5 \times 10^{5}$). This increase may reflect the putative inherent IRES activity of the BiP IRES; the fact that it was determined to be significant lends support to the hypothesis that IRES activity may be at least partially responsible for the CAT cistron activation. Alternatively, a splice site (ss) or cryptic promoter located in the BiP IRES sequence could also explain this increase. If this were the case, the CAT mRNA could be translated and CAT expressed independently of IRES activity. Specifically, a promoter located in the IRES sequence could direct transcription of the downstream message, or a 3' ss in the IRES could result in the 5' cistron

being spliced out, resulting in a monocistronic transcript encompassing the CAT mRNA.

As noted in subsequent sections (3.4) this BiP IRES-dependent increase in CAT activity in the absence of vhs was not noted in all experiments. However, it is likely that low n-values and general experimental variation are responsible for a lack of significance. In most experiments, 3-4 replicates were used to generate statistically relevant data; this is in comparison to the 13 replicates used in the case of Figure 7. Regardless, the increase observed both in this case (biCAT vs. biBiP without vhs) and after addition of vhs for the no IRES control (biCAT with and without vhs) are much less pronounced than that observed for the reporter containing the BiP IRES after addition of vhs (biBiP with and without). More discussion into the relevance of these differences will follow.

To summarize, vhs has been shown both in published reports (Saffran *et al,* 2010) and in my study to be capable of strongly stimulating CAT expression in a bicistronic reporter containing the BiP IRES. What is still unclear is role of vhs and the BiP IRES and the mechanism by which this occurs. All ensuing experiments were designed to answer these questions.

3.3 VHS DOES NOT ACTIVATE CAT EXPRESSION IN BICISTRONIC REPORTER CONSTRUCTS BEARING THE EMCV IRES OR A NON-IRES RNA APTAMER

The report by Saffran *et al* (2010) also examined the effect of vhs on expression by the EMCV IRES. They reported that in contrast to the BiP IRES, CAT activity was high in the absence of vhs and declined after addition of the vhs expression plasmid. This result was confirmed in my study, using the experimental methods described previously. As expected, cap-independent, EMCV IRES-driven translation resulted in high levels of CAT activity in absence of vhs (Figure 8). This activity was significantly higher than that observed for the no IRES construct (biCAT) and the BiP IRES construct (biBiP) in the absence of vhs ($p = 6.9 \times 10^{-5}$ and 1.3×10^{-5} respectively). Specifically, levels of CAT activity for the EMCV IRES reporter construct (biEMCV) were 8.5 higher than biCAT (no IRES) and 4.8 fold higher than biBiP (BiP IRES).

The differences between the BiP IRES and the EMCV IRES are further highlighted after addition of vhs; for biEMCV, CAT activity is substantially repressed after addition of vhs. Specifically, the addition of vhs results in an approximate 3 fold reduction in CAT activity (Figure 8). This repression is distinctly different from the vhs-induced activation observed for both the BiP IRES construct (biBiP) and the no IRES construct (biCAT). These differences demonstrate that vhs does not activate all IRES elements, and indicate that the BiP IRES has

characteristics that are not present in the EMCV IRES that are responsible for its activation by vhs. One interpretation is that this uniqueness is a function of the specific structure of the BiP IRES RNA; it is widely known that the structural complexity of IRES RNA contributes to its activity (reviewed in Chapter 1).

As another test of this conclusion, I examined the effect of a highly structured non-IRES aptamer sequence. This RNA sequence was originally used by Paige *et al* (2011) to image RNA in live cells. In my case, I cloned the RNA sequence into the intercistronic region of biCAT (described in detail in Chapter 2) and thus created a reporter plasmid (deemed biSC) containing the non-IRES RNA sequence in place of the BiP IRES. This biSC reporter was then transiently transfected into HeLa cells and CAT activation was assessed as previously described.

As shown in Figure 9, the non-IRES RNA sequence does not support CAT translation in the absence of vhs; levels of CAT activity are similar for all three constructs (biCAT, biBiP and biSC) in the absence of vhs. As previously noted in section 3.2 (Figure 7), a significant increase in CAT activity can be attributed to the BiP IRES in the absence of vhs (biCAT vs. biBiP; $p = 0.04$) in this experiment. Conversely, no significant increase could be attributed to the RNA aptmer (biCAT vs. biSC; $p = 0.09$). After addition of vhs, no significant increase in CAT activity is observed for the biSC construct ($p = 0.17$); this in contrast to the striking increase once again observed for the BiP IRES construct (biBiP). These

data suggest that vhs-induced CAT activation is dependent on the presence of the BiP IRES specifically, not just any IRES or highly structured RNA sequence.

3.4 FRAGMENTATION OF THE BIP IRES DOES NOT DESTROY ITS ABILITY TO STIMULATE CAT EXPRESSION

As mentioned above, substantial levels of vhs-induced CAT activation are dependent on the presence of an intercistronic BiP IRES. Neither the EMCV IRES nor a highly structured, non-IRES RNA sequence elicits the same response, indicating something specific about the BiP IRES is responsible for the observed CAT activation. In an effort to determine if a specific region of the BiP IRES sequence contributes more than others to the vhs-dependent CAT activation, an attempt to map the BiP IRES was undertaken.

3.4.1 5 PARTIALLY OVERLAPPING FRAGMENTS (biBIP 1-5)

Initially, 5 partially overlapping fragments of the BiP IRES were constructed and analyzed; this was done to avoid any end-effects and encompass all regions of the IRES sequence (Figure 10; specific details of the fragment construction are outlined in Chapter 2). Briefly, oligonucleotides containing the fragment sequence were annealed and cloned into a bicistronic biCAT reporter vector at the intercistronic XhoI site. These fragment constructs (named biBiP 1-5, Figure 10) were then

transiently transfected into HeLa cells and CAT activity was assayed as described previously. Fragments tested in a single experiment are shown together; i.e., biBiP 2-4 were assayed together (Figure 12) while biBiP 1 and biBiP 5 were assayed in separate experiments (Figures 11 and 13 respectively).

As shown in these figures, none of the fragment constructs support significant levels of CAT translation in the absence of vhs (Figures 11-13; $p < 0.05$ in all cases). Instead, levels of CAT activity in the absence of vhs were similar for all 5 BiP IRES fragment reporter constructs as well as for the no IRES control (biCAT) and the full-length BiP IRES reporter (biBiP). Thus, no significant increase in CAT activity could be attributed to the full-length BiP IRES in the absence of vhs (biCAT vs. biBiP; $p < 0.05$ in all cases) in these experiments. This result is not consistent with the results obtained in prior experiments (for example, comparison of biCAT to biBiP in Figure 7 and Figure 9). To reiterate, in these experiments significant increases in CAT activity could be attributed to the BiP IRES, as CAT expression for biBiP was significantly greater than that for biCAT (no BiP IRES) in the absence of vhs. As mentioned previously (section 3.2), I believe these discrepancies are due to experimental variation and low n-value in the cases where no significant was achieved.

After addition of vhs, all 5 fragment reporter constructs are capable of stimulating CAT activity. In all cases, the vhs-induced CAT activation was highly reproducible and determined to be statistically significant (biBiP

1-5 with vs. without vhs; p = 0.0012, 0.00022, 0.00076, 0.00093 and 3.6 x 10^-5). Additionally, this activation in response to vhs was significantly greater than the no IRES control (biCAT vs. biBiP 1-5 with vhs; p = 0.0064, 0.00085, 0.0046, 0.0085, 0.00027). However, for all these fragments, CAT activity was significantly lower than that observed for the full length BiP IRES ($p < 0.05$ in all cases). Consequently, response to vhs could not be mapped to any specific region of the IRES based on the data acquired thus far. Rather, activity appears to be distributed across the sequence.

3.4.2 ADDITIONAL BIP IRES FRAGMENTS (biBiP 4.1, 1-88, 5x2, 1/3 and 4x3)

Next, several additional fragments of the BiP IRES were constructed and assayed as previously described. Listed from shortest to longest these were; a shortened version of biBiP 4 (4.1), a longer version of biBiP 1 (biBiP 1-88), a duplicated version of biBiP 5 (biBiP 5x2), a BiP fragment 1 and 3 fusion (biBiP 1/3) and a triplicated version of biBiP 4 (biBiP 4x3). A schematic representation of these fragments is shown in Figure 14. Again, fragments tested in a single experiment are shown together; i.e., biBiP 1-88 and biBiP 1/3 were assayed together (Figure 16) and biBiP 4.1, biBiP 5x2 and biBiP4x3 were assayed in separate experiments (Figure 15 and 17-18 respectively).

None of the aforementioned fragment constructs supported significant levels of CAT translation in the absence of vhs (biCAT vs. biBiP 4.1, 1-88, 5x2, 1/3 or 4x3; $p < 0.05$ in all cases). However, these data are difficult to interpret, as a significant increase in CAT activity could be attributed to the full-length BiP IRES (biCAT vs. biBiP) in some but not all experiments. In the case of Figure 15 (analysis of biBiP 4.1; $p = 0.002$), Figure 16 (analysis of biBiP 1-88 and 1/3; $p = 0.04$) and Figure 18 (analysis of 4x3; $p = 0.0003$) significance was achieved. However, no significant increase in CAT activity could be attributed to the BiP IRES (biCAT vs. biBiP) in Figure 17 (analysis of biBiP 5x2; $p = 0.9$). As previously noted, experimental variation explains why this particular experiment did not achieve significance while other did. In the cases where significance is achieved, it is possible to conclude that fragmentation of the BiP IRES does eliminate the ability of the BiP IRES to activate CAT expression in the absence of vhs. However, this conclusion is tentative at best, considering the dependence on high n-values to get statistically reliable data.

Conversely, all additional fragments of the BiP IRES showed a reproducible and significant increase in CAT activity after addition of vhs. The shortest fragment (biBiP 4.1, Figure 15) was the closest to the no IRES control; although the amount of vhs-induced activation achieved significance (biBiP 4.1 with vs. without vhs; $p = 0.0041$), the activation was minimal in comparison to the other, longer, fragments (only about 2.4 fold

increase after addition of vhs). However, this activity was significantly greater than the no IRES control (biCAT vs. biBiP 4.1 with vhs; p = 0.041). All of the longer fragments showed substantial and significant levels of CAT activation after addition of vhs; biBiP 1-88 (p = 0.0012), biBiP 1/3 (p = 0.00054), biBiP 4x3 (p = 0.00071) and biBiP 5x2 (p = 0.00091). Additionally, all of these differed significantly from the no IRES control (biCAT vs. biBiP construct with vhs; biBiP 1-88 (p = 0.0028), biBiP 1/3 (p = 0.0008), biBiP 4x3 (p = 0.00058) and biBiP 5x2 (p = 0.0021). The fragment 1 and 3 fusion (biBiP 1/3, Figure 16) differed very little from the full-length BiP IRES in terms of the level of CAT activity after addition of vhs, even though the entire middle region of the IRES sequence had been deleted. The other longer fragments (biBiP 1-88, biBiP 5x2 and biBiP 4x3, Figures 16, 17 and 18 respectively) also showed substantial levels of CAT activation in the presence of vhs, however activity was reduced by about half from that observed for the full-length BiP IRES.

The data presented above suggest a correlation between length of the intercistronic BiP IRES sequence and the amount of vhs-dependent CAT activation. The identity of the sequence does not appear to have any effect on the amount of CAT activation, as duplicate, triplicate and fusion fragments showed similar increases in CAT activity in response to vhs. Thus, although activity could not be mapped to a specific region of the BiP IRES, it is apparent that the length of the RNA sequence does have an effect. One interpretation is that the increased length of the IRES

sequence results in increased structural complexity. Although the data obtained from the non-IRES aptamer (biSC) construct suggested that the contribution from structure alone is negligible, it is possible that within the context of the BiP IRES sequence, structural complexity is important. Another interpretation is that each of the 5 original BiP IRES fragments (biBiP 1-5) contains one or more response elements within their sequence. If this were the case, tandemizing these elements (as in biBiP 5x2 and biBiP 4x3) would increase the number of response elements and thus the response to vhs. Regardless, the relative contribution of sequence and structure in the context of the BiP IRES is still unclear; all of the fragments, regardless of length, show reproducible and significant CAT activation in the presence of vhs.

Assuming that the IRES ability of the BiP IRES is involved in stimulating CAT expression in response to vhs, these data are profoundly different from what occurs after alterations to other IRES sequences, such as the EMCV IRES or the Poliovirus IRES. In these cases, even small (1-2 nucleotide) deletions or insertions completely obliterate IRES activity (Svitkin *et al*, 1985, Kuge and Nomoto, 1987, Trono *et al*, 1988 and Van Der Velden, 1995). The cause of this discrepancy in unclear; however, unlike the putative cellular BiP IRES, these viral IRES are well characterized and *bonafide* IRES's (Pestova *et al,* 1996a/b and de Breyne *et al,* 2009). This is confirmed in the context of my study (Figure 8); EMCV is capable of strongly stimulating CAT expression in the absence of vhs,

indicating it does indeed function as an IRES to stimulate cap-independent translation. Additionally, the EMCV IRES has previously been confirmed to have IRES activity through alternative methods (for example, see Elroy-Stein *et al,* 1989).

Although the BiP IRES is also capable of stimulating CAT expression in the absence of vhs, the magnitude is much smaller than that for the EMCV IRES. In fact, as noted and discussed previously (section 3.2-3.4) in several of the experiments this significant increase in CAT expression attributed to the BiP IRES does not occur. Although this is most likely due to experimental variation and low n-values, this inconsistency makes these data difficult to interpret. For example, if we assume this BiP IRES-dependent increase is real, then fragmenting the BiP IRES did kill its ability to activate CAT expression (as none of the fragments were capable of activating a significant levels of CAT activity in the absence of vhs). However, although this would be in agreement with the previously mentioned literature on IRES fragmentation, it is impossible to make this conclusion based on these data. Thus, it is currently unclear if the BiP IRES is actually functioning as an IRES in the context of this experiment. It is clear that the sequences with the ability to activate 3' cistron expression appear to be evenly distributed throughout the BiP IRES sequence. Additionally, not all IRES sequences or structured RNA sequences have this ability. However, these data do not address the mechanism of 3' cistron activation and do little to distinguish between the

two models (IRES activity vs. RNase activity). Thus, subsequent experiments were designed to address these issues.

3.5 MONOCISTRONIC CONSTRUCTS EXHIBIT MUCH GREATER LEVELS OF CAT EXPRESSION IN THE ABSENCE OF VHS THAN THEIR BICISTRONIC COUNTERPARTS

As noted in section 3.3, the activity of the BiP IRES in the bicistronic construct (biBiP) in the absence of vhs is much smaller than that for the EMCV IRES. In fact, in some experiments this low level of activity was not even statistically significant (discussed in section 3.4). Thus, it is questionable whether this low level of activity in actually due to internal initiation; perhaps instead it is due to the unintentional production of monocistronic RNAs via splicing, cryptic promoter activity or RNA breakage. In addition, the BiP IRES is normally found in the 5' UTR of monocistronic BiP mRNA, not in an intercistronic location (as it is in the biBiP construct). Thus, assessment of the activity of the BiP IRES sequence and its response to vhs in monocistronic constructs was of great importance. These results could then be compared to those obtained using the bicistronic reporters.

3.5.1 MONOBIP VS. BIBIP

Firstly, a monocistronic construct containing the BiP IRES upstream of the CAT cistron (monoBiP; see Figure 19) was assayed for CAT activity in the absence of vhs as previously described and compared to its bicistronic counterpart (biBiP). As shown in Figure 20, the BiP IRES is much more active in the monocistronic construct (monoBiP). Specifically, levels of CAT expression in the absence of vhs are 97 fold higher than the bicistronic no IRES control (biCAT) and 50 fold higher than the bicistronic BiP IRES reporter (biBiP). Although this difference in striking, it is unclear how much traditional cap-dependent translation is contributing to this activity. Thus, monoBiP was compared to its monocistronic IRES-less partner (monoCAT; see Figure 19).

3.5.2 MONOBIP VS. MONOCAT

As shown in Figure 21, significantly more CAT expression is driven from the monoBiP construct than the monoCAT construct ($p = 0.00008$). Given the only difference in the two constructs is the presence of the BiP IRES, it appears as if the IRES is conferring the additional activation and somehow enhancing translation. How this is occurring is unclear; previous data has determined that the BiP IRES confers very little inherent IRES activity in a bicistronic construct. Additionally, the cap-dependent translation should overshadow any minute contribution of cap-independent translation. One interpretation is that the BiP IRES can only function

properly when it is located in the 5' UTR region. This explanation is biologically reasonable, as bicistronic transcripts do not actually exist *in vivo;* in actual cells, IRES's are always located in the 5' UTR of RNA transcripts. Perhaps the BiP IRES is only fully functional when placed in a biologically relevant location, i.e., at the 5' end of the transcript. If this were the case, the additional CAT expression seen for the monoBiP construct would be a result of both traditional cap-dependent translation and also IRES-mediated translational initiation.

3.5.3 CONFIRMATION OF INCREASED CAT EXPRESSION FROM MONOCISTONIC CONSTRUCTS VIA WESTERN BLOT

To confirm that high levels of CAT activity in an enzymatic based CAT assay correlate to actual increases in protein expression, a western blot was performed. This allowed for quantification and comparison of CAT protein expression in the monocistronic and bicistronic constructs. The western blot corroborates the results of the CAT assay; much higher levels of CAT protein are expressed from the monocistronic constructs (Figure 22). However, this is not surprising given the high levels of cap-dependent translation predicted to occur.

It is worthwhile to note that the additional expression driven from the monoBiP construct is much more evident in the CAT enzymatic assay (Figures 20-21) than the western blot (Figure 22). However this discrepancy is not unexpected; the enzymatic CAT assay is known to be

linear (previously tested) but the western blot may not be; i.e., the LiCOR signal may not be linearly related to the amount of protein added.

3.6 ADDITION OF A HAIRPIN DECREASES CAT ACTIVATION IN MONOCAT BUT NOT MONOBIP

To help determine the contribution of IRES activity to the increased activation in the monocistronic constructs, a hairpin sequence (previously described by Attal *et al*, 2000) which blocks downstream ribosomal scanning was inserted either upstream of the CAT cistron (HP in monoCAT) or upstream of the BiP IRES (HP in monoBiP). Details of this procedure are outlined in Chapter 2. These constructs were then transfected into HeLa cells and assayed for CAT activity as previously described. If the BiP IRES sequence is indeed functioning as an IRES, the addition of the hairpin should only effect the initiation of translation in the construct without an IRES (HP in monoCAT). When the IRES is present (HP in monoBIP) ribosomes would be recruited directly to the IRES sequence and thus have no effect on downstream CAT cistron translation.

As expected for the monoCAT construct (HP in monoCAT), the addition of the hairpin significantly decreased CAT activity in the absence of vhs ($p = 0.0038$; see Figure 23). In contrast, for the monoBiP construct (HP in monoBIP) the addition of the hairpin had no significant effect on CAT expression in the absence of vhs ($p = 0.15$; see Figure 24). These data indicate that the enhanced activity of monoBiP relative to monoCAT

(see Figure 21) stems from IRES activity. If this were the case, it appears as if the BiP IRES can only function properly when it is located in the 5' UTR region; if located in the intercistronic region (for example in biBiP), it functions very poorly. Alternatively, it is possible that the hairpin and the BiP IRES are folding together (i.e., not acting as separate entities) and thus the hairpin is not functioning properly to block downstream ribosomal scanning.

3.7 VHS DECREASES CAT ACTIVITY IN MONOCISTRONIC CONSTRUCTS

As described above, monocistronic constructs show much higher levels of CAT activity in the absence of vhs than their bicistronic counterparts. Additionally, monoBiP is significantly more active than monoCAT (even when ribosomal scanning is inhibited by a hairpin), suggesting IRES activity contributes to this additional activity. Next, the effect of vhs on these monocistronic constructs was assessed and compared to their bicistronic counterparts. Additionally, the effect of the same hairpin on the bicistronic BiP IRES reporter (HP.BiP in biCAT) was compared to its monocistronic counterpart (monoBiP).

As shown in Figure 25, the addition of vhs significantly decreases CAT activity for both monoBiP and HP in monoBiP. In contrast, the addition of vhs significantly increased CAT expression in both the bicistronic counterparts (biBiP and HP.BiP in biCAT; see Figure 26).

Although this vhs-dependent response was slightly reduced when the hairpin is present (HP.BiP in biCAT), it was still substantial and statistically significant ($p = 0.00044$). Thus, this indicates that in the bicistronic reporter, the hairpin did not effectively block translation of the downstream CAT mRNA.

In summary, it appears as if the response of the BiP IRES sequence to vhs depends on the location of the IRES on the RNA. Specifically, if it is located in the 5' UTR (monoBiP and HP in monoBiP) vhs inhibits CAT expression. Conversely, if it is located in the intercistronic region (biBiP and HP.BiP in biCAT) vhs stimulates CAT expression. While this is not fully consistent with the IRES activity hypothesis, it is consistent with the RNase hypothesis. In short, if vhs acts to promote CAT expression from the bicistronic constructs by degrading the 5' cistron, this would result in a translatable monocistronic transcript encompassing the CAT ORF. In contrast, if the construct is already monocistronic, there is no 5' cistron for vhs to target. Instead, vhs may be targeting the CAT cistron, resulting in the observed decrease in CAT activity. According to this model, the BiP IRES sequence promotes CAT expression either by (a) blocking 5' to 3' degradation and thus enhancing accumulation of truncated mRNA, or (b) enhancing translation of uncapped degradation products, or (c) a combination of both. Perhaps arguing against this hypothesis, Saffran *et al* (2010) could not show a detectable level of vhs-induced truncated monocistronic RNA with a northern blot; however, these

data do not definitively discount this hypothesis (also, further investigation into this will follow in subsequent sections).

Despite mounting evidence to support the RNase hypothesis, it is still unclear if vhs is acting alone or in concert with cellular nucleases to promote 5' to 3' degradation. The experiments described in the following sections attempt to elucidate the role of other nucleases (specifically, the cellular exonuclease Xrn1) in the 5' to 3' RNA degradation predicted by the RNase model.

3.8 ADDITION OF A XRN1 NUCLEASE INHIBITING SLII SEQUENCE UPSTREAM OF THE CAT CISTRON RESULTED IN AN INCREASE OF CAT ACTIVITY

As mentioned in the previous section (3.7), the RNase model predicts that the BiP IRES may be enhancing CAT expression by blocking 5' to 3' degradation and thus enhancing accumulation of truncated mRNA. I next asked if inserting an RNA that blocks 5' to 3' degradation of the products of vhs action (by impeding the cellular 5' to 3' exonuclease Xrn1) could mimic this effect. To this end, I inserted a flavivirus derived SLII element (described in Pijlman *et al*, 2008) between cistrons in place of the BiP IRES. Details of this construct and its construction are outlined in Chapter 2.

This SLII sequence has been shown by other groups to block nuclease activity, specifically, the cellular Xrn1 nuclease (Gaglia *et al*,

2010). Based on the experiments performed in this report, Gaglia *et al* hypothesize that vhs makes an initial endonucleolytic cleavage close to the 5' end of the mRNA transcript, at which point the cellular exonuclease XrnI completes the degradation, proceeding in a 5' to 3' direction. In the context of my study, insertion of the SLII element in the intercistronic region should block any downstream nuclease activity. In this case, the CAT RNA should be preserved and thus translated as normal. On the other hand, if the IRES activity hypothesis is correct, no translation should occur, as there is no longer an IRES present to participate in translation initiation.

As shown in Figure 27, the SLII element functions identically to the BiP IRES in terms of its ability to stimulate CAT activity in response to vhs. Specifically, a significant increase in CAT activity was observed in response to vhs ($p = 0.00058$) for the SLII element construct. This increase was also significantly greater than the no IRES control (biCAT vs. SLII element with vhs; $p = 0.00022$). Additionally, no significant difference in CAT activity was found between the wild-type biBiP and biSLII element constructs ($p = 0.22$). In the absence of vhs, no significant change between the SLII element construct and either biCAT or biBiP is observed ($p = 0.45$ or 0.4 respectively). This is not unexpected, as the SLII element has no IRES activity. In this experiment, the BiP IRES also does not promote a significant increase in CAT activity ($p = 0.1$; likely due to experimental variation, see section 3.4 for discussion on this issue).

As shown in Figure 28, combining both elements (the SLII element upstream of the BiP IRES in the intercistronic region) results in the same effect; a substantial and significant increase of CAT activity ($p = 0.00021$). Again, this increase was also significantly greater than the no IRES control (biCAT vs. SLII element + BiP IRES with vhs; $p = 0.00012$). In the absence of vhs, there is a significant increase in CAT activity levels with the SLII/BiP IRES construct (SLII with BiP IRES) compared to the no IRES control (biCAT) ($p = 0.02$). As noted above, this significant increase was not achieved when the SLII element was alone (no BiP IRES present). In this experiment, the increase CAT activity imparted by the BiP IRES alone (biCAT vs. biBiP in the absence of vhs) does achieve significance ($p = 0.04$).

In summary, these data indicate that the BiP IRES likely employs 2 strategies to simulate CAT expression in response to vhs. Firstly, the CAT cistron stimulation in response to vhs was mimicked by the SLII element, which has no IRES ability and functions to block Xrn1 nuclease activity. Therefore, it seems likely that the BiP IRES and the SLII element both function by blocking 5' to 3' degradation (mediated by Xrn1) and thus enhance accumulation of truncated mRNA. Secondly, only the BiP IRES is capable of stimulating CAT expression in the absence of vhs. As noted above, the SLII element had no effect on CAT activity in the absence of vhs; a significant increase was only observed when the BiP IRES was downstream (SLII/BiP IRES construct). Interestingly, the level of CAT

activity in the absence of vhs was actually significantly higher for the SLII/BiP IRES construct than for the BiP IRES construct ($p = 0.03$; see Figure 28). Additionally, for the SLII/BiP IRES construct, levels of CAT activity after addition of vhs were actually higher than that observed with the BiP IRES or SLII element constructs alone. Thus, it appears as if the BiP IRES is also acting to enhancing translation of uncapped degradation products, perhaps via IRES activity.

Given the likelihood of the RNase model, it seems probable that other viral host shutoff nucleases would have a similar effect as vhs on both β-galactosidase and CAT activity. Thus, the next series of experiments were designed to address this issue.

3.9 EFFECT OF BGLF5, SOX and NSP1 EXPRESSION PLASMIDS ON β-GALACTOSIDASE AND CAT ACTIVITY IN BICISTRONIC REPORTERS

As evidenced by the data presented thus far, the addition of vhs has very specific and notable effects on both β-galactosidase and CAT activity for a variety of different bicistronic constructs. Next, I wanted to examine the effect of other nucleases on β-galactosidase and CAT activity. Unrelated herpesvirus host shutoff nucleases EBV BGLF5 and KHSV SOX as well as the SARS coronavirus Nsp1 nuclease were transiently transfected into HeLa cells and levels of β-gal and CAT activity were assessed as previously described. None of nucleases are directly

related to vhs; BGLF5 and SOX are alkaline exonucleases that have been shown to contribute to RNA instability and degradation, although the mechanism by which this occurs is currently unclear (Clyde and Glaunsinger, 2011). SARS coronavirus Nsp1 protein induces mRNA degradation by binding the 40S subunit and modifying capped mRNA so it cannot be translated (Kamitani *et al,* 2009). Also, Nsp1 has been shown to target regions of mRNA downstream of certain IRES elements (Kamitani *et al,* 2009 and Huang *et al*, 2011). This observation is similar what Elgadi and Smiley reported in their 1999 publication (summarized in Chapter 1); sequences 3' to certain IRES's could selectively target vhs. Critically, degradation of mRNAs by all of these nucleases involves 5' to 3' decay mediated by Xrn1, and can be blocked by the SLII element. Therefore, these alternate nucleases were assayed for their ability to (a) inhibit expression of the 5' β-gal cistron and/or (b) stimulate translation of the 3' CAT cistron.

3.9.1 BGLF5 BUT NOT SOX OR NSP1 CONSISTENTLY INHIBIT 5' CISTRON (β-GALACTOSIDASE) EXPRESSION

The same bicistronic constructs used for previously described experiments (biCAT, biBiP, biSLII +/- the BiP IRES) were transiently transfected into HeLa cells alongside the nuclease of interest. β-gal activity was first assessed as previously described. As shown in Figures 29 and 30, the only non-vhs nuclease that significantly inhibited β-gal

activity specified by all constructs was BGLF5 ($p < 0.05$). However, SOX significantly inhibited β-gal activity for the biBiP construct ($p = 0.007$) and Nsp1 significantly inhibited β-gal activity for biCAT ($p = 0.034$). It is worthwhile to note that in all cases, an increased number of replicates may allow for more of these comparisons to achieve significance. Although something may not achieve significance with 3 replicates, it may still be biologically relevant; albeit requiring additional tests to achieve statistical relevance.

Interestingly, in the absence of vhs, neither SLII construct (+/- the BiP IRES) can support high levels of β-gal activity (Figure 29 and 30). This is in contrast to both biCAT and biBiP, which consistently show high levels of β-gal activity in the absence of vhs; presumably due to cap-dependent translation of the 5' cistron. Why the SLII constructs do not support translation of the 5' β-gal cistron is not clear. Next, the effect of these alternative nucleases on 3' CAT activity was examined.

3.9.2 SOX, BGLF5 AND NSP1 ARE ALL ABLE TO ACTIVATE 3' CAT CISTRON EXPRESSION

In contrast to the effect on β-gal activity, all 3 alternative host shutoff nucleases affected CAT activity, although the extent varied. As shown in Figures 31 and 32, none of the alternative nucleases (BGLF5, SOX or Nsp1) were able to significantly increase CAT activity ($p > 0.05$ for

both). As previously described, in all cases, the addition of vhs resulted in a significant increase in CAT activity for the biCAT construct.

In contrast, for the biBiP and biSLII element constructs, all three nucleases (BGLF5, SOX and Nsp1) were capable of significantly simulating CAT expression (Figures 31 and 32). P-values were as follows; for biBiP (BGLF5; p = 0.005), (SOX; p = 0.0005), (Nsp1; p = 0.0006) and for biSLII (BGLF5; p = 0.04), (SOX; p = 0.02), (Nsp1; p = 7.8x10^-6). The majority of these increases were also determined to be significantly greater than the no IRES control in the presence of the host shutoff protein. biCAT vs. biBiP/biSLII with host shutoff protein, p-values were as follows; for biBiP (BGLF5; p = 0.0064), (SOX; p = 0.00093), (Nsp1; p = 0.0015) and for biSLII (BGLF5; p = 0.074), (SOX; p = 0.011), (Nsp1; p = 0.0039). Although biSLII + BGLF5 did not achieve significance it is likely that a low number of replicates was responsible for this.

As shown in Figures 31 and 32, the amount of CAT activation induced by BGLF5 and SOX (for both biBiP and biSLII) and Nsp1 (for biBiP) was substantially less than that induced by vhs, despite achieving significance. Conversely, for the SLII constructs, the addition of Nsp1 stimulated CAT expression both substantially and significantly (Figures 32 and 33; 7.8 x 10^-6 and 0.0052 respectively). Again, these increases were significantly higher than the no IRES control (biCAT vs. biSLII with BiP IRES/without BiP IRES with Nsp1; p = 2.8 x 10^-6 and 0.0039). The effect on biBiP (no SLII element) was less dramatic; specifically, an average 7.3

fold increase is observed for the SLII construct, whereas an average 2.6 fold increase for the biBiP construct. As shown in Figure 33, excision of the BiP IRES did not greatly alter the CAT expression profile for either vhs or Nsp1; significant levels of CAT activation are still achieved ($p = 0.0077$ and 0.0052, respectively). The only notable difference was a slight decrease in vhs-induced CAT activation in the SLII construct. Assuming the RNase model, this is likely due to the BiP IRES enhancing translation of the uncapped degradation products generated via nuclease mediated decay.

The data presented in this section are consistent with the RNase hypothesis; I have shown that several unrelated nucleases are capable of stimulating CAT expression in a similar way to vhs. Again, it seems as if the BiP IRES likely employs 2 strategies to simulate CAT expression in response to vhs; blocking 5' to 3' degradation (mediated by Xrn1) and thus enhancing accumulation of truncated mRNA and enhancing translation of uncapped degradation products, perhaps via IRES activity.

In the last series of experiments, I attempted to detect these putative monocistronic transcripts via Northern blot.

3.10 VHS MEDIATED mRNA DECAY REVEALED VIA NORTHERN BLOT

As described previously, the RNase hypothesis predicts that all of the viral host shutoff nucleases (vhs, BGLF5, SOX and Nsp1) provoke the generation of monocistronic RNAs encompassing the CAT cistron when the substrate RNA contains the BiP IRES or the SLII element. This model is supported by the CAT assay data described in section 3.9.2. However, this evidence is suggestive; no actual loss of RNA has been detected. As described previously, Holly Saffran was unsuccessful at detecting any monocistronic RNAs; however, this does not mean they were not generated. Instead, it is possible that only a small subset of RNAs are rendered monocistronic; in this case, the Northern blot would not be sensitive enough to detect these minute levels. Thus, I attempted to increase the amount of monocistronic RNAs available for detection by mimicking an experiment designed by Gaglia *et al* (2012).

As previously outlined in this thesis and in Gaglia *et al* (2012), the RNase hypothesis predicts that vhs activates the 3' CAT cistron by making an initial cleavage near the 5' end of the RNA, followed by 5' → 3' degradation mediated by vhs and/or cellular exoribonucleases. This leads to transient production of uncapped monocistronic mRNA encompassing the 3' CAT cistron. Gaglia *et al* (2012) predicted that the cellular exonuclease Xrn1 is mediating 5' → 3' degradation following the initial cleavage by vhs. Thus, they used the previously described SLII element to protect downstream mRNA from Xrn1 nuclease degradation. This allows

the RNA downstream of the SLII element to be detected on a northern blot using a radionucleotide-labeled probe.

I was able to replicate this experiment (detailed in Gaglia *et al* (2012) and Chapter 2) using HeLa cells (they used HEK293T cells) and the SLII-containing GFP reporter plasmid generously provided by this group (pD2EGFP-N1_3'SLII; contains GFP reporter cistron downstream of SLII element). In short, HeLa cells were transiently transfected with a reporter plasmid (biBiP with no SLII element or pD2EGFP-N1_3'SLII) and the vhs effector plasmid as needed. Lysates were harvested and total RNA isolated as described in Chapter 2. RNA samples were electrophoresed through an agarose-formaldehyde gel then transferred to a nitrocellulose membrane. A ^{32}P radiolabeled probe against the GFP 3' UTR (see Chapter 2 for details) was used to detect RNA downstream of the SLII element. As predicted by Gaglia *et al* (2012), the SLII element should function to block Xrn1-mediated degradation downstream of the SLII element, allowing for detection of an ~450 bp protected fragment (PF) with the 3' UTR probe, as well as an ~1,381 bp intact fragment (http://www.snapgene.com/resources/plasmid_files/fluorescent_protein_genes_and_plasmids/pd2EGFP-N1/). Gaglia *et al* (2012) confirmed this prediction, indicating that Xrn1 completes the exonucleolytic degradation following the primary endonucleolytic cleavage by the viral host shutoff nuclease. As shown in Figure 34, I was also able to confirm this result. The addition of vhs resulted in the appearance of the protected fragment

(PF; indicted by arrowhead), indicating that the SLII element successfully functioned to block downstream Xrn1-mediated degradation. Although the exact sizes of the fragments could not be confirmed (the ladder was not properly denoted on the blot and is thus not well visualized) the relative locations appear to be as predicted by Gaglia *et al* (2012). Additionally, a general reduction in total RNA levels was observed after addition of vhs (evidenced by reduction in GFP RNA, indicated on Figure 34).

These data are fully consistent with the RNase hypothesis, specifically, that both vhs and Xrn1 contribute to the 5' to 3' RNA degradation and subsequent generation of truncated mRNA. As previously mentioned, this hypothesis also predicts that CAT activation in response to vhs (or another viral host shutoff nuclease) is dependent on the presence of either the BiP IRES or the SLII element on the substrate RNA. The data presented in sections 3.8 and 3.10 of my study support this model, as I have shown the SLII element is able to stimulate CAT expression in response to vhs (section 3.8), likely by blocking Xrn1-mediated degradation of the downstream RNA (successfully shown in this section using northern blotting techniques). Thus, the effect of the BiP IRES in a similar context is of interest; in the future, experiments designed to test the ability of the BiP IRES to protect the downstream CAT RNA should be initiated.

Figure 3: Schematic representation of bicistronic biBiP reporter construct (not to scale). The BiP IRES element was inserted between the 5' β-galactosidase (β-gal) cistron and the 3' chloramphenicol acetyl transferase (CAT) cistron. Locations of the CMV IE promoter and 2 alternate polyadenylation symbols are indicated.

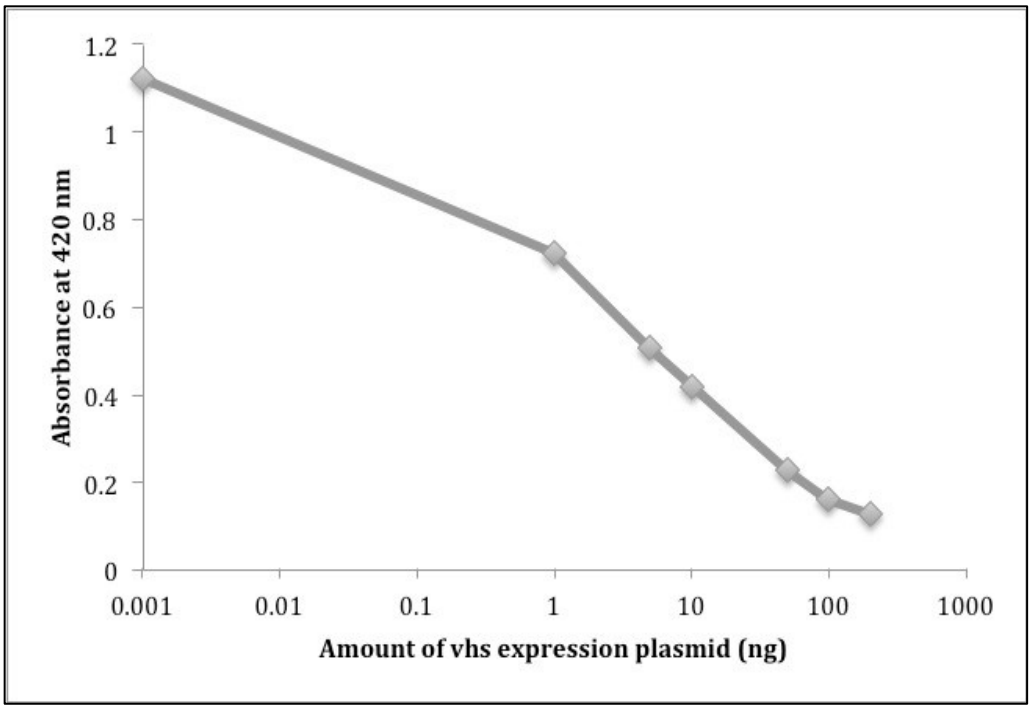

Figure 4: Vhs reduces the expression of β-Galactosidase encoded by the bicistronic biBiP reporter plasmid. Note: x-axis is a log scale.

HeLa cells were transfected with specified bicistronic biBiP reporter plasmid, 'filler' plasmids pUC19 and pCDNA3.1, and effector plasmid of interest (vhs expression plasmid) using Lipofectamine 2000 (Invitrogen; according to manufacturer's instructions). After 48 hours, cells were washed 2X with Phospho-buffered saline (PBS) and lysates were prepared using 200μL of 1X reporter lysis buffer (Promega). β-Galactosidase assays were performed on a portion of the lysate as outlined by ProMega, available online at www.promega.com/tbs and detailed in Chapter 2 (section 2.4). Levels of nitrophenol (a yellow product) were then quantified via spectrophotometer (Thermo Fisher) at 420nm.

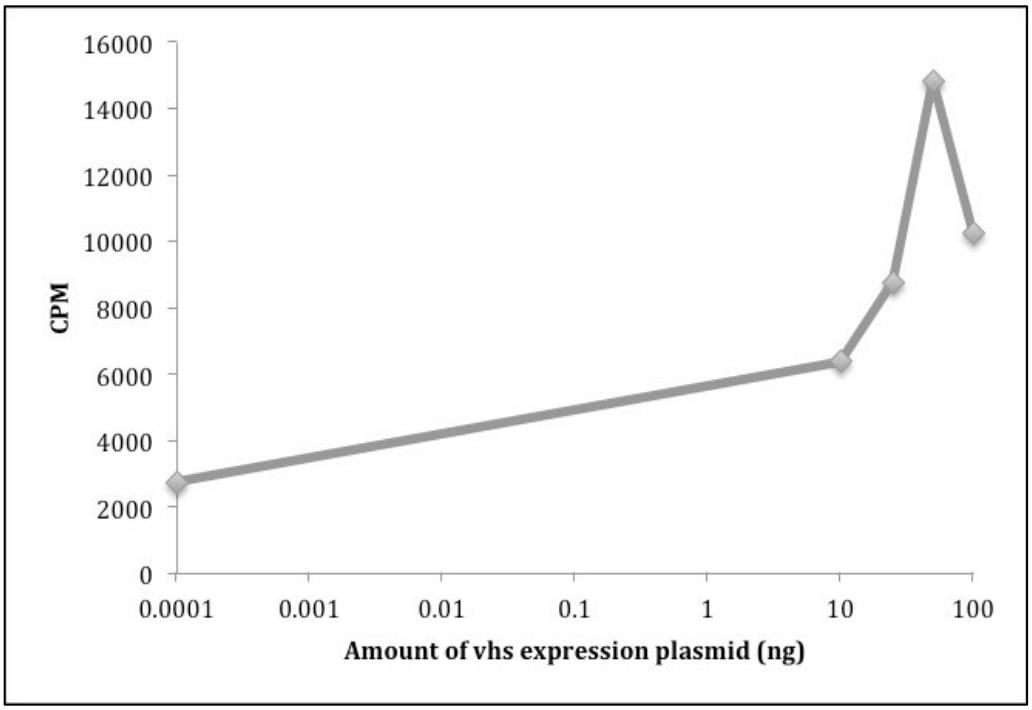

Figure 5: Effect of increasing amounts of vhs on CAT activity specified by the bicistronic biBiP reporter plasmid. Note: x-axis is a log scale.

HeLa cells were transfected with specified bicistronic biBiP reporter plasmid, 'filler' plasmids pUC19 and pCDNA3.1, and effector plasmid of interest (vhs expression plasmid) using Lipofectamine 2000 (Invitrogen; according to manufacturer's instructions). After 48 hours, cells were washed 2X with Phospho-buffered saline (PBS) and lysates were prepared using 200µL of 1X reporter lysis buffer (Promega). CAT assays were performed on a portion of the lysate as outlined by ProMega, available online at www.promega.com/tbs and detailed in Chapter 2 (section 2.5). The amount of radioactive, butyrylated chloramphenicol product was then measured in a liquid scintillation counter as counts per minute (CPM).

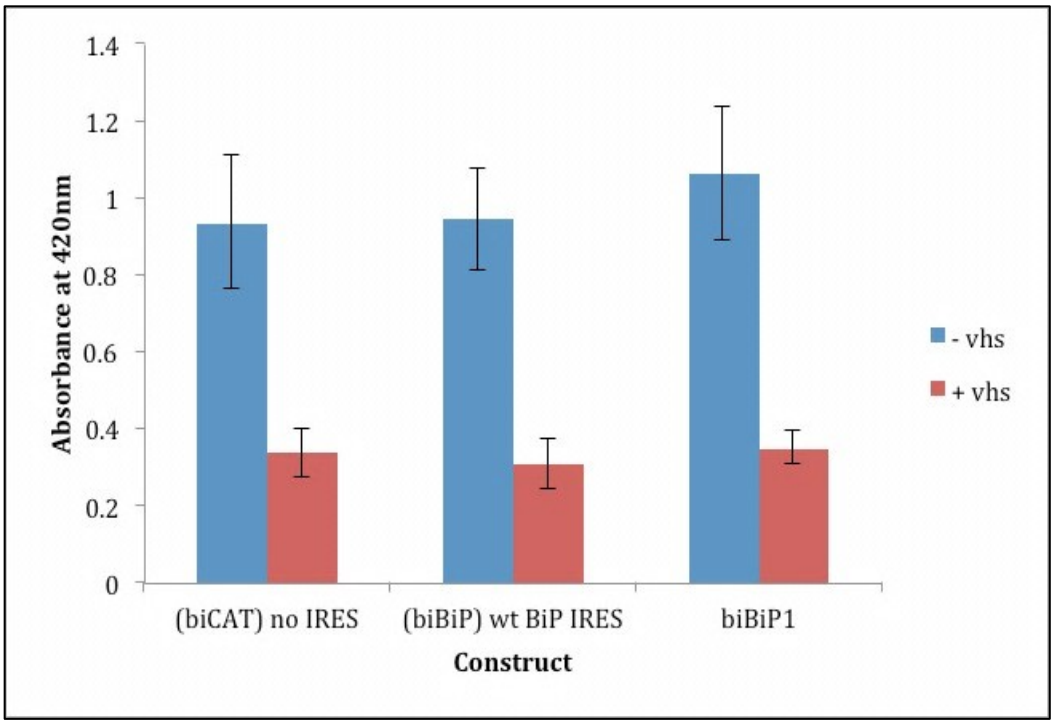

Figure 6: Vhs represses β-galactosidase activity specified by bicistronic constructs biCAT, biBiP and biBiP1. Error bars represent standard error of the mean. N=4.

HeLa cells were transfected with specified bicistronic reporter plasmid, 'filler' plasmids pUC19 and pCDNA3.1, and effector plasmid of interest (vhs expression plasmid) using Lipofectamine 2000 (Invitrogen; according to manufacturer's instructions). Lysates were harvested and assayed for CAT activity as previously described Chapter 2 (section 2.5) and summarized in Figure 5 legend.

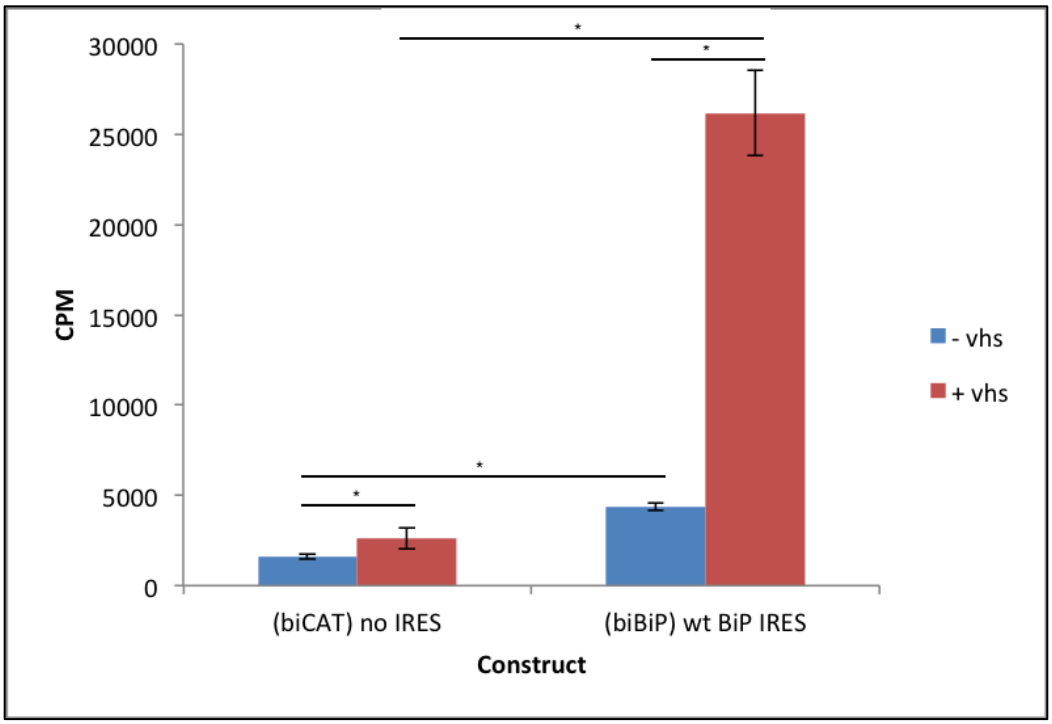

Figure 7: Addition of vhs increases CAT activity specified by bicistronic constructs biCAT and biBiP. Error bars represent standard error of the mean. N=13. * Indicates statistical significance ($p < 0.05$).

HeLa cells were transfected with specified bicistronic biBiP reporter plasmid, 'filler' plasmids pUC19 and pCDNA3.1, and effector plasmid of interest (vhs expression plasmid) using Lipofectamine 2000 (Invitrogen; according to manufacturer's instructions). Lysates were harvested and assayed for CAT activity as previously described Chapter 2 (section 2.5) and summarized in Figure 5 legend.

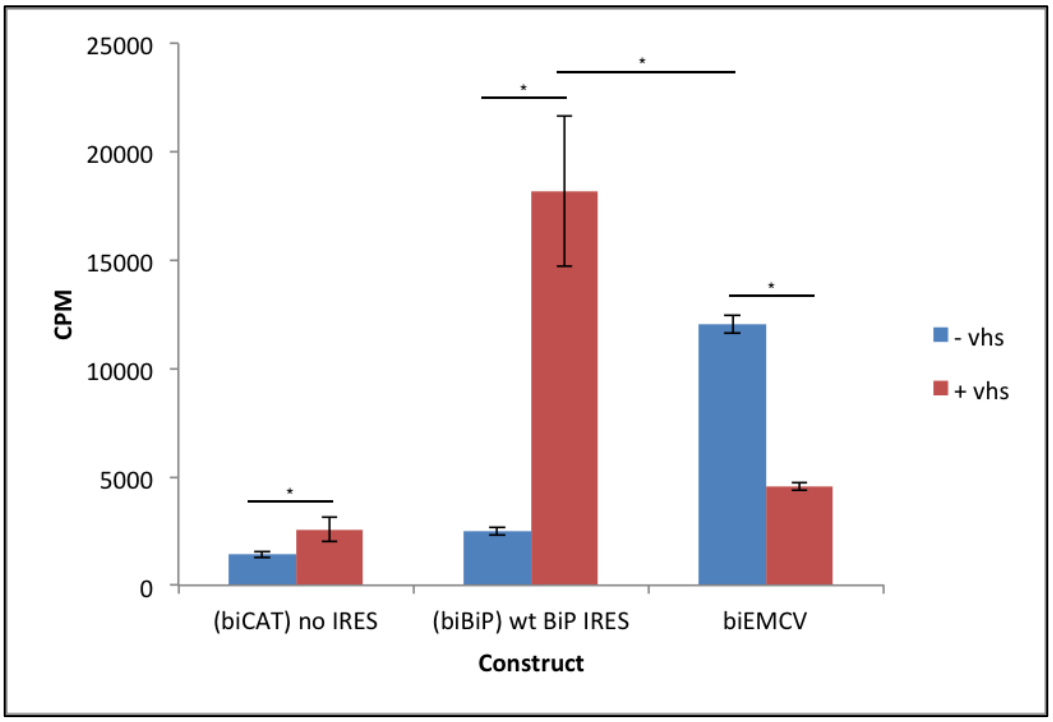

Figure 8: Effect of vhs on the EMCV IRES containing biEMCV construct in comparison to biCAT and biBiP. Error bars represent standard error of the mean. N = 3. * Indicates statistical significance ($p < 0.05$).

HeLa cells were transfected with specified bicistronic reporter plasmid, 'filler' plasmids pUC19 and pCDNA3.1, and effector plasmid of interest (vhs expression plasmid) using Lipofectamine 2000 (Invitrogen; according to manufacturer's instructions). Lysates were harvested and assayed for CAT activity as previously described Chapter 2 (section 2.5) and summarized in Figure 5 legend.

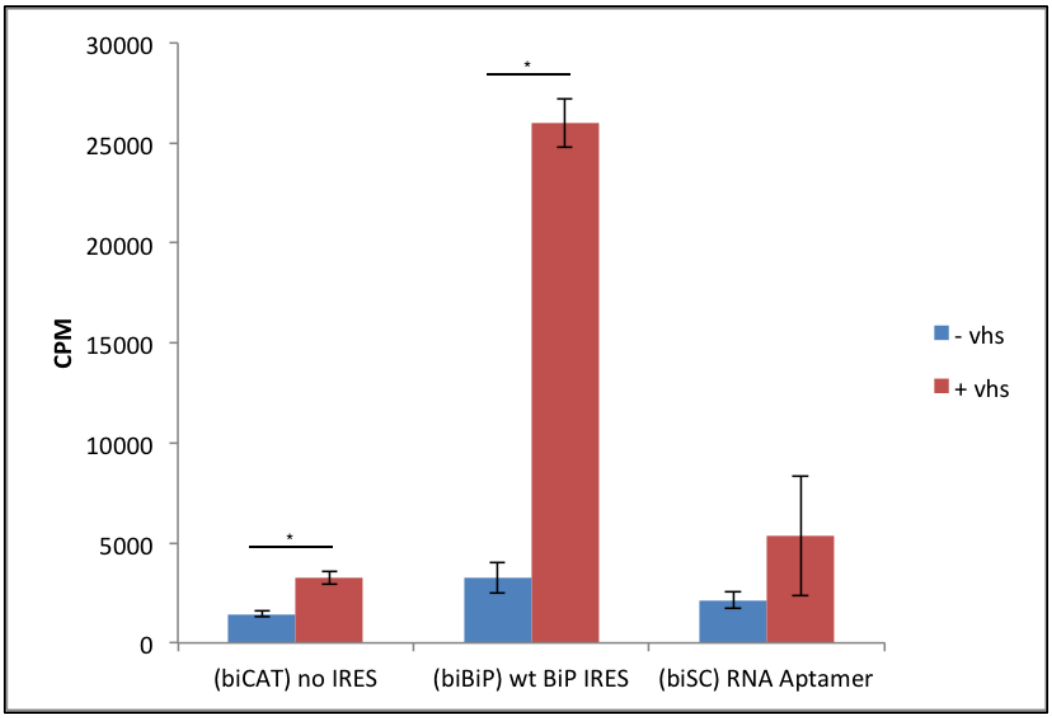

Figure 9: Effect of vhs on the non-IRES containing structured RNA sequence construct (biSC) in comparison to biCAT and biBiP. Error bars represent standard error of the mean. N = 3. * Indicates statistical significance ($p < 0.05$).

HeLa cells were transfected with specified bicistronic reporter plasmid, 'filler' plasmids pUC19 and pCDNA3.1, and effector plasmid of interest (vhs expression plasmid) using Lipofectamine 2000 (Invitrogen; according to manufacturer's instructions). Lysates were harvested and assayed for CAT activity as previously described Chapter 2 (section 2.5) and summarized in Figure 5 legend.

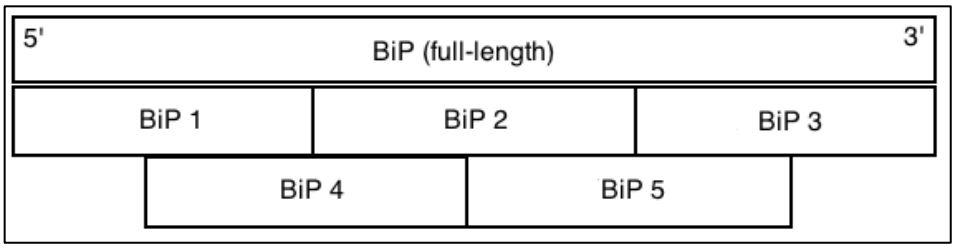

Figure 10: Schematic representation of the 5 partially overlapping BiP IRES fragments. Nucleotide positions are as follows: BiP 1 (1-69), BiP 2 (69-139), BiP 3 (139-221), BiP 4 (34-104) and BiP 5 (104-174).

Further details on fragment sequences and length shown in Chapter 2.

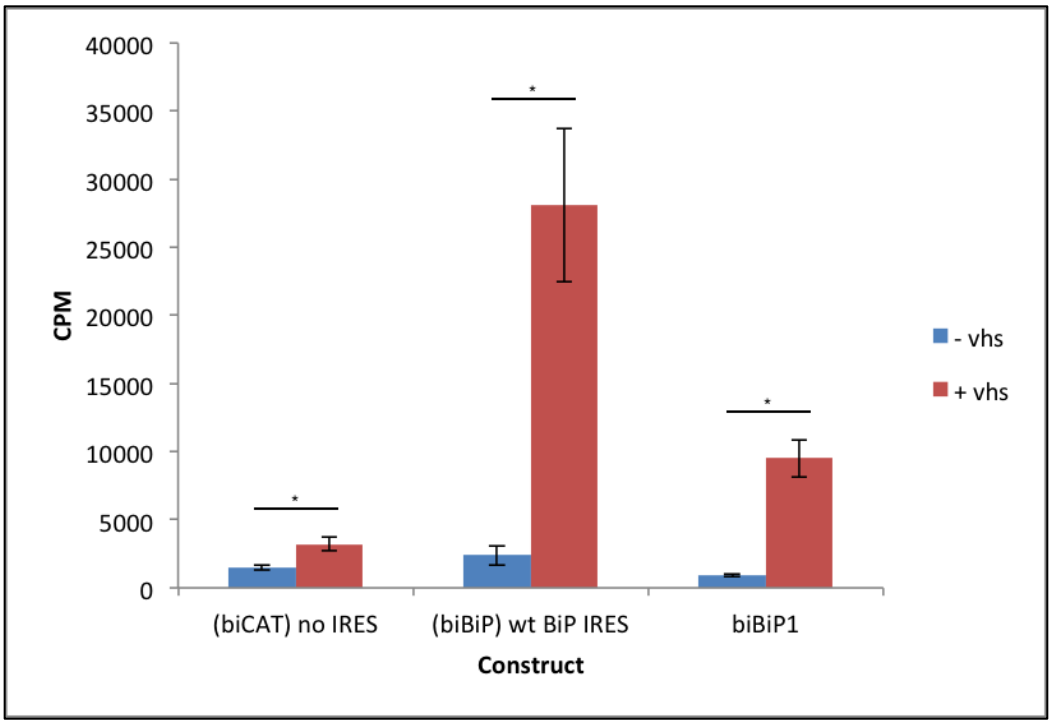

Figure 11: Effect of vhs on BiP IRES fragment 1 (biBiP1). Error bars represent standard error of the mean. N=3. * Indicates statistical significance ($p < 0.05$).

HeLa cells were transfected with specified bicistronic reporter plasmid, 'filler' plasmids pUC19 and pCDNA3.1, and effector plasmid of interest (vhs expression plasmid) using Lipofectamine 2000 (Invitrogen; according to manufacturer's instructions). Lysates were harvested and assayed for CAT activity as previously described Chapter 2 (section 2.5) and summarized in Figure 5 legend.

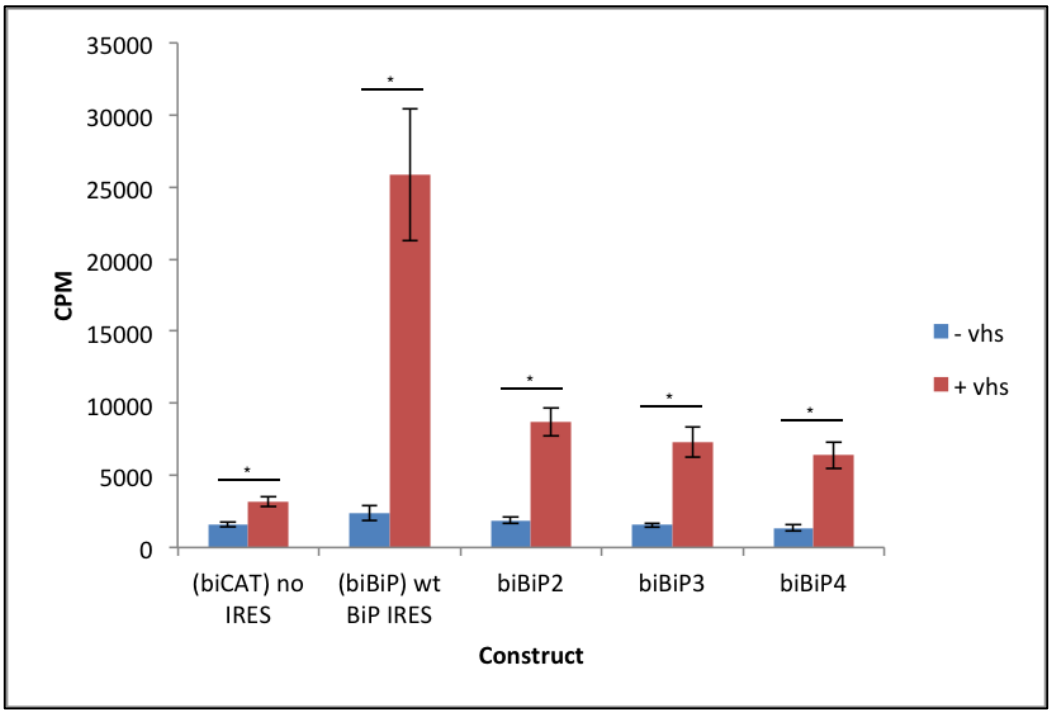

Figure 12: Effect of vhs on BiP IRES fragments 2-4 (biBiP2-4). Error bars represent standard error of the mean. N=4. * Indicates statistical significance ($p < 0.05$).

HeLa cells were transfected with specified bicistronic reporter plasmid, 'filler' plasmids pUC19 and pCDNA3.1, and effector plasmid of interest (vhs expression plasmid) using Lipofectamine 2000 (Invitrogen; according to manufacturer's instructions). Lysates were harvested and assayed for CAT activity as previously described Chapter 2 (section 2.5) and summarized in Figure 5 legend.

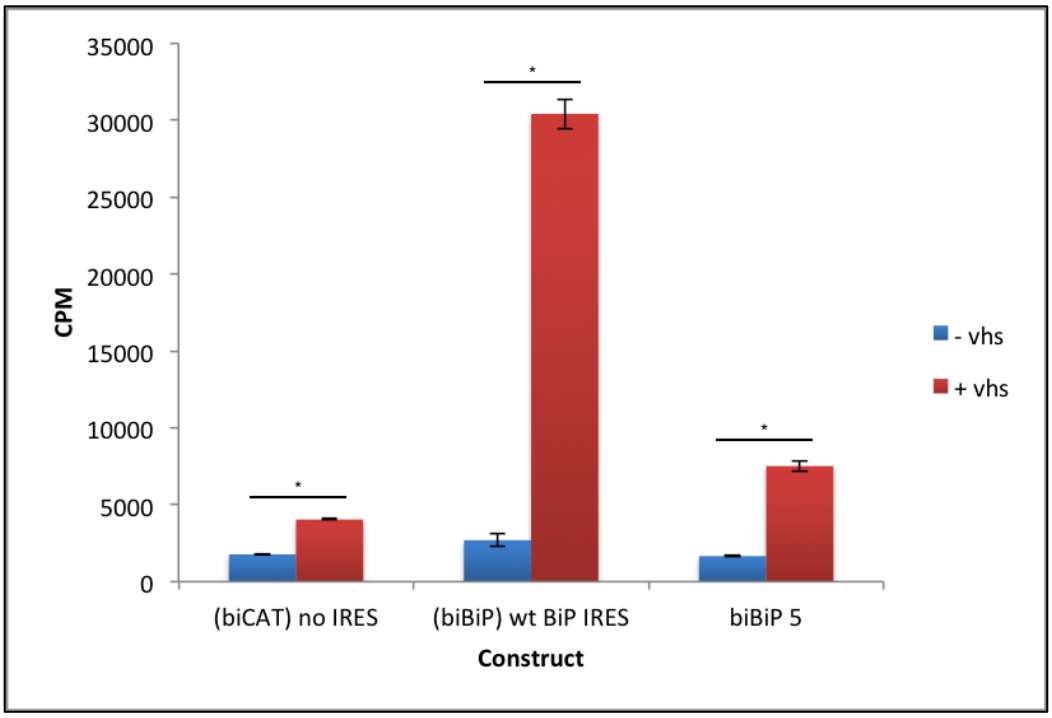

Figure 13: Effect of vhs on BiP IRES fragment 5 (biBiP5). Error bars represent standard error of the mean. N=3. * Indicates statistical significance ($p < 0.05$).

HeLa cells were transfected with specified bicistronic reporter plasmid, 'filler' plasmids pUC19 and pCDNA3.1, and effector plasmid of interest (vhs expression plasmid) using Lipofectamine 2000 (Invitrogen; according to manufacturer's instructions). Lysates were harvested and assayed for CAT activity as previously described Chapter 2 (section 2.5) and summarized in Figure 5 legend.

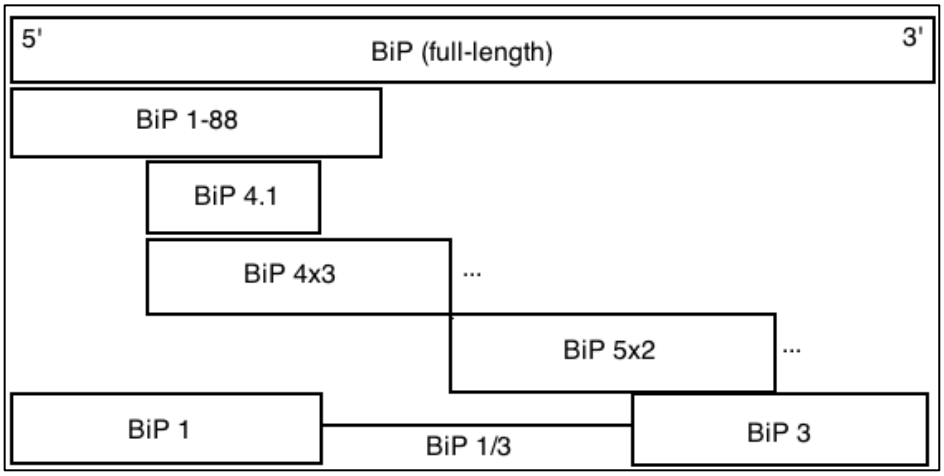

Figure 14: Schematic representation of the longer, shorter and fusion fragments of the BiP IRES (not to scale). Nucleotide positions are as follows: BiP 1-88 (1-88), BiP 4.1 (34-68), BiP 4x3 (34-104 triplicated), BiP 5x2 (104-174 duplicated) and BiP 1/3 (1-69 fused to 139-221).

Further details on fragment sequences and length shown in Chapter 2.

*** Duplicate (BiP 5x2) and triplicate (BiP 4x3) fragments are the indicated fragments annealed to one another via their XhoI sites, for example, BiP 1/3 includes BiP fragment 1 and 3 but excludes the middle portion of the IRES sequence.

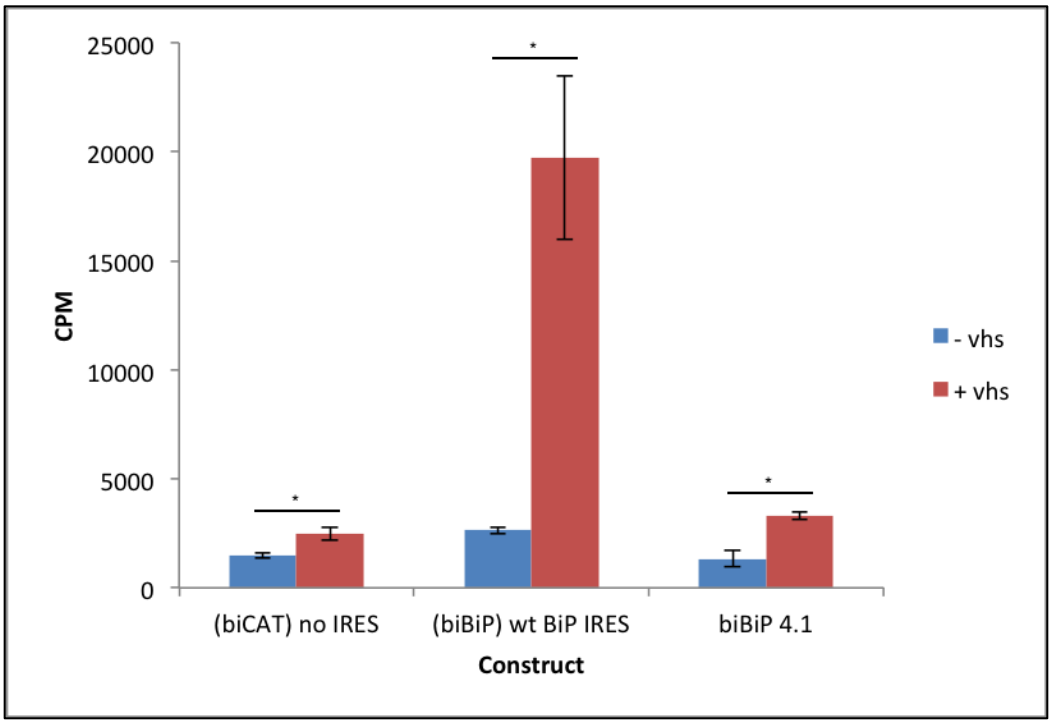

Figure 15: Effect of vhs on shortened BiP IRES fragment 4 (biBiP4.1). Error bars represent standard error of the mean. N=3. * Indicates statistical significance ($p < 0.05$).

HeLa cells were transfected with specified bicistronic reporter plasmid, 'filler' plasmids pUC19 and pCDNA3.1, and effector plasmid of interest (vhs expression plasmid) using Lipofectamine 2000 (Invitrogen; according to manufacturer's instructions). Lysates were harvested and assayed for CAT activity as previously described Chapter 2 (section 2.5) and summarized in Figure 5 legend.

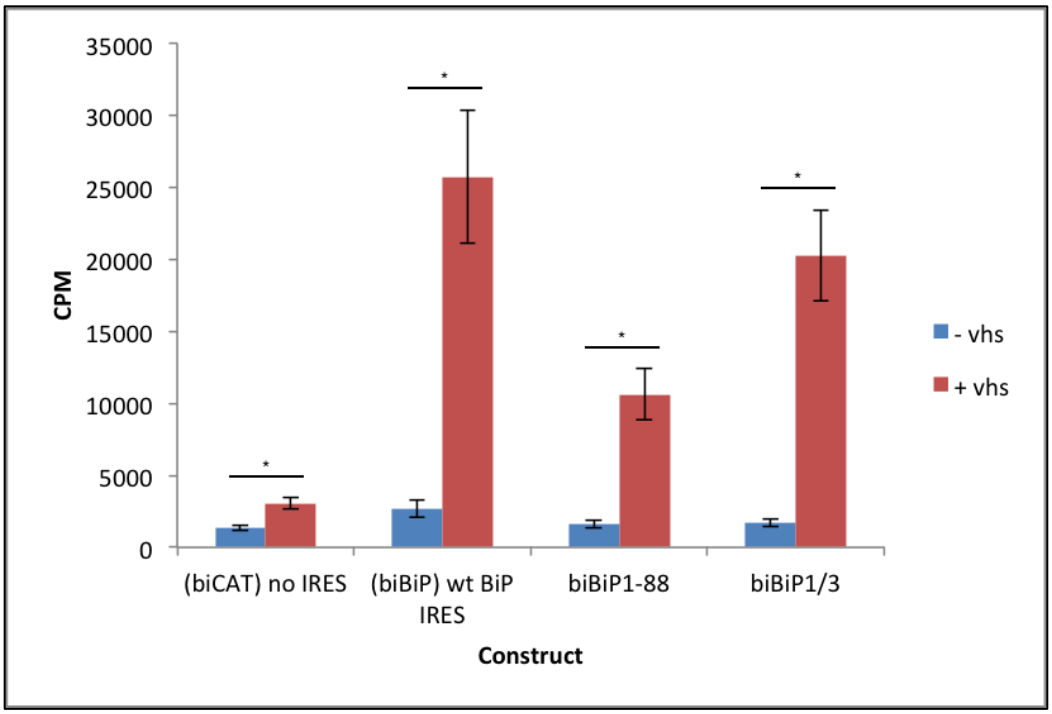

Figure 16: Effect of vhs on longer BiP IRES fragment biBiP 1-88 and fusion fragment biBiP 1/3. Error bars represent standard error of the mean. N=4. * Indicates statistical significance ($p < 0.05$).

HeLa cells were transfected with specified bicistronic reporter plasmid, 'filler' plasmids pUC19 and pCDNA3.1, and effector plasmid of interest (vhs expression plasmid) using Lipofectamine 2000 (Invitrogen; according to manufacturer's instructions). Lysates were harvested and assayed for CAT activity as previously described Chapter 2 (section 2.5) and summarized in Figure 5 legend.

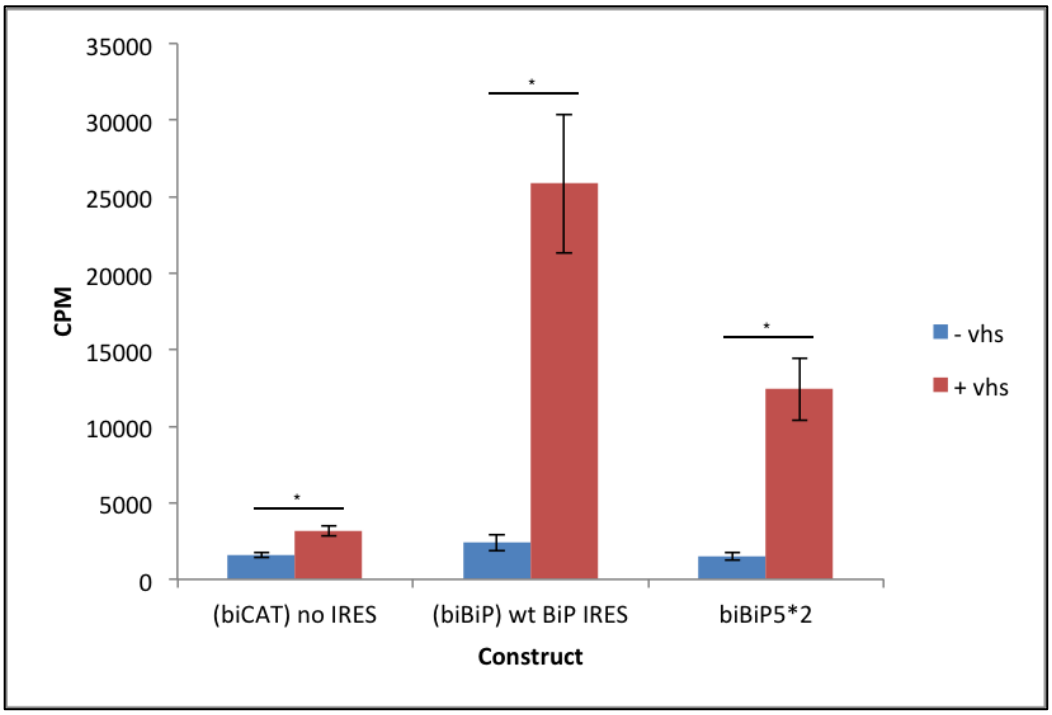

Figure 17: Effect of vhs on duplicated BiP IRES fragment 5 (biBiP5x2). Error bars represent standard error of the mean. N=4. * Indicates statistical significance ($p < 0.05$).

HeLa cells were transfected with specified bicistronic reporter plasmid, 'filler' plasmids pUC19 and pCDNA3.1, and effector plasmid of interest (vhs expression plasmid) using Lipofectamine 2000 (Invitrogen; according to manufacturer's instructions). Lysates were harvested and assayed for CAT activity as previously described Chapter 2 (section 2.5) and summarized in Figure 5 legend.

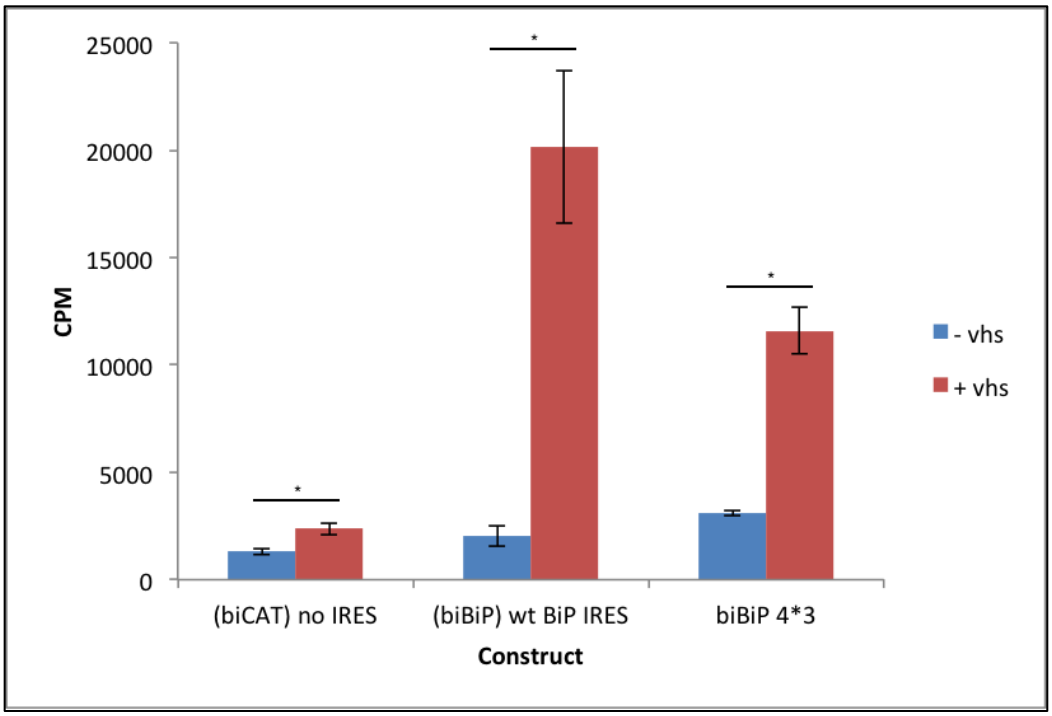

Figure 18: Effect of vhs on triplicated BiP IRES fragment 4 (biBiP4x3). Error bars represent standard error of the mean. N=3. * Indicates statistical significance ($p < 0.05$).

HeLa cells were transfected with specified bicistronic reporter plasmid, 'filler' plasmids pUC19 and pCDNA3.1, and effector plasmid of interest (vhs expression plasmid) using Lipofectamine 2000 (Invitrogen; according to manufacturer's instructions). Lysates were harvested and assayed for CAT activity as previously described Chapter 2 (section 2.5) and summarized in Figure 5 legend.

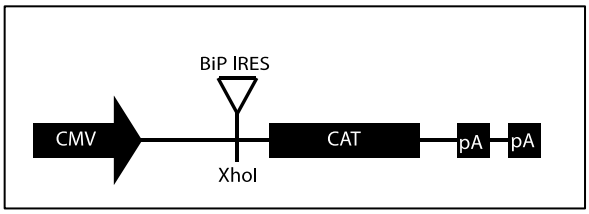

Figure 19: Schematic representation of monocistronic monoBiP reporter construct (not to scale). MonoCAT is identical save for the BiP IRES is not present. Locations of the CMV IE promoter and 2 alternate polyadenlyation symbols are indicated.

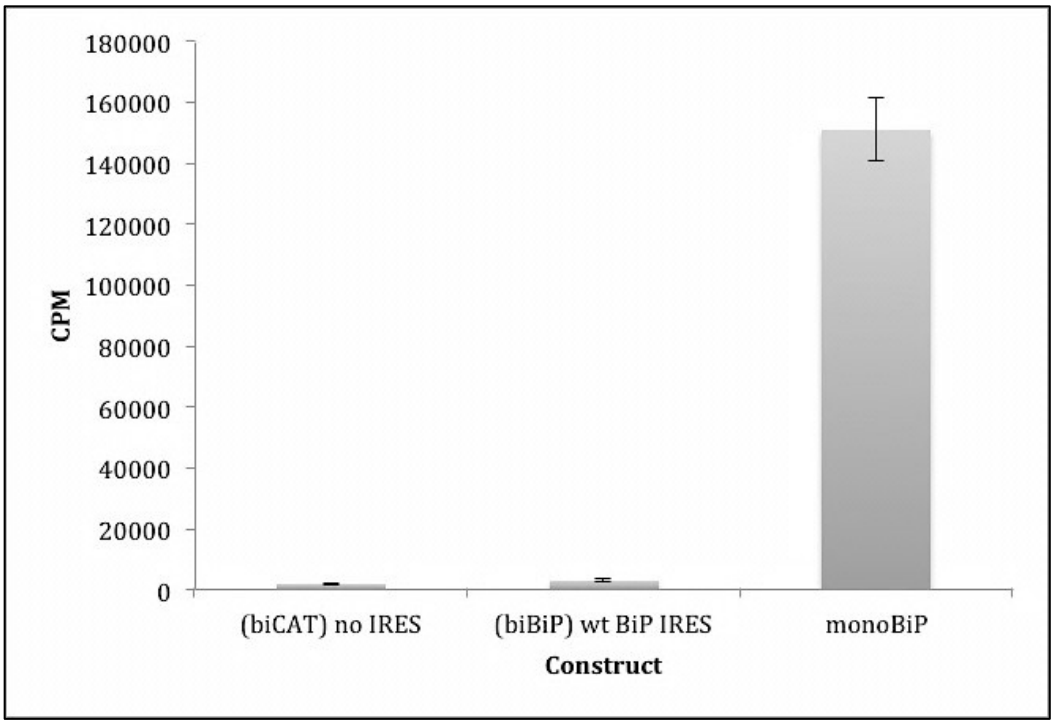

Figure 20: The BiP IRES is much more active in a monocistronic construct (monoBiP) than a bicistronic construct (biBiP). Error bars represent standard error of the mean. N=5.

HeLa cells were transfected with specified bicistronic or monocistronic reporter plasmid, 'filler' plasmids pUC19 and pCDNA3.1, and effector plasmid of interest (vhs expression plasmid) using Lipofectamine 2000 (Invitrogen; according to manufacturer's instructions). Lysates were harvested and assayed for CAT activity as previously described Chapter 2 (section 2.5) and summarized in Figure 5 legend.

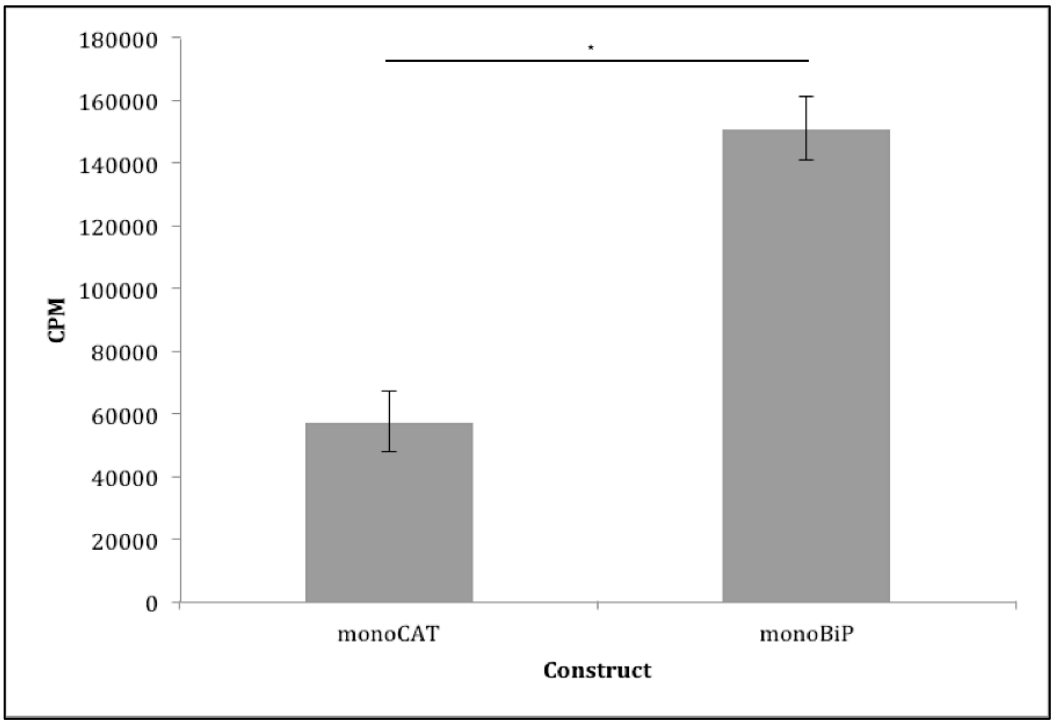

Figure 21: MonoBiP is more active than monoCAT in the absence of vhs. Error bars represent standard error of the mean. N=5. * Indicates statistical significance ($p < 0.05$).

HeLa cells were transfected with specified monocistronic reporter plasmid, 'filler' plasmids pUC19 and pCDNA3.1, and effector plasmid of interest (vhs expression plasmid) using Lipofectamine 2000 (Invitrogen; according to manufacturer's instructions). Lysates were harvested and assayed for CAT activity as previously described Chapter 2 (section 2.5) and summarized in Figure 5 legend.

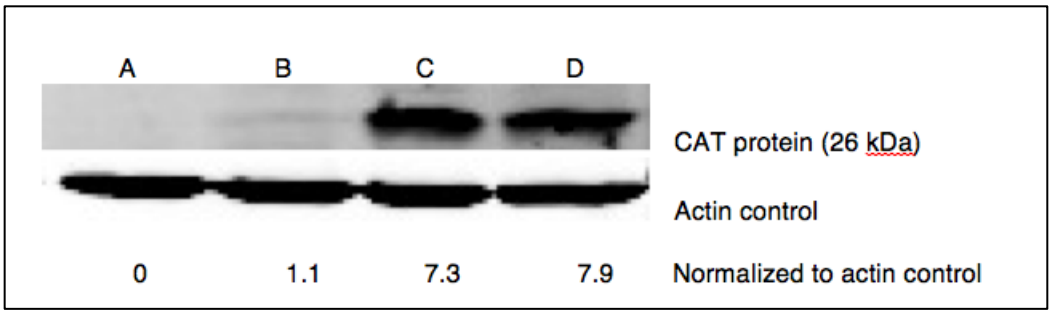

Figure 22: Western blot of the 26 kDa CAT protein, showing higher levels of CAT protein expression from monocistronic constructs. (A) Negative control, (B) biBiP, (C) monoCAT and (D) monoBiP.

HeLa cells were transiently transfected with appropriate reporter plasmid (bicistronic biCAT/biBiP or monocistronic monoCAT/monoBiP) and effector plasmid (pCMV vhs). Cell lysates were harvested using 1X reporter lysis buffer as previously described. A 15% SDS-PAGE polyacrylamide gel was prepared and samples were run at 100V for 1.5-2 hours. Samples were then transferred to a nitrocellulose membrane using a semi-dry transfer apparatus for 45 minutes at 0.45 A. Membrane was then blocked in Odyssey blocking buffer and TBST buffer for 1 hour at room temperature. Primary antibodies (rabbit polyclonal anti-chloramphenicol acetyltransferase (10µg/mL) and mouse anti-actin (1:5000 dilution) were incubated with membrane in 1:1 Odyssey buffer:TBST at 4°C overnight. The membranes were then washed in TBST and secondary antibodies (Alexa Fluor 680 goat anti-rabbit and Anti-mouse IgG IRDye800, both at 1:10000) were incubated with membrane in 1:1 Odyssey buffer:TBST at room temperature for 1 hour. The membranes were again washed in TBST buffer. Levels of CAT protein were detected using an Odyssey infrared imaging system (Li-COR). Levels of CAT protein were then normalized to the actin control and relative expression levels were assessed.

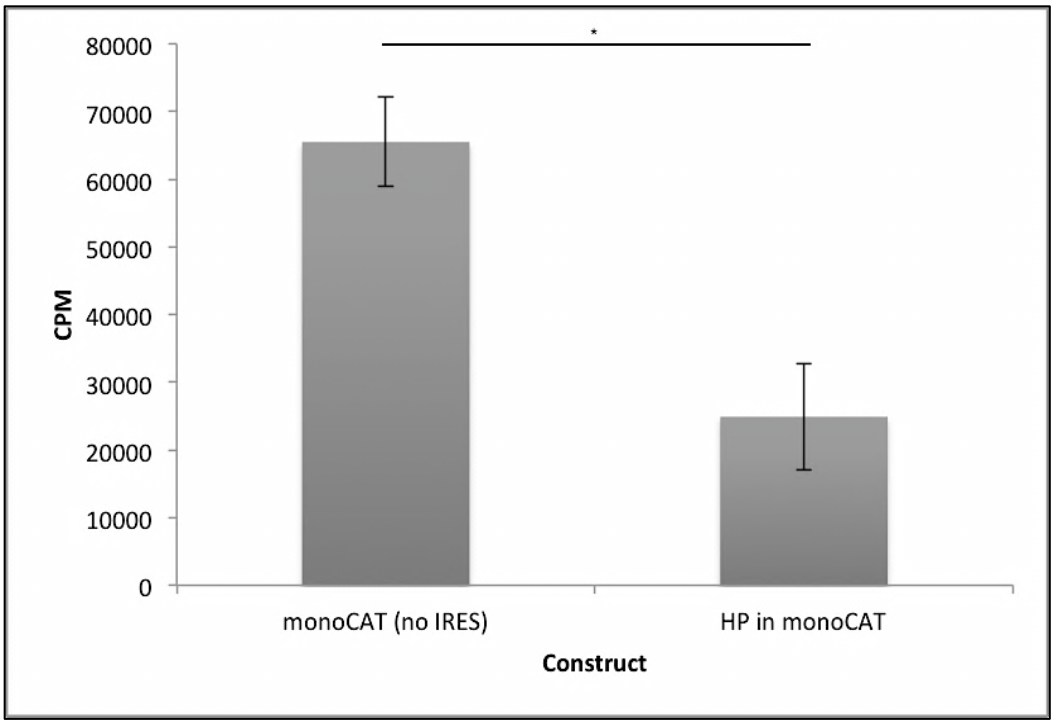

Figure 23: Addition of the hairpin upstream of the CAT cistron significantly decreased CAT activity for the monocistronic constructs in the absence of vhs. Error bars represent standard error of the mean. N=4. * Indicates statistical significance ($p < 0.05$).

HeLa cells were transfected with specified monocistronic reporter plasmid, 'filler' plasmids pUC19 and pCDNA3.1, and effector plasmid of interest (vhs expression plasmid) using Lipofectamine 2000 (Invitrogen; according to manufacturer's instructions). Lysates were harvested and assayed for CAT activity as previously described Chapter 2 (section 2.5) and summarized in Figure 5 legend.

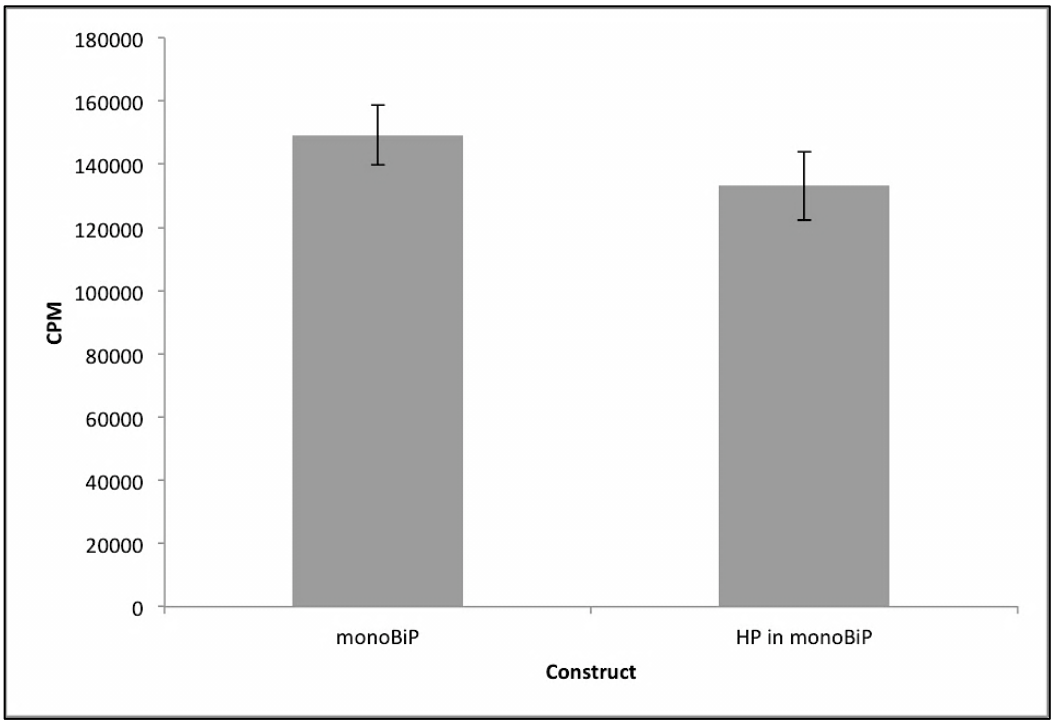

Figure 24: Addition of the hairpin upstream of the BiP IRES had no significant effect on CAT activity for the monocistronic constructs in the absence of vhs. Error bars represent standard error of the mean. N=4.

HeLa cells were transfected with specified monocistronic reporter plasmid, 'filler' plasmids pUC19 and pCDNA3.1, and effector plasmid of interest (vhs expression plasmid) using Lipofectamine 2000 (Invitrogen; according to manufacturer's instructions). Lysates were harvested and assayed for CAT activity as previously described Chapter 2 (section 2.5) and summarized in Figure 5 legend.

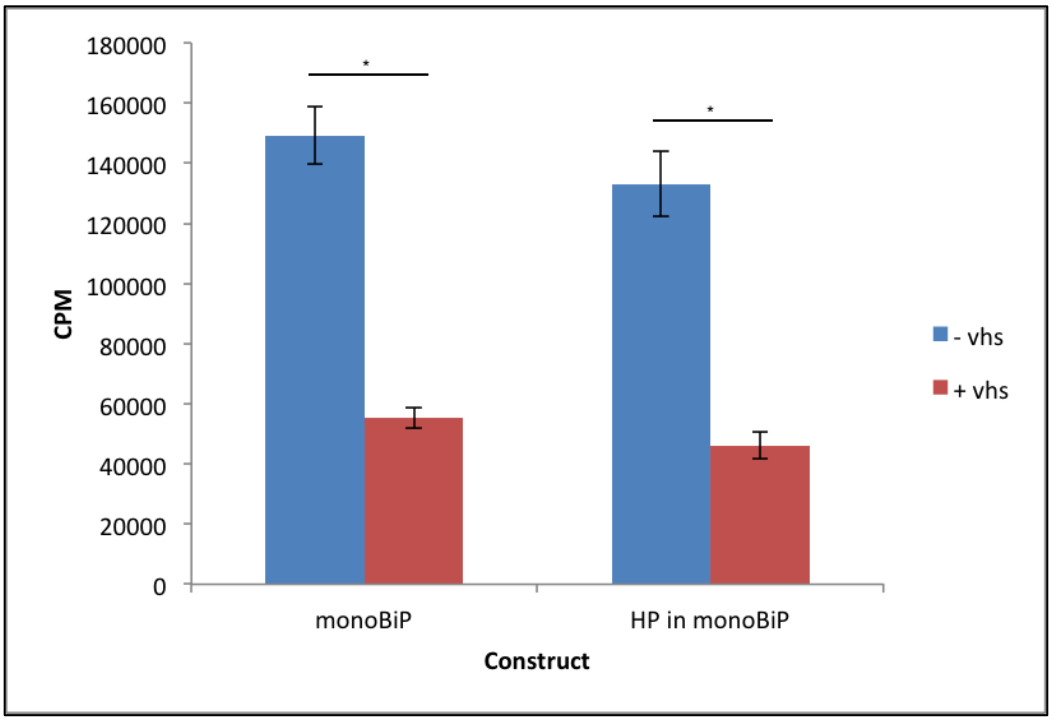

Figure 25: Addition of vhs significantly decreases CAT activity for both monoBiP and HP in monoBiP. N=4. * Indicates statistical significance ($p < 0.05$).

HeLa cells were transfected with specified monocistronic reporter plasmid, 'filler' plasmids pUC19 and pCDNA3.1, and effector plasmid of interest (vhs expression plasmid) using Lipofectamine 2000 (Invitrogen; according to manufacturer's instructions). Lysates were harvested and assayed for CAT activity as previously described Chapter 2 (section 2.5) and summarized in Figure 5 legend.

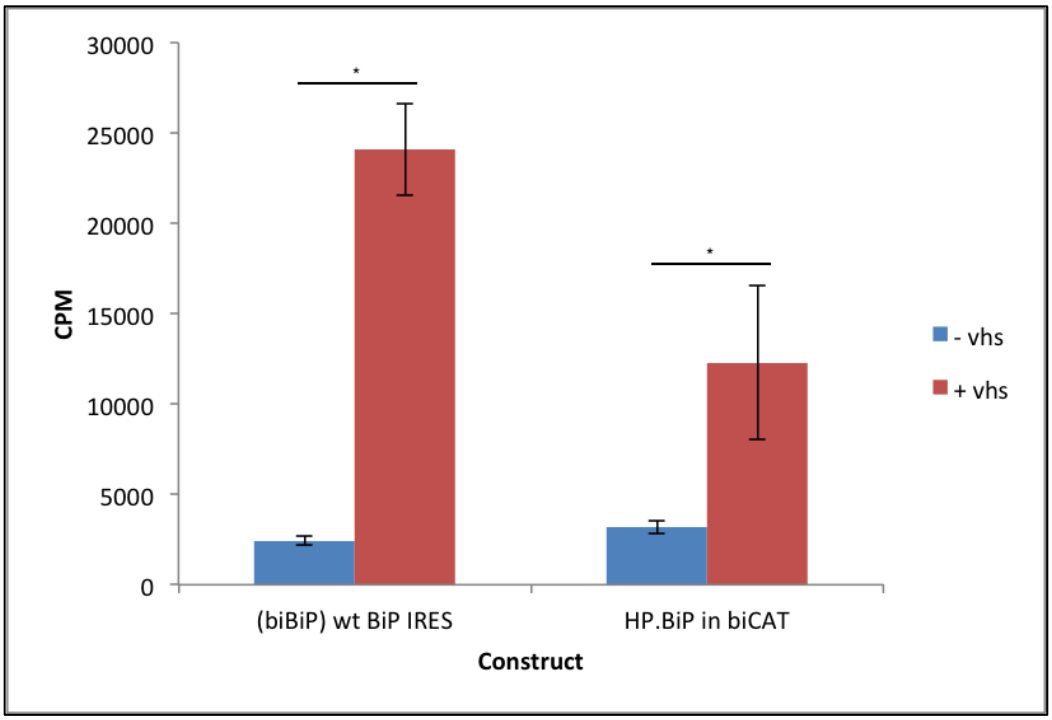

Figure 26: Addition of vhs stimulates CAT activity for both biBiP and HP.BiP in biCAT. Error bars represent standard error of the mean. N=3. * Indicates statistical significance ($p < 0.05$).

HeLa cells were transfected with specified bicistronic reporter plasmid, 'filler' plasmids pUC19 and pCDNA3.1, and effector plasmid of interest (vhs expression plasmid) using Lipofectamine 2000 (Invitrogen; according to manufacturer's instructions). Lysates were harvested and assayed for CAT activity as previously described Chapter 2 (section 2.5) and summarized in Figure 5 legend.

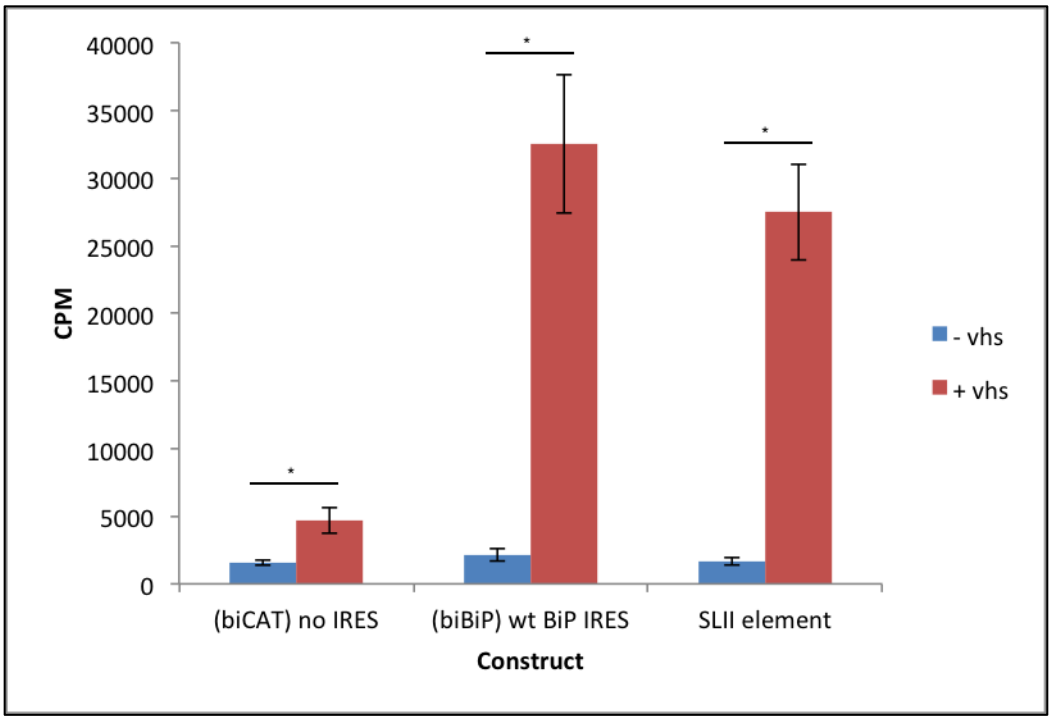

Figure 27: The addition of the intercistronic SLII element significantly increases CAT activity in response to vhs. Error bars represent standard error of the mean. N=5. * Indicates statistical significance ($p < 0.05$).

HeLa cells were transfected with specified bicistronic reporter plasmid, 'filler' plasmids pUC19 and pCDNA3.1, and effector plasmid of interest (vhs expression plasmid) using Lipofectamine 2000 (Invitrogen; according to manufacturer's instructions). Lysates were harvested and assayed for CAT activity as previously described Chapter 2 (section 2.5) and summarized in Figure 5 legend.

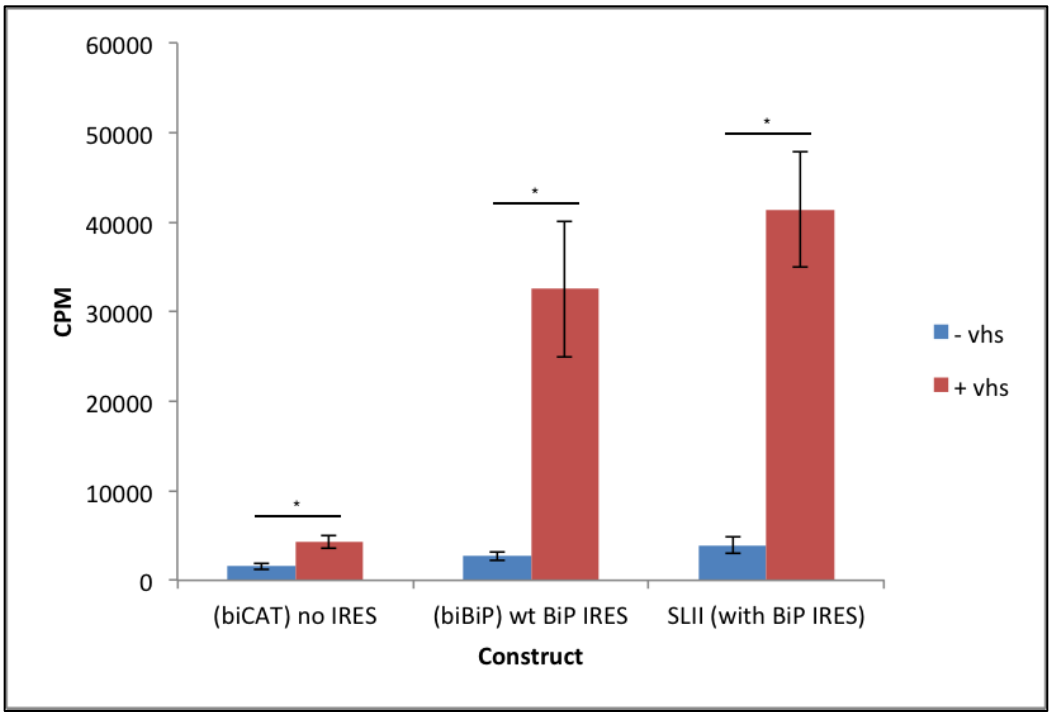

Figure 28: Combining the SLII element and the BiP IRES still results in a significant increase in CAT activity in response to vhs. Error bars represent standard error of the mean. N=5. * Indicates statistical significance ($p < 0.05$).

HeLa cells were transfected with specified bicistronic reporter plasmid, 'filler' plasmids pUC19 and pCDNA3.1, and effector plasmid of interest (vhs expression plasmid) using Lipofectamine 2000 (Invitrogen; according to manufacturer's instructions). Lysates were harvested and assayed for CAT activity as previously described Chapter 2 (section 2.5) and summarized in Figure 5 legend.

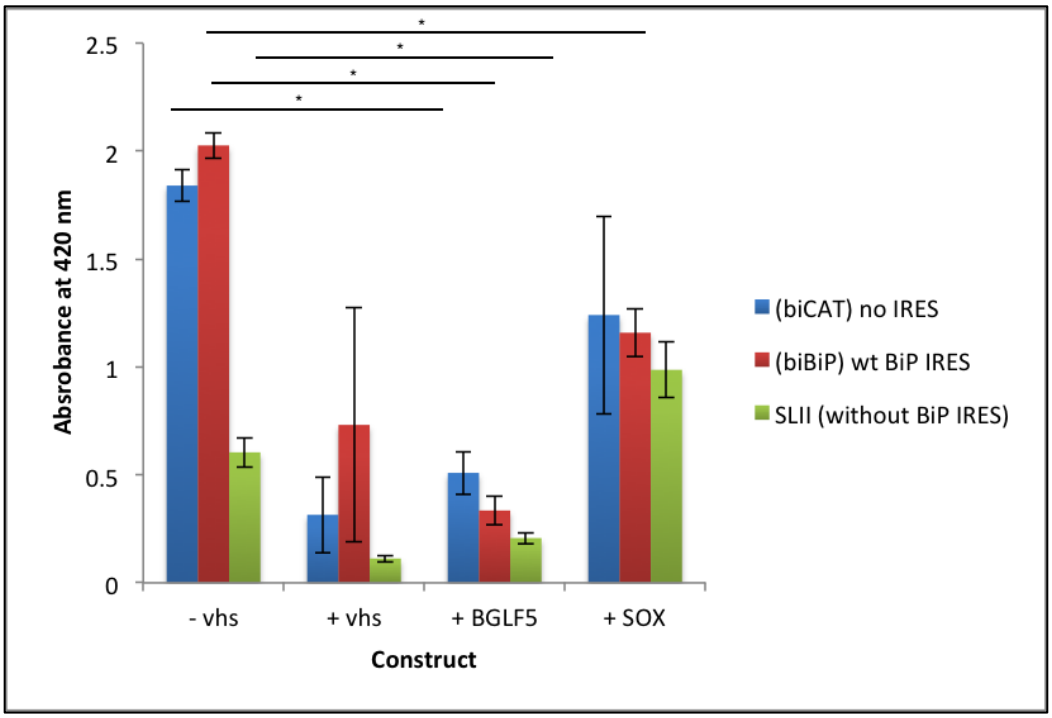

Figure 29: Effect of vhs, BGLF5 or SOX on β-galactosidase activity for biCAT, biBiP and SLII (with BiP IRES). Error bars represent standard error of the mean. N=4. Results for SLII (without BiP IRES) construct (not shown) are similar.

HeLa cells were transfected with specified bicistronic reporter plasmid, 'filler' plasmids pUC19 and pCDNA3.1, and effector plasmid of interest using Lipofectamine 2000 (Invitrogen; according to manufacturer's instructions). Lysates were harvested and assayed for CAT activity as previously described Chapter 2 (section 2.5) and summarized in Figure 5 legend.

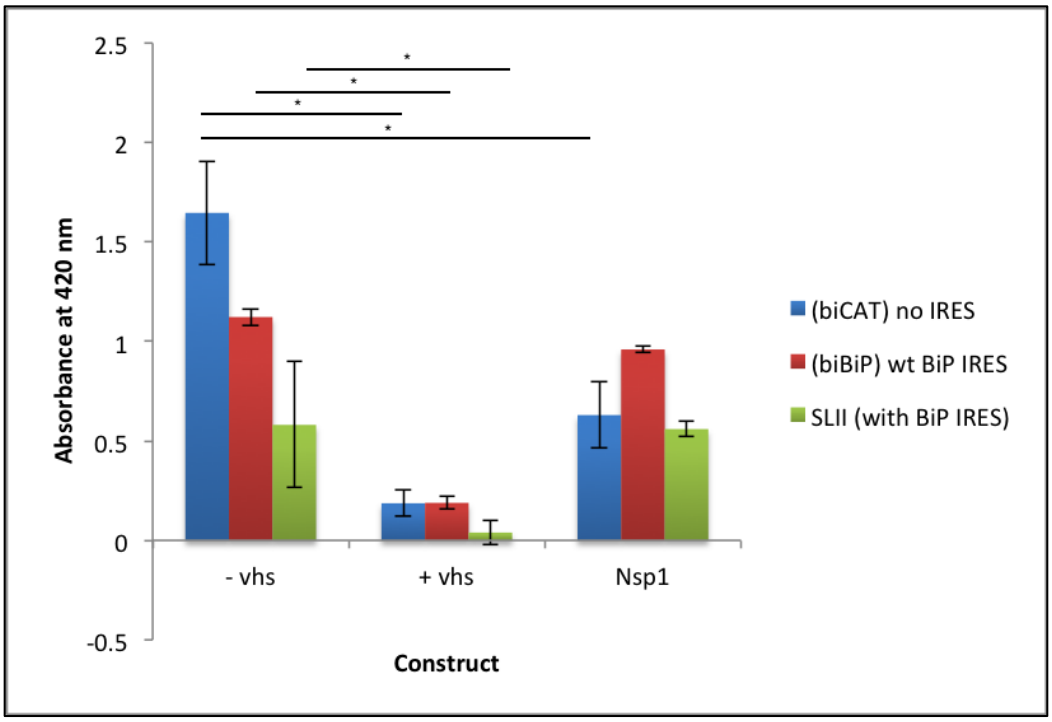

Figure 30: Effect of vhs or Nsp1 on β-galactosidase activity for biCAT, biBiP and biSLII (with BiP IRES). Error bars represent standard error of the mean. N=3. Results for SLII (without BiP IRES) construct (not shown) are similar.

HeLa cells were transfected with specified bicistronic reporter plasmid, 'filler' plasmids pUC19 and pCDNA3.1, and effector plasmid of interest using Lipofectamine 2000 (Invitrogen; according to manufacturer's instructions). Lysates were harvested and assayed for CAT activity as previously described Chapter 2 (section 2.5) and summarized in Figure 5 legend.

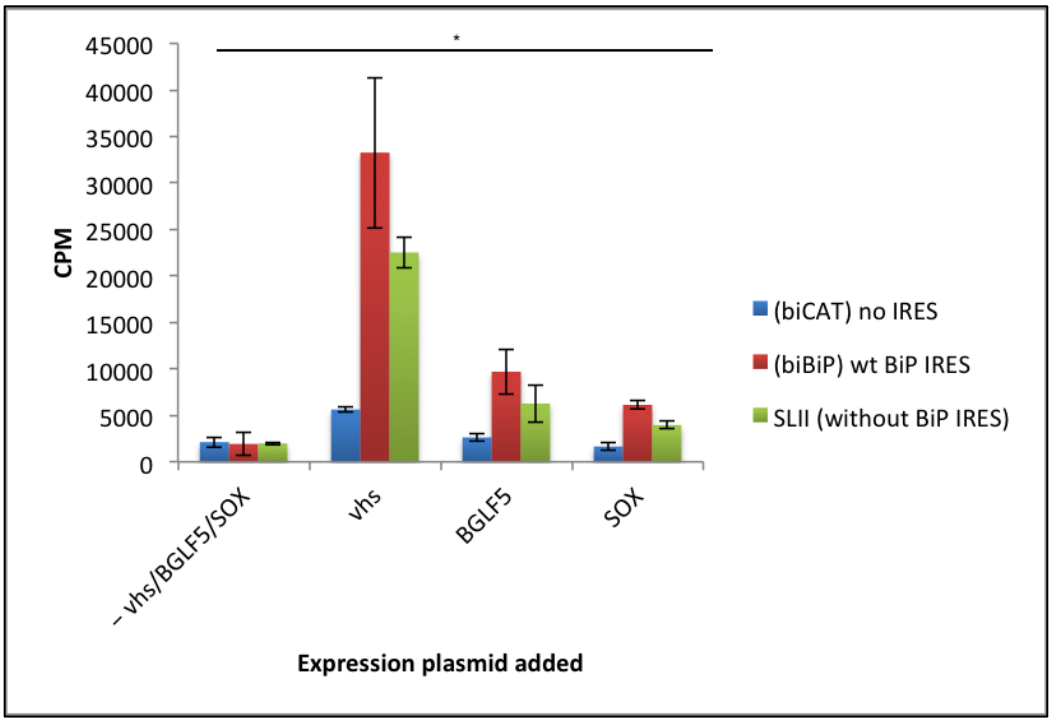

Figure 31: BGLF5 and SOX significantly increase CAT activity. Error bars represent standard error of the mean. N=3. Results for SLII (with BiP IRES) construct (not shown) are similar. * Indicates statistical significance ($p < 0.05$). In this case, all comparisons (except biCAT -/+ BGLF5 and SOX) were determined to be significant.

HeLa cells were transfected with specified bicistronic reporter plasmid, 'filler' plasmids pUC19 and pCDNA3.1, and effector plasmid of interest using Lipofectamine 2000 (Invitrogen; according to manufacturer's instructions). Lysates were harvested and assayed for CAT activity as previously described Chapter 2 (section 2.5) and summarized in Figure 5 legend.

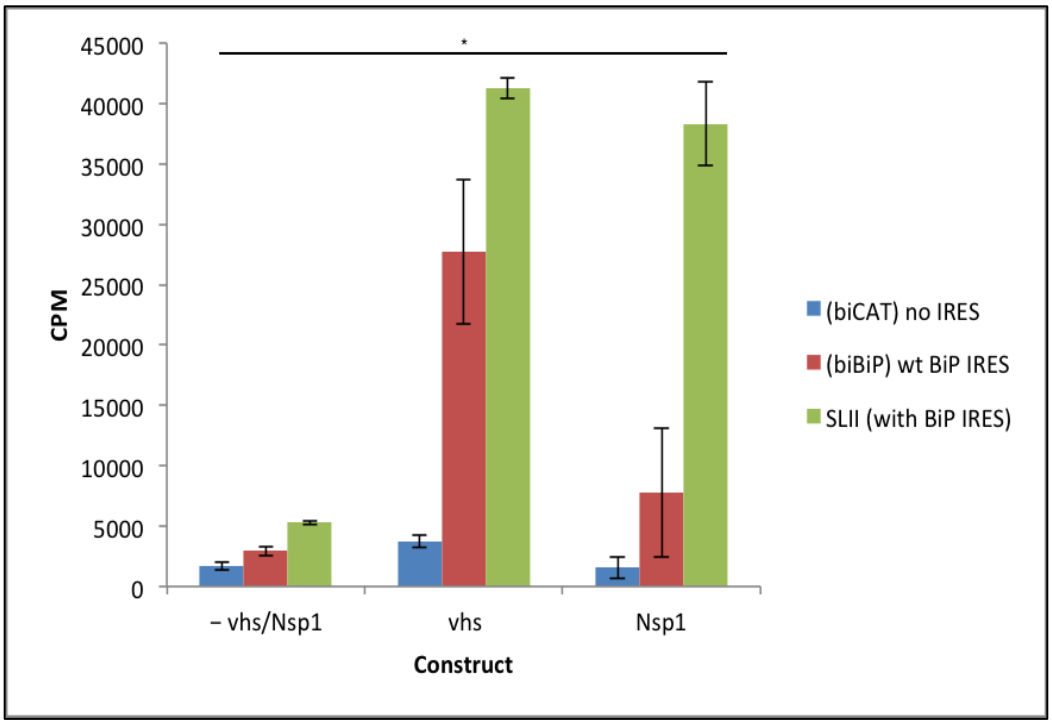

Figure 32: Nsp1 significantly increases CAT activity. Error bars represent standard error of the mean. N=5. * Indicates statistical significance ($p < 0.05$). In this case, all comparisons (except biCAT -/+ Nsp1) were determined to be significant.

HeLa cells were transfected with specified bicistronic reporter plasmid, 'filler' plasmids pUC19 and pCDNA3.1, and effector plasmid of interest using Lipofectamine 2000 (Invitrogen; according to manufacturer's instructions). Lysates were harvested and assayed for CAT activity as previously described Chapter 2 (section 2.5) and summarized in Figure 5 legend.

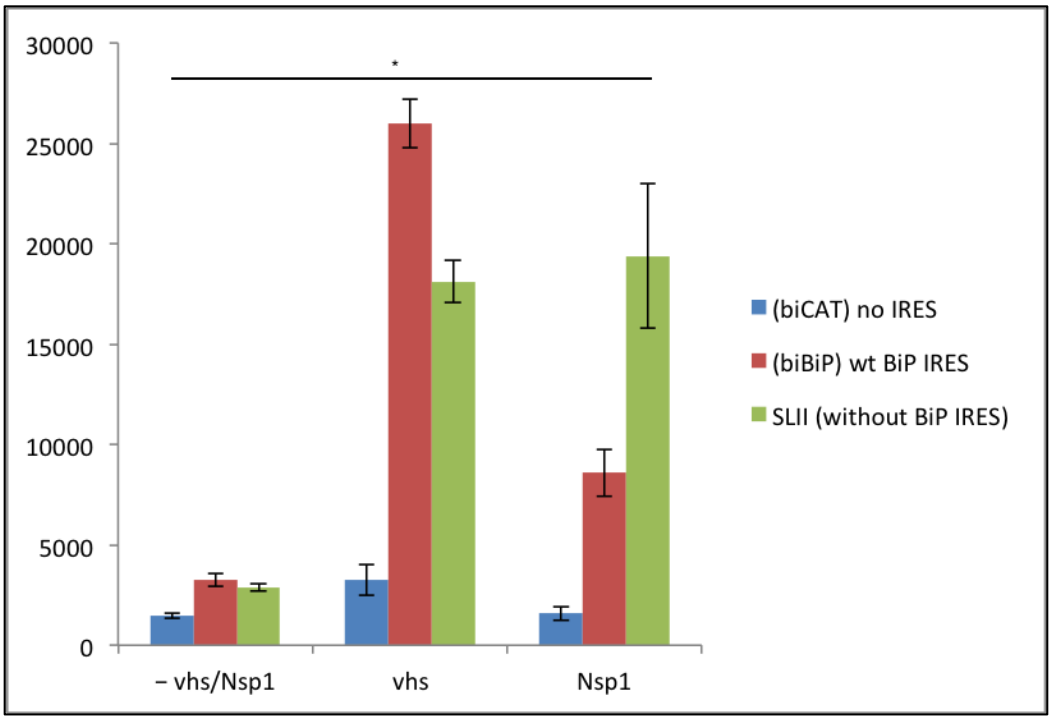

Figure 33: Addition of Nsp1 significantly increases CAT activity when the SLII element is present, even if the BiP IRES is not. Error bars represent standard error of the mean. N=3. * Indicates statistical significance ($p < 0.05$). In this case, all comparisons (except biCAT -/+ Nsp1) were determined to be significant.

HeLa cells were transfected with specified bicistronic reporter plasmid, 'filler' plasmids pUC19 and pCDNA3.1, and effector plasmid of interest using Lipofectamine 2000 (Invitrogen; according to manufacturer's instructions). Lysates were harvested and assayed for CAT activity as previously described Chapter 2 (section 2.5) and summarized in Figure 5 legend.

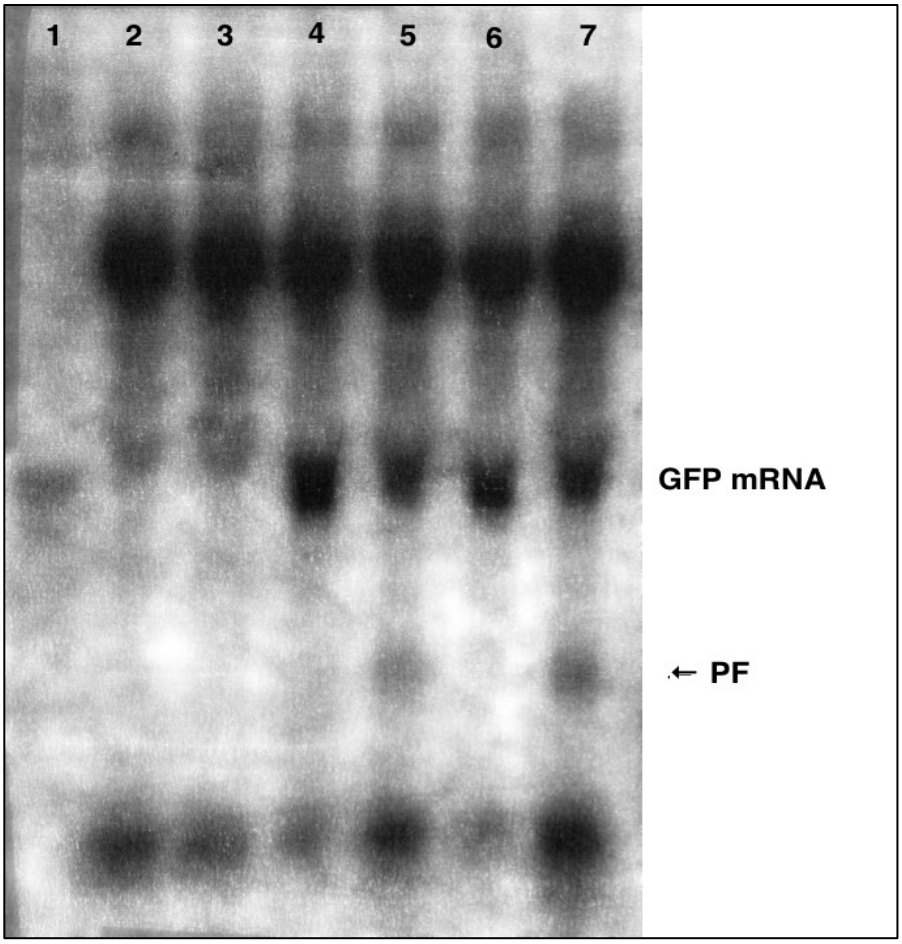

Figure 34: Appearance of the protected fragment (PF, denoted by arrow) indicates that Xrn1 participates in exonucleolytic degradation of the reporter mRNA after the primary endonucleolytic cleavage. (1) 0.5 -10 kB RNA Ladder (Invitrogen), (2) Cells only, (3) Negative control plasmid (biBiP; no SLII element), (4) SLII containing GFP reporter plasmid (pD2EGFP-N1_3'SLII) without vhs, (5) SLII containing GFP reporter plasmid (pD2EGFP-N1_3'SLII) with vhs, (6) Second replicate of (4), (7) Second replicate of (5).

Note: Ladder was not properly denoted, thus accurate prediction of fragment sizes is not possible. However, relative positions are in agreement with Gaglia *et al* (2012).

Experiment modified from Gaglia *et al* (2010; see Figure 3). Briefly, HeLa cells were transfected with a GFP construct containing a flavivirus-derived Xrn1 blocking element in its 3′ untranslated region (pD2EGFP-N1_3'SLII, see Table 1) or a non-SLII containing control plasmid (biBiP), 'filler' plasmids pUC19 and pCDNA3.1, along with vhs effector plasmid (pCMVvhs) as necessary. Total RNA levels were visualized using a Northern blot, probing for the 3′ UTR of the reporter RNA. The data were then evaluated using a Phosphoimager.

CHAPTER 4: DISCUSSION

4.1 SUMMARY OF THESIS RATIONALE

As previously discussed, my study began as a follow-up to the unexpected results obtained by Holly Saffran (Saffran *et al,* 2010). To reiterate, Holly found that in a bicistronic reporter system, vhs is capable of (a) repressing the expression of a 5' β-gal cistron and (b) strongly stimulating expression of the 3' CAT cistron while under the influence of certain putative cellular IRES's, a mutant (non-functional) EMCV IRES and HSV 5′ UTR sequences. The 5' cistron repression was not surprising given the known shutoff activity of vhs. However, the activation of the CAT cistron was both unexpected and novel.

As noted in Holly's report, the most striking response in terms of vhs-induced CAT stimulation was that driven from the putative cellular BiP IRES (see Saffran *et al,* 2010 or Chapter 1 for details). This observed vhs-dependent activation of 3' CAT cistron while under the influence of the BiP IRES was attributed to at least one of two hypotheses: (1) Activation of IRES activity or (2) RNase activity. To reiterate, (1) suggests that vhs promotes cap-independent translation by activating the BiP IRES and (2) suggests that vhs truncates the bicistronic mRNA either alone or in concert with cellular nucleases, resulting in the generation of monocistronic transcripts encompassing the CAT ORF. As previously detailed, the IRES activity hypothesis (1) was originally favored; however, evidence for the RNase hypothesis also exists. Thus, the experiments

described and performed in my study sought to determine which of the above two hypothesis is most correct.

4.2 SUMMARY OF RESULTS

Firstly, I was able to replicate the results obtained by Saffran *et al* (2010) and show that in a bicistronic construct containing an intercistronic BiP IRES (Figure 3), vhs is capable of simultaneously repressing 5' cistron activity and strongly stimulating 3' cistron activity (Figures 4-6).

This stimulation of CAT activity was seemingly specific to the BiP IRES, as it was not observed for the EMCV IRES or a structured non-IRES RNA aptamer (Figures 7-9). Additionally, fragmentation of the BiP IRES did not eliminate the stimulatory response; in all cases, vhs-induced CAT activation was observed (Figures 11-13 and 15-18). A correlation between length of the intercistronic BiP IRES sequence and amount of CAT activation was evident, as longer fragments generally elicited a stronger response.

The BiP IRES does appear to have inherent IRES ability, as this sequence stimulates CAT activity in bicistronic constructs in the absence of vhs (Figure 7). In the absence of vhs, monocistronic constructs show much higher levels of CAT activity than their bicistronic counterparts (Figure 20). Additionally, monoBiP is significantly more active than monoCAT (even when ribosomal scanning is inhibited by a hairpin), suggesting IRES activity contributes to this additional activity. After

addition of vhs, CAT activity for both monoBiP and HP in monoBiP in significantly repressed (Figure 25). In contrast, the addition of vhs significantly increased CAT expression in both the bicistronic counterparts (biBiP and HP.BiP in biCAT; see Figure 26). Thus, it is clear that the response of the BiP IRES sequence to vhs depends on the location of the IRES on the RNA. Specifically, if it is located in the 5' UTR (a biologically relevant location) vhs inhibits CAT expression. Conversely, if it is located in the intercistronic region (not biologically relevant) vhs stimulates CAT expression. These data are fully consistent with the RNase hypothesis, although the details of the mechanism have not yet been elucidated.

Interestingly, a Xrn1 (cellular exonuclease) blocking element (SLII) had the same effect as the BiP IRES in the bicistronic reporter assay in the presence of vhs. Specifically, if the SLII element was present in the intercistronic region, vhs-induced CAT activation still occurred (Figures 27 and 28). Examination of other unrelated nucleases (KHSV SOX, EBV BGLF5 and SARS coronavirus Nsp1) on both 5' cistron repression and 3' cistron stimulation revealed that although only BGLF5 consistently repressed 5' cistron activity, all were capable of stimulating CAT activity.

To summarize, the data presented in this section are consistent with the RNase hypothesis. It seems as if the BiP IRES likely employs 2 strategies to simulate CAT expression in response to vhs; blocking 5' to 3' degradation and enhancing transaction of uncapped degradation products.

Specifically, I hypothesize that vhs activates the 3' CAT cistron according to the following model:

1. Initial vhs-induced cleavage near the 5' end of the RNA upstream of the lacZ gene
2. Subsequent Xrn1-mediated degradation proceeding in a general 5' → 3' direction
3. Enhanced production of transient uncapped monocistronic mRNA encompassing the 3' CAT cistron
4. Enhanced translation of the CAT cistron from monocistronic mRNA, perhaps via IRES activity.

The following sections will detail how the data obtained in my study and other relevant literature support this model.

4.3 DOES THE BIP IRES HAVE INHERENT IRES ACTIVITY?

As detailed in Chapter 1, translation of mRNA can occur independently of the 5’ cap structure. In this case, ribosomes are recruited directly to areas of mRNA containing *cis*-acting, highly structured regulatory elements termed internal ribosome entry sites (IRES’s). One such example is the cellular BiP IRES, which is the focus of this thesis.

Previous reports by several researchers have shown that the BiP IRES sequence does have IRES activity. First of all, Sarnow (1989)

reported that the BiP mRNA was translated at an increased rate in poliovirus infected cells even when components of the cap-binding complex were inhibited. Thus, they proposed that this translation was a result of cap-independent translation via a yet-undetermined mechanism. A decade later, Johannes and Sarnow (1998) proposed that the BiP IRES element was in fact functional in its natural mRNA. Their experiments showed that the BiP IRES containing mRNA not only associates with the translation apparatus but is in fact translated when cap-dependent translation is inhibited by poliovirus infection. Thus, these data suggest that the BiP IRES sequence can indeed promote cap-independent translation of natural monocistronic BiP mRNA.

In my study, the activity of the cellular BiP IRES was first assessed by comparing it to the *bonafide* viral EMCV IRES in terms of its ability to stimulate translation of a 3' CAT ORF when located in a bicistronic reporter plasmid (Figure 3). This bicistronic assay is commonly used to assess IRES ability; if the 3', presumably IRES-controlled cistron is expressed, it is assumed that internal, IRES-mediated translation is responsible.

4.3.1 EVIDENCE FOR IRES ACTIVITY

As initially shown in previous literature (Saffran *et al,* 2010) and confirmed in my study, both the cellular BiP IRES and the viral EMCV IRES area capable of stimulating CAT expression in the absence of vhs;

however, expression driven from the EMCV IRES was substantially greater than that driven from the BiP IRES. Specifically, levels of CAT activity for the EMCV IRES-containing construct (biEMCV) were approximately 5 fold higher than the BiP IRES containing construct (biBiP). Thus, in the absence of vhs, the EMCV IRES is more efficient at stimulating 3' CAT cistron expression when located between cistrons in a bicistronic reporter. This stimulation without influence from vhs presumably reflects inherent IRES activity and it's ability to drive translation of the downstream 3' cistron. Hence, because the presence of either the EMCV IRES or the BiP IRES results in a significant increase in CAT activity, it can be proposed that both have inherent IRES activity.

Additional evidence for the IRES activity of the BiP IRES comes from the analysis of the monocistronic constructs. Specifically, the monocistonic construct containing the BiP IRES (monoBiP) consistently and significantly showed much higher levels of CAT activation than the IRES-less monocistronic construct (monoCAT) in the absence of vhs. Although this result supports the argument that the BiP IRES has inherent IRES activity, it is still uncertain how much of this contribution is due to cap-dependent translation and how much is due to IRES-driven, internal cap-independent initiation. Thus, I used a stable hairpin that blocks ribosomal scanning to impede cap-dependent translation. Consistent with the idea that the BiP IRES has IRES activity, the hairpin had no effect on CAT expression for the monoBiP construct. Conversely, addition of the

hairpin caused a substantial reduction in CAT expression for the monoCAT construct (no IRES) suggesting that the enhanced activity of monoBiP relative to monoCAT stems from IRES activity.

Additionally, monoBiP consistently and significantly showed much higher levels of CAT activation than the bicistronic counterpart biBiP. This indicates that the location of the BiP IRES on the mRNA is important; specifically, the IRES functions significantly better when located at the 5' end of the mRNA transcript. Because no bonafide mammalian bicistronic RNAs have been yet described, this makes biological sense. This interpretation also corresponds with the evidence presented by Sarnow (1989) and Johannes and Sarnow (1998); specifically, that the BiP IRES sequence promotes cap-independent translation of monocistronic BiP mRNA, presumably via IRES activity.

4.3.2 IS THIS EVIDENCE VALID?

Although these data are consistent with the hypothesis that BiP IRES is functioning to stimulate cap-independent translation via its IRES activity, they do not prove this. As previously mentioned, the very existence of cellular IRESs (such as the BiP IRES) is a matter of debate and controversy (Schneider *et al*, 2001 and Kozak, 2001/2005). Criticism of the experimental design (specifically bicistronic reporter assays) has led some researchers to believe a positive result in a bicistronic reporter assay does not indicate the presence of a cellular IRES.

Instead, the seemingly IRES-controlled 3' cistron activation may be the result of a 3′ splice site (ss) located in the IRES sequence or cryptic promoter activity. In these cases, translation of the second (3') cistron is not occurring because of IRES activity; instead, monocistronic mRNAs are either generated via splicing or transcribed from cryptic promoters (Kozak, 2001/2005, Van Eden *et al,* 2004 and Young *et al*, 2008). These alternate mechanisms of 3' cistron activation have lead to many putative cellular IRESs being discounted (Kozak, 2001/2005, Van Eden *et al,* 2004, Bert *et al,* 2006 and Baranick *et al,* 2008). Interestingly, Young *et al* (2008) argue that in their bicistronic reporter assay, apparent BiP IRES-driven activation of the 3' cistron is actually due to cryptic promoter activity, not IRES activity. Thus, in my bicistronic constructs, the observed 3' CAT cistron activation could also be attributed to cryptic promoter activity, not BiP IRES activity.

4.4 DOES IRES ACTIVITY CONTRIBUTE TO VHS-DEPENDENT STIMULATION OF CAT EXPRESSION?

As evidenced in Figure 7 and discussed in the above section (4.3), the BiP IRES may have inherent IRES activity. Whether this putative IRES activity contributes to the average 10-fold increase in CAT activity in response to vhs is unclear. However, it is clear that something specific to the BiP IRES confers CAT expression in response to vhs.

4.4.1 THE ABILITY TO ACTIVATE CAT EXPRESSION IS SPECIFIC TO THE BIP IRES

Initially, I hypothesized that this increased CAT activation is simply a result of increased structural complexity (characteristic of IRES's). However, a construct containing a highly structured non-IRES RNA sequence in the intercistronic regions (biSC) did not elicit any CAT activation. Thus, structured RNA alone is not sufficient to elicit an increase in CAT activity; instead, something specific about the BiP IRES sequence was doing so.

Further to this point, not all IRES's acted like the BiP IRES in response to vhs. For example, the EMCV IRES does not promote CAT expression in the presence of vhs; in fact, CAT activity is substantially reduced by the addition of vhs. Additionally, it has been previously shown that a mutant version of the EMCV IRES (which no longer has IRES activity) is capable of stimulating CAT expression (Saffran et al, 2010). Thus, it seems possible that the vhs-dependent CAT activation is not a function of the IRES activity of the BiP IRES; as the *bonafide* EMCV IRES only displays vhs-dependent activation of CAT expression when it no longer functions as an IRES.

4.4.2 THE BIP IRES DOES NOT RESPOND LIKE OTHER IRES'S

In confirmed IRES's (such as the EMCV IRES) activity can be attributed to the presence of highly specific structures or sequences that

act to recruit either translation factors or the ribosome itself (reviewed in Shatsky *et al*, 2010). Thus, these commonalities are in a way characteristic of IRES's. In contrast, no such commonalities in either structure or sequence have been found amongst putative cellular IRES's, including the BiP IRES. According to Kozac (2005), this alone is evidence that cellular IRES's do not exist. These specific structural features are so important to viral IRES's (such as the EMCV IRES and the Poliovirus IRES) that even small deletions or point mutations completely eradicate the IRES's ability to initiate translation (Svitkin *et al*, 1985, Kuge and Nomoto, 1987, Trono *et al*, 1988 and Van Der Velden, 1995).

This is in direct contrast to the BiP IRES; even large manipulations and fragmentations did not kill its ability to stimulate CAT expression in response to vhs. As described in Chapter 3, all of the BiP IRES fragments tested showed an increase in CAT activity above the no IRES control, and all of these differences were determined to be significant ($p < 0.05$). These data clearly indicate that the full-length IRES sequence is not needed to stimulate expression of the CAT cistron when vhs is present.

These data are consistent with that reported by Yang and Sarnow (1997). These researchers performed similar experiments and found that fragmentation of the BiP IRES did not kill its ability to stimulate 3' cistron (in their case, luciferase) expression. Additionally, Yang and Sarnow's constructs lacking the middle portion of the BiP IRES (analogous to my BiP 1/3 fusion fragment) conferred nearly 100% of wild-type activity. This

was consistent with my data, which clearly show that this BiP 1/3 fusion fragment stimulates 3' CAT expression as well as the full-length BiP IRES sequence. However, not all of Yang and Sarnow's results were consistent with my data. For example, in their experiments the 3' fragment (analogous to my BiP 3) conferred nearly 100% of wild-type activity, where as the 5' and middle fragments (analogous to my BiP 1 and 2 respectively) only conferred between 37-64% of wild-type activity. This is in contrast to my data; BiP 3 did not confer any more activation than BiP 1,2,4 or 5. These researchers propose that this 3' region of the BiP IRES contains binding sites for RNA-binding proteins p60 and p95, which are proposed to contribute to internal initiation (Yang and Sarnow, 1997).

Although it is still unclear how the BiP IRES (either full-length or fragmented) is stimulating CAT activity, a relationship between length of the intercistronic BiP RNA and amount of vhs-induced CAT expression did emerge. As shown in Chapter 3, longer fragments were capable of supporting levels of vhs-dependent CAT expression close to that of the full-length BiP IRES sequence. Given the proposed sensitivity of IRES sequences to manipulation, this result does not lend support to the idea that the vhs-induced stimulation of the CAT cistron stems from IRES activity in this study; rather, some other feature of the BiP IRES is likely responsible. It is possible that within the context of the BiP IRES sequence, structural complexity is important. Another interpretation is that one or more response elements are present within the BiP IRES

sequence. If this were the case, tandemizing these elements would increase the number of response elements and thus the response to vhs. It is possible that the proposed RNA-binding protein binding sites thought to contribute to internal initiation by Yang and Sarnow (1997) act as these response elements.

In summary, it is currently unclear if the IRES activity of the BiP is contributing to the increase in CAT expression in response to vhs. However, is it clear that the sequences with the ability to activate 3' cistron expression appear to be evenly distributed throughout the BiP IRES sequence. Additionally, not all IRES sequences or structured RNA sequences have this ability.

4.5 EVIDENCE FOR RNASE ACTIVITY

As discussed in section 4.3.1, monocistronic constructs show much higher levels of CAT activity in the absence of vhs than their bicistronic counterparts. Additionally, monoBiP is significantly more active than monoCAT (even when ribosomal scanning is inhibited by a hairpin), suggesting IRES activity contributes to this additional activity. Despite these data providing evidence for the IRES activity of the BiP IRES, there is no evidence to support the idea that the IRES activity of the BiP IRES is directly responsible for the increase in CAT expression in response to vhs. Thus, the alternate hypothesis (RNase activity) must be considered.

4.5.1 VHS-INDUCED INHIBITION OF CAT ACTIVITY ENCODED BY MONOCISTRONIC TRANSCRIPTS

According to the RNase hypothesis, vhs promotes CAT expression by degrading the 5' cistron, thus generating monocistronic transcripts encompassing the CAT ORF. If this were the case, the effect of vhs on CAT expression should be very different when that construct is already monocistronic. As predicted by the RNase model, the addition of vhs significantly repressed CAT expression from the monocistronic constructs. Thus, the data suggest vhs acts to promote CAT expression from the bicistronic constructs by degrading the 5' cistron, resulting in a translatable monocistronic transcript encompassing the CAT ORF. In contrast, if the construct is already monocistronic, there is no 5' cistron to degrade and the CAT cistron is targeted instead, resulting in the observed decrease in CAT activity.

4.5.2 5' β-GAL CISTRON REPRESSION AND VISIBLE LOSS OF mRNA

As initially reported by Saffran *et al* (2010) and confirmed in my study, vhs is capable of strongly repressing 5' cistron activity (β-gal assays; Figures 4 and 6). This vhs-induced repression was observed in all constructs tested and was shown to be dose-dependent (Figure 4).

According to the RNase activity model, this repression is presumably due to loss of mRNA containing the 5' β-gal cistron due to nuclease-mediated degradation. As discussed above, this theory is

supported by the data thus far. However, as mentioned in previous sections, the IRES activity hypothesis was originally favored because no visible loss of RNA could be detected. Thus, the most likely interpretation was that both the vhs-induced 5' cistron repression and 3' cistron stimulation were due to translational effects. Thus, without visible loss of RNA, the RNase model does not most accurately explain these data.

In my study, I was able to show a loss of mRNA in response to vhs (Northern blot; Figure 34), albeit not using the biBiP plasmid. Preliminary experiments indicate this may also occur using poly-A isolated mRNA (data not shown). If this were the case, this result is in agreement with this presumption that 5' cistron repression is due to loss of mRNA containing the 5' β-gal cistron due to nuclease-mediated degradation. Taken in conjunction with the monocistronic construct data (shows the addition of vhs consistently resulted in repression of the now 5' CAT cistron) the most likely interpretation is that the mRNA directly downstream of the 5' cap-structure is targeted for degradation.

These data corroborate previous studies regarding the mechanism of vhs-induced degradation. Specifically, it is proposed that vhs is recruited exclusively to mRNA, targeting regions of translation initiation presumably through documented interactions with translation initiation factors and the cap-binding complex (Karr and Read, 1999, Feng *et al,* 2001/2005 Doepker *et al,* 2004 and Page and Read, 2010). Perez-Parada *et al* (2004) initially proposed a mechanism involving removal of the 5' cap

structure by vhs, followed by a directed 5' to 3' degradation of the mRNA transcript. Thus, according to this model, addition of vhs should result in a loss of mRNA and a marked decrease in 5' cistron translation products (β-gal). Both of the predictions were confirmed in my study.

More recently, Gaglia *et al* (2012) elaborated on this model by suggesting that vhs is only responsible for the initial endonucleolytic cleavage; subsequent 5' to 3' degradation is completed by the cellular exonuclease XrnI. Interestingly, this same mechanism was proposed for other nucleases, such as KSHV SOX, EBV BGLF5 and the betacoronavirus SARS coronavirus Nsp1 nuclease (Gaglia *et al*, 2010). In my study, only BGLF5 was capable of repressing 5' β-gal cistron activity in the bicistronic constructs. However, it is known that these nucleases are recruited differently to the mRNA; it is the dependence on the host degradation machinery (specifically Xrn1) that is stressed as the commonality in the report by Gaglia *et al* (2012). Perhaps, SOX and Nsp1 are not effectively recruited to the mRNA, and thus cannot make the initial endonucleolytic cleavage required for repression of β-gal activity.

Unfortunately, β-gal assays have a major limitation; they cannot by themselves determine the relative contribution of vhs and other nucleases (such as Xrn1) to the observed repression. Thus, although the role of vhs in this context appears to be relatively clear, the role of Xrn1 cannot be determined based on the β-gal assays alone. In future experiments, siRNAs blocking Xrn1 expression could be used to assess the contribution

of Xrn1. Following transient transfection with the reporter plasmid, vhs, and the siRNA, RNA could isolated and intact β-gal RNA detected on a Northern blot by a radiolabelled probe specific to the β-gal sequence.

4.6 ROLE OF XRN1 IN RNA DEGRADATION

As discussed in the previous section (4.5), the 5' β-gal cistron repression consistently observed in response to vhs is consistent with the RNase activity hypothesis, and also fits the model proposed by other researchers (Perez-Parada *et al,* 2004 and Gaglia *et al,* 2010). However, as discussed, these β-gal data only provide evidence that vhs is participating in the degradation; the contribution of other nuclease (specifically Xrn1) is unclear.

To help determine the contribution of this nuclease, a flavivirus derived Xrn1-blocking SLII element was inserted into the intercistronic region. If model proposed by Gaglia *et al* (2012) is correct, this element should protect the downstream CAT RNA, allowing it to be translated. Examination of constructs containing the SLII element show that the addition of vhs resulted in a substantial increase in CAT expression. Thus, the Xrn1 nuclease-blocking element has the same effect on CAT expression as the BiP IRES.

This finding provides additional evidence that IRES activity of the BiP IRES is not responsible for the increase in CAT expression. Rather, this provides further support for the Gaglia *et al* (2012) model; that is, vhs

performs an initial endonucleolytic cleavage and Xrn1 completes degradation in a 5' to 3' direction. If this were the case, then the BiP IRES sequence likely acts in a similar way as the SLII element to block Xrn1 mediated degradation. According to this model, the downstream CAT RNA is protected and can be translated.

Interestingly, a recent report by Hutin *et al* (2013) shows that a specific sequence in the 3' UTR of the mRNA encoding IL-6 is capable of inhibiting cleavage by SOX. They have deemed this sequence the SOX-resistant element (SRE). Although it is thus unclear how exactly the SRE confers resistance, they suggest that it functions in association with other proteins to promote transcript instability. Perhaps, a similar mechanism is at work in the case of the BiP IRES and vhs, leading to stabilization of the RNA spanning the CAT cistron.

4.7 OTHER VIRAL HOST SHUTOFF NUCLEASES STIMULATE CAT ACTIVITY

Given the proposed model for vhs-induced CAT activation, it stands to reason that other, unrelated viral host shutoff nucleases may have a similar effect on CAT activity. As shown in Chapter 3, other herpesvirus nucleases (BGLF5 and SOX) and the SARS coronavirus nuclease Nsp1 have differing effects on both 5' β-gal cistron and the 3' CAT cistron. Their effect on 5' β-gal cistron expression was discussed in section 3.8

In terms of their ability to stimulate the 3' CAT cistron, all three nucleases were capable of significantly stimulating CAT expression. Interestingly, only Nsp1 was capable of stimulating the substantial increases in CAT activity consistent with addition of vhs. Additionally, the presence of the SLII element was required for this substantial Nsp1-induced CAT activation. Thus, in this experiment, the SLII element is to Nsp1 what the BiP IRES is to vhs.

Given the apparent similarities of SLII and the BiP IRES in this experiment, perhaps the BiP IRES is functioning to block the nuclease activity of vhs, thus protecting the downstream CAT RNA from nuclease degradation and allowing it to be translated. This would be consistent with the model suggested by Gaglia *et al* (2012); to reiterate, they suggest that vhs makes an initial endonucleolytic cleavage close to the 5' end of the mRNA transcript, and the cellular exonuclease XrnI completes the degradation, proceeding in a 5'-to-3' direction. Interestingly, this report suggested a similar mechanism of action for SOX, BGLF5 and Nsp1.

4.8 POSSIBLE BIOLOGICAL RELEVANCE

Many HSV mRNAs fall into 3' coterminal families and thus contain more than one open reading frame on a single piece of RNA (Figure 36; Attrill *et al,* 2002). Although the current hypothesis is that each ORF is translated only when located at the 5' end (for example, only UL14 is made from the largest mRNA; see Figure 36) it seems conceivable that

vhs allows for translation of internal ORF's (J. Smiley, personal communication). As evidenced by my study, vhs allows translation of ORF's that are not located at the 5' end of a transcript. As predicted by the data obtained in my study (consistent with the RNase model) this most likely begins with removal of the 5' cap and subsequent directed 5' to 3' degradation of the mRNA, mediated by vhs and Xrn1. This degradation may be halted by the presence of specific secondary structures in the UTR region of the newly uncapped mRNA. If this were the case, vhs may allow for translation of internal ORF's such as those depicted in Figure 35.

4.9 CONCLUSION

Based on the data presented in my study, I believe that the RNase activity hypothesis is most likely. This conclusion and the model it generates are in agreement with previous literature on the topic (most relevant: Gaglia *et al*, 2010).

Specifically, I hypothesize that vhs (or BGFL5, SOX or Nsp1) cleave the RNA near the 5' end, upstream of the lacZ gene. This results in repression of the 5' β-gal cistron. This initial cleavage is followed by Xrn1-mediated degradation in a general 5' to 3' direction. This degradation can be blocked by RNA elements such as the SLII element and the BiP IRES. Thus, an excess of uncapped monocistronic mRNAs encompassing the 3' CAT cistron are produced. These transcripts are then translated and CAT

is synthesized. When the BiP IRES/SLII element is not present, nuclease-mediated degradation continues and repression of the CAT cistron occurs.

Translation of the CAT mRNA from these uncapped monocistronic mRNAs occurs presumably via a 5' end-dependent, cap-independent mechanism. Recently, Andreev *et al* (2013) not only confirmed the occurrence of 5' end-dependent, cap-independent translation, but also linked this to the presence of specific secondary structure in the 5' UTR of the uncapped mRNA. These researchers propose that this secondary structure acts to recruit components of the scanning apparatus (such as initiation factors) allowing scanning to begin at the 5' end, independent of the cap. Perhaps, the BiP IRES (and the SLII element) are enhancing translation by functioning as the specialized secondary structures described by this group. Specifically, they may be acting to attract initiation factors (and thus vhs; recall, vhs binds several initiation factors) and thus enhances 5' end-dependent, cap-independent translation of the CAT mRNA. Alternatively, the IRES activity of the BiP IRES may be contributing to the enhanced translation from the uncapped monocistronic RNA's.

This RNase degradation model could be tested using Northern blots similar to those presented in this study. Specifically, by probing for CAT mRNA generated from constructs containing the SLII element (biSLII) or the BiP IRES (biBiP) and those which do not contain these elements (biCAT) both in the presence and absence of vhs. If the proposed model

is true, those constructs that contain ‘protective’ RNA elements such as the SLII element and the BiP IRES should show detectable levels of CAT mRNA; those that do not contain these elements should not. The former was confirmed in my study, however the latter could not be due to experimental difficulties. Further refining of the experimental procedures should allow this question to be answered.

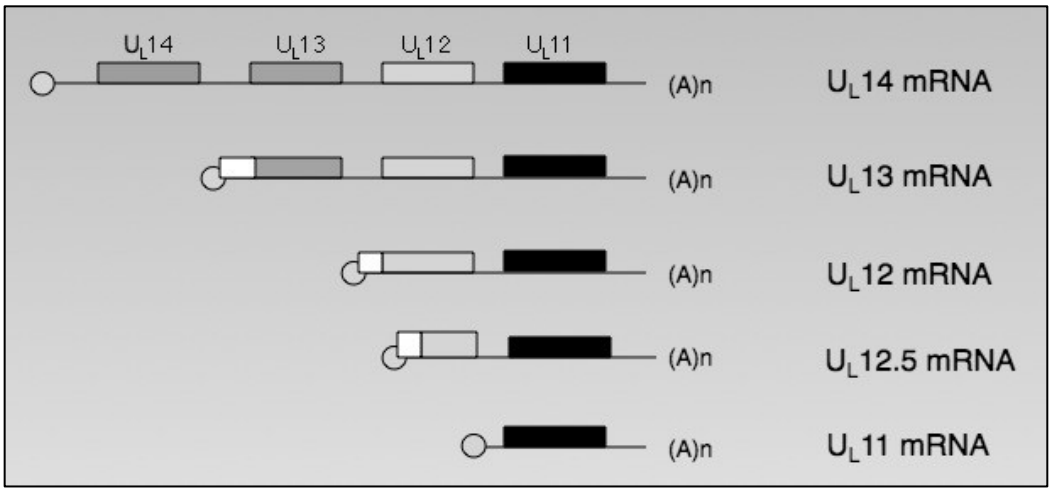

Figure 35: Schematic representation of mRNA's arising from the UL14 to UL11 region of the viral genome. The 5' cap is indicated by the circle on the left hand (5') region of the mRNA.

CHAPTER 5: REFERENCES

Abaitua F, Souto RN, Browne H, Daikoku T, O'Hare P. "Characterization of the Herpes Simplex Virus (HSV)-1 Tegument Protein Vp1-2 During Infection with the HSV Temperature-Sensitive Mutant Tsb7." *J Gen Virol* 90, no. 10 (2009): 2353-2363.

Adelman K, et al. "Herpes Simplex DNA Packaging Sequences Adopt Novel Structures That Are Specifically Recognized by a Component of the Cleavage and Packaging Machinery." *Proc Natl Acad Sci* 98, (2001): 3086-3091.

Advani SJ, Brandimarti R, Weichselbaum RR, Roizman B "The Disappearance of Cyclins a and B and the Increase in Activity of the G(2)/M-Phase Cellular Kinase Cdc2 in Herpes Simplex Virus 1-Infected Cells Require Expression of the Alpha22/U(S)1.5 and U(L)13 Viral Genes." *J Virology* 74, no. 1 (2000): 8-15.

Advani SJ, Weichselbaum RR, Roizman B. "The Role of Cdc2 in the Expression of Herpes Simplex Virus Genes." *Proc Natl Acad Sci* 97, no. 20 (2000): 10996-11001.

Andreev DE, Dmitriev SE, Terenin IM and Shatsky IN. “Cap-Independent Translation Initiation of Apaf-1 mRNA Based on a Scanning Mechanism Is Determined by Some Features of the Secondary Structure of Its 5’ Untranslated Region”. *Biochemistry (Mosc)* 78(2013):157-165.

Aslani A, Olsson M, Elias P. "Atp-Dependent Unwinding of a Minimal Origin of DNA Replication by the Origin-Binding Protein and the Single-Strand DNA-Binding Protein ICP8 from Herpes Simplex Virus Type I." *J Biol Chem* 277, (2002): 41204–41212.

Atanasiu D, Saw WT, Cohen GH, Eisenberg RJ. "Cascade of Events Governing Cell-Cell Fusion Induced by Herpes Simplex Virus Glycoproteins gD, gH/gl, and gB." *J Virology* 84, (2010): 12292–12299.

Attrill HL, Cumming SA, Clements JB and Graham SV. “The Herpes Simplex Virus Type 1 US11 Protein Binds the Coterminal UL12, UL13, and UL14 RNAs and Regulates UL13 Expression In Vivo.” *J Virol* 76, (2002): 8090.

Baird SD, Turcotte M, Korneluk RG, Holcik M "Searching for IRES." *RNA* 12, (2006): 1755-1785.

Baranick BT, Lemp NA, Nagashima J, Hiraoka K, Kasahara N, Logg CR. "Splicing Mediates the Activity of Four Putative Cellular Internal Ribosome Entry Sites." *Proc Natl Acad Sci* 105, no. 12 (2008).

Bastian TW, Livingston CM, Weller SK, Rice SA. "Herpes Simplex Virus Type 1 Immediate-Early Protein ICP22 Is Required for Vice Domain Formation During Productive Viral Infection." *J Virology* 84, no. 5 (2010): 2384–2394.

Beinert D, Neumann L, Uebel S, Tampé R. "Structure of the Viral Tap-Inhibitor ICP47 Induced by Membrane Association." *Biochemistry* 36, no. 15 (1997): 4694-4700.

Bert AG, Grépin R, Vadas MA, Goodall GJ. “Assessing IRES activity in the HIF-1alpha and other cellular 5' UTRs.” *RNA* 12, (2006):1074-83.

Boehmer PE, Lehman, IR "Herpes Simplex Virus DNA Replication." *Annu Rev Biochem* 66, (1997): 347-351.

Bogani F, Corredeira I, Fernandez V, Sattler U, Rutvisuttinunt W, Defais M, Boehmer PE. "Association between the Herpes Simplex Virus-1 DNA Polymerase and Uracil DNA Glycosylase." *J Biol Chem* 285, (2010): 27664–27672.

Boissiere O, Hughes T, Hare P. "Hcf-Dependent Nuclear Import of Vp16. " *EMBO J* 18480, (1999): 489-489.

Bole DG, Hendershot LM, and Kearney JF**.** “Posttranslational association of immunoglobulin heavy chain binding protein with nascent heavy chains in nonsecreting and secreting hybridomas.” *J. Cell Biol.* 102 (1986)**:**1558-1566.

Booy FP, et al. "Liquid Crystalline, Phage-Like Packaging of Encapsidated DNA in Herpes Simplex Virus." *Cell* 64, (1991): 1007-1015.

Boutell C, Canning M, Orr A, Everett RD. "Reciprocal Activities between Herpes Simplex Virus Type 1 Regulatory Protein ICP0, a Ubiquitin E3 Ligase, and Ubiquitin-Specific Protease Usp7." *J Virology* 79, (2005): 12342-12354.

Boutell C, Everett RD. “Regulation of alphaherpesvirus infections by the ICP0 family of proteins.” *J Gen Virology* 94, (2013): 465–481.

Brady RC, Bernstein DI. "Review Treatment of Herpes Simplex Virus Infections." *Antiviral Res* 61, (2004): 73-81.

Bryan HE, Wadd SE, Lamond AI, Silverstein SJ, Clements JB "Herpes Simplex Virus Ie63 (ICP27) Protein Interacts with Spliceosome-Associated Protein 145 and Inhibits Splicing Prior to the First Catalytic Step." *J Virology* 75, (2001): 4376-4395.

Cairns TM, Landsburg DJ, Whitbeck JC, Eisenberg RJ, Cohen GH. "Contribution of Cysteine Residues to the Structure and Function of Herpes Simplex Virus Gh/G." *Virology* 332, (2005): 550–562.

Cardone G, Newcomb WW, Cheng N, Wingfield PT, Benes LT, Brown JC, Steven AC. "The Ul36 Tegument Protein of Herpes Simplex Virus 1 Has a Composite Binding Site at the Capsid Vertices." *J Virology* 86, no. 8 (2012): 4058-4064.

Carfi A, Willis SH, Whitbeck JC, et al. "Herpes Simplex Virus Glycoprotein D Bound to the Human Receptorhvea." *Molecular Cell* 8, no. 1 (2001): 169- 179.

Carrozza MJ, DeLuca NA. "Interaction of the Viral Activator Protein ICP4 with Tfiid through Taf250." *Mol. Cell Biol* 16, (1996): 3085–3093.

Challberg M. *Herpesvirus DNA Replication*: Cold Spring Harbor Monograph Archive, 1996.

Chaurushiya MS, Lilley CE, Aslanian A, Meisenhelder J, Scott DC, Landry S, Ticau S, Boutell C, Yates JR, Schulman BA, Hunter T, Weitzman MD. "Viral E3 Ubiquitin Ligase-Mediated Degradation of a Cellular E3: Viral Mimicry of a Cellular Phosphorylation Mark Targets the Rnf8 Fha Domain." *Mol. Cell* 49, (2012): 79-90.

Chen IB, Sciabica KS, Sandri-Goldin RM. "ICP27 Interacts with the Export Factor Aly/Ref to Direct Herpes Simplex Virus 1 Intronless Rnas to the Tap Export Pathway." *J Virology* 76, (2002): 12877-12889.

Chen Y, Bai P, Mackay S, Korza G, Carson JH, Kuchta RD, Weller SK. "Herpes Simplex Virus Type 1 Helicase-Primase: DNA Binding and Consequent Protein Oligomerization and Primase Activation." *J Virology* 85, (2011): 968–978.

Connolly SA, Landsburg DJ, Carfi A, et al. . "Structure- Based Analysis of the Herpessimplex Virus Glycoproteind Binding Site Present on Herpesvirus Entry Mediatorhvea(Hvem)." *J Virology* 76, (2002): 10894- 10904.

Connolly SA, Landsburg DJ, Carfi A, et al. "Potential Nectin- 1 Binding Site on Herpes Simplex Virusglycoprotein D." *J Virology* 79, no. 2 (2005): 1282- 1295.

Corey L, Spear PG. "Infections with Herpes Simplex Viruses " *N Engl J Med* 314, (1986): 686-691.

Costanzo F, Campadelli-Fiume G, Foa-Tomasi L, Cassai E. "Evidence That

Herpes Simplex Virus DNA Is Transcribed by Cellular RNA Polymerase B." *J Virology* 21, (1977): 996-1001.

Clyde K and Glaunsinger BA. “Deep sequencing reveals direct targets of gammaherpesvirus-induced mRNA decay and suggests that multiple mechanisms govern cellular transcript escape.” *PLoS One* 6, (2011)

Dai-Ju JQ, Li L, Johnson LA, Sandri-Goldin RM "ICP27 Interacts with the C-Terminal Domain of RNA Polymerase Ii and Facilitates Its Recruitment to Herpes Simplex Virus-1 Transcription Sites, Where It Undergoes Proteasomal Degradation During Infection." *J Virology* 80, (2006): 3567-3581.

Dauber B, Pelletier J, Smiley JR. "The Herpes Simplex Virus 1 Vhs Protein Enhances Translation of Viral True Late MRNAs and Virus Production in a Cell Type-Dependent Manner." *J Virology* 85, (2011): 5363-5373.

de Breyne S, Yu Y, Unbehaun A, Pestova TV, Hellen CUT. "Direct Functional Interaction of Initiation Factor Eif4g with Type 1 Internal Ribosomal Entry Sites." *Proc Natl Acad Sci* 106, (2009): 9197-9202.

DeLuca NA, Schaffer PA. "Activation of Immediate-Early, Early, and Late Promoters by Temperature-Sensitive and Wild-Type Forms of Herpes Simplex Virus Type 1 Protein ICP4." *Mol Cell Biol* 5, (1985): 1997–2008.

DM, Knipe. *Fields Virology*. Vol. 2. 5 ed. Philadelphia, PA: Lippincott Williams & Wilkins, 2007.

Doepker RC, Hsu WL, Saffran HA, Smiley JR. "Herpes Simplex Virus Virion Host Shutoff Protein Is Stimulated by Translation Initiation Factors Eif4b and Eif4h." *J Virology* 78, (2004): 4684-4699.

Duerst RJ, Morrison LA. "Herpes Simplex Virus 2 Virion Host Shutoff Protein Interferes with Type I Interferon Production and Responsiveness." *Virology* 322, (2004): 158-167.

Eisenberg RJ, Atanasiu D, Cairns TM, Gallagher JR, Krummenacher C, Cohen GH. . "Herpes Virus Fusion and Entry: A Story with Many Characters." *Review, Viruses* 13, (2012): 800–832.

Elgadi MM, Hayes CE, Smiley JR. "The Herpes Simplex Virus Vhs Protein Induces Endoribonucleolytic Cleavage of Target Rnas in Cell Extracts." *J Virology* 70, (1999): 2411-2419.

Elgadi MM, Hayes CE, Smiley JR. "The Herpes Simplex Virus Vhs Protein Induces Endoribonucleolytic Cleavage of Target Rnas in Cell Extracts." *J*

Virology 73, (1999): 7153-7164.

Elgadi MM, Smiley JR. "Picornavirus Internal Ribosome Entry Site Elements Target RNA Cleavage Events Induced by the Herpes Simplex Virus Virion Host Shutoff Protein." *J Virology* 73, (1999): 9222-9231.

Ellison KS, Maranchuk RA, Mottet KL, Smiley JR. "Control of Vp16 Translation by the Herpes Simplex Virus Type 1 Immediate-Early Protein ICP27." *J Virology* 79, (2005): 4120-4131.

Elroy-Stein O, Fuerst TR and Moss B. “Cap-independent translation of mRNA conferred by encephalomyocarditis virus 5′ sequence improves the performance of the vaccinia virus/bacteriophage T7 hybrid expression system”. *Proc. Natl. Acad. Sci. USA* 86. (1989): 6126-6130.

Esclatine A, Taddeo B, Roizman B. "The Ul41 Protein of Herpes Simplex Virus Mediates Selective Stabilization or Degradation of Cellular MRNAs." *Proc Natl Acad Sci* 101, no. 52 (2004): 18165-18170.

Esclatine A, Taddeo B, Evans L,Roizman B. "The Herpes Simplex Virus 1 Ul41 Gene-Dependent Destabilization of Cellular Rnas Is Selective and May Be Sequence-Specific." *Proc Natl Acad Sci* 101, no. 10 (2004): 3603-3608.

Everly DNJ, Feng P, Mian IS, Rea GS. "MRNA Degradation by the Virion Host Shutoff (Vhs) Protein of Herpes Simplex Virus: Genetic and Biochemical Evidence That Vhs Is a Nuclease." *J Virology* 76, (2002): 8560-8571.

Falkenberg M, Lehman IR, Elias P. "Leading and Lagging Strand DNA Synthesis in Vitro by a Reconstituted Herpes Simplex Virus Type 1 Replisome." *Proc Natl Acad Sci* 97, (2000): 3896–3900.

Farnsworth A, Goldsmith K, Johnson DC. “Herpes simplex virus glycoproteins gD and gE/gI serve essential but redundant functions during acquisition of the virion envelope in the cytoplasm.” *J Virology* 77 (2003):8481–8494.

Fatahzadeh M, Schwartz RA. "Human Herpes Simplex Virus Infections: Epidemiology, Pathogenesis, Symptomatology, Diagnosis, and Management " *J Am Acad Dermatol* 57, no. 5 (2007): 737-763.

Feng P, Everly DN, Read GS. "MRNA Decay During Herpesvirus Infections: Interaction between a Putative Viral Nuclease and a Cellular Translation Factor." *J Virology* 75, (2001): 10272-10280.

Feng P, Everly DN, Read GS. "MRNA Decay During Herpes Simplex Virus (HSV) Infections: Protein-Protein Interactions Involving the HSV Virion Host Shutoff Protein and Translation Factors Eif4h and Eif4a." *J Virology* 79,

(2005): 9651-9664.

Fenwick ML, Clark J. "Early and Delayed Shut-Off of Host Protein Synthesis in Cells Infected with Herpes Simplex Virus." *J Gen Virol* 61, (1982): 121-125.

Fenwick ML, Clark J. "Early and Delayed Shut-Off of Host Protein Synthesis in Cells Infected with Herpes Simplex Virus." *J Gen Virol* 61, (1982): 121-125.

Fontaine-Rodriguez EC, Knipe DM. "Herpes Simplex Virus ICP27 Increases Translation of a Subset of Viral Late MRNAs." *J Virology* 82, (2008): 3538-3545.

Fontaine-Rodriguez EC, Taylor TJ, Olesky M, Knipe DM. "Proteomics of Herpes Simplex Virus Infected Cell Protein 27: Association with Translation Initiation Factors." *Virology* 330, (2004): 487-492.

Fraser KA, Rice SA "Herpes Simplex Virus Immediate-Early Protein ICP22 Triggers Loss of Serine 2-Phosphorylated RNA Polymerase II." *J Virology* 81, (2007): 5091–5101.

Früh K, Ahn K, Djaballah H, Sempe P, van Endert PM, Tampe R, Peterson PA, Yang Y. "A Viral Inhibitor of Peptide Transporters for Antigen Presentation." *Nature* 375, (1995): 415-418.

Fusco D, Forghieri C, Campadelli-Fiume G. "The Pro-Fusion Domain of Herpes Simplex Virus Glycoprotein D (Gd) Interacts with the Gd N Terminus and Is Displaced by Soluble Forms of Viral Receptors." *Proc Natl Acad Sci* 102, (2005): 9323–9328.

Gaglia MM, Covarrubias S, Wong W, Glaunsinger BA. “A common strategy for host RNA degradation by divergent viruses.” *J Virology* 86(2012): 9527-9530.

Gelman IH, Silverstein S. "Dissection of Immediate-Early Gene Promoters from Herpes Simplex Virus: Sequences That Respond to the Virus Transcriptional Activators." *J Virology* 61, (1987): 3167-3172.

Glaunsinger B, Chavez L and Ganem D. “The Exonuclease and Host Shutoff Functions of the SOX Protein of Kaposi's Sarcoma-Associated Herpesvirus Are Genetically Separable.” *J Virology* 79, (2005):7396-7401.

Godowski PJ, Knipe DM. "Transcriptional Control of Herpesvirus Gene Expression: Gene Functions Required for Positive and Negative

Regulation." *Proc Natl Acad Sci* 83, (1986): 256-260.

Gold MO, Tassan JP, Nigg EA, Rice AP, Herrmann CH. "Viral Transactivators E1a and Vp16 Interact with a Large Complex That Is Associated with Ctd Kinase Activity and Contains Cdk8." *Nucl Acids Res* 24, (1996): 3771–3777.

Goldmacher VS, Bartle LM, Skaletskaya A, Dionne CA, Kedersha NL, Vater CA, Han JW, Lutz RJ, Watanabe S, Cahir-McFarland ED, Kieff E, Mocarski ES, Chittenden T. "A Cytomegalovirus-Encoded Mitochondria-Localized Inhibitor of Apoptosis Structurally Unrelated to Bcl-2." *Proc Natl Acad Sci* 96, (1999): 12536-12541.

Greenberg MS. "Herpesvirus Infections." *Dent Clin North Am*, (1996): 359-368.

Grondin B, DeLuca N "Herpes Simplex Virus Type 1 ICP4 Promotes Transcription Preinitiation Complex Formation by Enhancing the Binding of Tfiid to DNA." *J Virology* 74, (2000): 11504–11510.

Gross JD, et al. "Ribosome Loading onto the MRNA Cap Is Driven by Conformational Coupling between Eif4g and Eif4e." *Cell* 115, (2003): 739-750.

Gu B, DeLuca N "Requirements for Activation of the Herpes Simplex Virus Glycoprotein C Promoter in Vitro by the Viral Regulatory Protein ICP4." *J Virology* 68, (1994): 7953-7965.

Gu H, Liang Y, Mandel G, Roizman B. "Components of the Rest/Corest/Histone Deacetylase Repressor Complex Are Disrupted, Modified, and Translocated in HSV-1-Infected Cells." *Proc Natl Acad Sci* 102, (2005): 7571-7576.

Hadigal S, Shukla D. "Exploiting Herpes Simplex Virus Entry for Novel Therapeutics." *Viruses* 5, no. 6 (2013): 1447-1465.

Hall DB, Struhl K. "The Vp16 Activation Domain Interacts with Multiple Transcriptional Components as Determined by Protein-Protein Cross-Linking in Vivo." *J Biol Chem* 277, (2002): 46043–46050.

Hardwicke MA, Sandri-Goldin RM "The Herpes Simplex Virus Regulatory Protein ICP27 Can Cause a Decrease in Cellular MRNA Levels During Infection." *J Virology* 68, (1994): 4797-4810.

Hardy WR, Sandri-Goldin RM. "Herpes Simplex Virus Inhibits Host Cell Splicing, and Regulatory Protein ICP27 Is Required for This Effect." *J Virology* 68, (1994): 7790-7799.

Hernandez FP, Sandri-Goldin RM. "Head-to-Tail Intramolecular Interaction of Herpes Simplex Virus Type 1 Regulatory Protein ICP27 Is Important for Its Interaction with Cellular MRNA Export Receptor Tap/Nxf1." *M Bio* 1, no. 5 (2010).

Herold BC, WuDunn D, Soltys N, et al. . "Glycoprotein C of Herpes Simplex Virus Type 1 Plays a Principal Role in the Adsorption of Virus to Cells and in Infectivity." *J Virology* 65, (1991): 1090-1098.

Herrera FJ, Triezenberg SJ. "Vp16-Dependent Association of Chromatin-Modifying Coactivators and Underrpresentation of Histones at Immediate-Early Gene Promoters During Herpes Simplex Virus Infection." *J Virology* 78, no. 18 (2004): 9689–9696.

Herrmann CH, Gold MO, Rice AP. "Viral Transactivators Specifically Target Distinct Cellular Protein Kinases That Phosphorylate the RNA Polymerase Ⅱ C-Terminal Domain." *Nucl Acids Res* 24, (1996): 501–508.

Heymann JB, et al. "Dynamics of Herpes Simplex Virus Capsid Maturation Visualized by Time-Lapse Cryo-Electron Microscopy." *Nat Struct Biol* 10, (2003): 334-341.

Hill A, Jugovic P, York I, Russ G, Bennink J, Yewdell J, Ploegh H, Johnson D. “Herpes simplex virus turns off the TAP to evade host immunity.” *Nature*, 375 (1995). 411–415.

Holland LE, Anderson KP, Shipman C, Wagner EK. "Viral DNA Synthesis Is Required for the Efficient Expression of Specific Herpes Simplex Virus Type 1 mRNA Species." *Virology* 101, (1980): 10-24.

Homa FL, Otal TM, Glorioso JC, Levine M. "Transcriptional Control Signals of a Herpes Simplex Virus Type 1 Late (Γ2) Gene Lie within Bases −34 to +124 Relative to the 5′ Terminus of the mRNA." *Mol Cell Biol* 6, (1986): 3652-3666.

Homa FL, Otal TM, Glorioso JC, Levine M. "Transcriptional Control Signals of a Herpes Simplex Virus Type 1 Late (Γ2) Gene Lie within Bases −34 to +124 Relative to the 5′ Terminus of the mRNA." *Mol Cell Biol* 6, (1986): 3652-3666.

Honess RW, Roizman B. "Regulation of Herpesvirus Macromolecular Synthesis: Cascade Regulation of the Synthesis of Three Groups of Viral Proteins." *J Virology* 1, (1974): 8-19.

Honess RW, Roizman B. "Regulation of Herpesvirus Macromolecular Synthesis:

Sequential Transition of Polypeptide Synthesis Requires IRES Functional Viral Polypeptides." *Proc Natl Acad Sci* 72, no. 4 (1975): 1276-1280.

Howley G, Roizman B, Knipe DM. *Fields Virology* Herpes Simplex Viruses and Their Replication. Philadelphia: Lippincott, Williams & Wilkins, 2001.

Hutin S, Lee Y, Glaunsinger BA. “An RNA element in human interleukin 6 confers escape from degradation by the gammaherpesvirus SOX protein.” *J Virology* 87(8):4672-82.

Huang CJ, Goodart SA, Rice MK, Guzowski JF, Wagner EK. "Mutational Analysis of Sequences Downstream of the Tata Box of the Herpes Simplex Virus Type 1 Major Capsid Protein (Vp5/Ul19) Promoter." *J Virology* 67, (1993): 5109-5116.

Huang CJ, Lokugamage KG, Rozovics JM, Narayanan K, Semler BL, Makino S. “SARS Coronavirus nsp1 Protein Induces Template-Dependent Endonucleolytic Cleavage of mRNAs: Viral mRNAs Are Resistant to nsp1-Induced RNA Cleavage.” *PLoS Pathog* 7, (2011)

Jackson RJ, et al. "Alternative Mechanisms of Initiating Translation of Mammalian MRNAs." *Biochem Soc Trans* 33, (2005): 1231-1241.

Jackson RJ, Hellen CUT, Pestova TV. "The Mechanism of Eukaryotic translation Initiation and Principles of Its Regulation." *Nat Rev Mol Biol* 10, (2010): 113-127.

Jang SK, et al. "A Segment of the 5 Nontranslated Region of Encephalomyocarditis Virus RNA Directs Internal Entry of Ribosomes During in Vitro Translation." *J Virology* 62, (1988): 2636-2643.

Jean S, LeVan KM, Song B, Levine M, Knipe DM. "Herpes Simplex Virus 1 ICP27 Is Required for Transcription of Two Viral Late (G2) Genes in Infected Cells." *Virology* 283, (2001): 273-284.

Jenkins HL, Spencer CA. "RNA Polymerase Ii Holoenzyme Modifications Accompany Transcription Reprogramming in Herpes Simplex Virus Type 1-Infected Cells." *J Virology* 75, (2001): 9872-9884.

Johannes G, Sarnow P. “Cap-independent polysomal association of natural mRNAs encoding c-myc, BiP, and eIF4G conferred by internal ribosome entry sites.” *RNA* 4(1998): 1500-1513.

Johnson DC, Baines JD. "Herpesviruses Remodel Host Membranes for Virus Egressdavid " *Nat Rev Micro* 9, (2011): 382-394.

Kamitani W, Huang C, Narayanan K, Lokugamage KG, Makino S. “A two-pronged strategy to suppress host protein synthesis by SARS coronavirus Nsp1 protein.” *Nat Struct Mol Biol* 16, (2009):1134-40.

Kapp LD, Lorsch JR. "Gtp-Dependent Recognition of the Methionine Moiety on Initiator Trna by Translation Factor Eif2." *J Mol Biol* 335, (2004): 923-936.

Karr BM, Read GS. "The Virion Host Shutoff Function of Herpes Simplex Virus Degrades the 5′ End of a Target mRNA before the 3′ End." *Virology* 264, (1999): 195-204.

Karr BM, Read GS. "The Virion Host Shutoff Function of Herpes Simplex Virus Degrades the 5′ End of a Target mRNA before the 3′ End." *Virology* 264, (1999): 195-204.

Kelly BJ, Fraefel C, Cunningham AL, Diefenbach RJ. "Functional Roles of the Tegument Proteins of Herpes Simplex Virus Type 1” *Virus Res* 145, no. 173-186 (2009).

Kibler PK, Duncan J, Keith BD, Hupel T, Smiley JR. "Regulation of Herpes Simplex Virus True Late-Gene Expression: Sequences Downstream from the Us11 Tata Box Inhibit Expression from an Unreplicated Template." *J Virology* 65, (1991): 6749-6760.

Kleizen B, Braakman I. "Protein Folding and Quality Control in the Endoplasmic Reticulum." *Curr Opin Cell Biol* 16, (2004): 343-349.

Knipe DM, Howley PM, Roizman B, Sears AE. *Fundamental Virology* Herpes Simplex Viruses and Their Replication. Philadelphia: Lippincott-Raven Publishers, 1996.

Koppers-Lalic D., Rijsewijk FA, Verschuren SB, van Gaans-Van den Brink JA, Neisig A, Ressing ME, Neefjes J, Wiertz EJ. "The Ul41-Encoded Virion Host Shutoff (Vhs) Protein and Vhs-Independent Mechanisms Are Responsible for Down-Regulation of Mhc Class I Molecules by Bovine Herpesvirus 1." *J Gen Virol* 82, (2001): 2071-2081.

Kozak M. "Structural Features in Eukaryotic mRNAs That Modulate the Initiation of Translation." *J Biol Chem* 266, (1991): 19867-19870

Kozac M. "New Ways of Initiating Translation in Eukaryotes?." *Mol Cell Biol* 21, (2001): 1899-1907.

Kozac M. "A Second Look at Cellular mRNA Sequences Said to Function as Internal Ribosome Entry Sites." *Nucleic Acid Res.* 33, (2005): 6593-6602.

Kristie TM, Sharp PA. "Interactions of the Oct-1 Pou Subdomains with Specific DNA Sequences and with the HSV Alpha-Trans-Activator Protein." *Genes Dev* 4, (1990): 2383–2396.

Kristie TM. *Human Herpesviruses: Biology, Therapy, and Immunoprophylaxis* Vol. 8 Early Events Pre-Initiation of Alphaherpes Viral Gene Expression, Edited by Campadelli-Fiume G Arvin A, Mocarski E, et al. Cambridge: Cambridge University Press, 2007.

Kuge S and Nomoto A. "Construction of viable deletion and insertion mutants of the Sabin strain of type 1 poliovirus: Function of the 5' noncoding sequence in viral replication." *J. Virol.* 61 (1987):1478–1487.

Kwong AD, Frenkel N. "Herpes Simplex Virus-Infected Cells Contain a Function(S) That Destabilizes Both Host and Viral MRNAs." *Proc Natl Acad Sci* 84, (1987): 1926-1930.

Kwong AD, Kruper JA, Frenkel N. "Herpes Simplex Virus Virion Host Shutoff Function." *J Virology* 62, (1988): 912-921.

Kwong AD, Kruper JA and Frenkel N. "Herpes Simplex Virus Virion Host Shutoff Function." *J Virology* 62, no. 3 (1988): 912.

Lai JS, Herr W "Interdigitated Residues within a Small Region of Vp16 Interact with Oct-1, Hcf, and DNA." *Mol Cell Biol* 17, (1997): 3937–3946.

Lam Q, et al. "Herpes Simplex Virus Vp16 Rescues Viral MRNA from Destruction by the Virion Host Shutoff Function." *EMBO J* 15, no. 10 (1996): 2575-2581.

Lazear E, Carfi A, Whitbeck JC, Cairns TM, Krummenacher C, Cohen GH, Eisenberg RJ. "Engineered Disulfide Bonds in Herpes Simplex Virus Type 1 Gd Separate Receptor Binding from Fusion Initiation and Viral Entry." *J Virology* 82, (2008): 700-709.

Leopardi R, Ward PL, Ogle WO, Roizman B. "Association of Herpes Simplex Virus Regulatory Protein ICP22with Transcriptional Complexes Containing Eap, ICP4, Rnapolymerase Ii, and Viral DNA RequIRES Posttranslationalmodification by the U(L)13 Proteinkinase." *J Virology* 71, (1997): 1133-1139.

Lilley CE, Chaurushiya MS, Boutell C, Landry S, Suh J, Panier S, Everett RD, Stewart GS, Durocher D, Weitzman MD. "A Viral E3 Ligase Targets Rnf8 and Rnf168 to Control Histone Ubiquitination and DNA Damage Responses." *EMBO J* 29, (2010): 943-955.

Liu F, Hong Zhou Z. *Human Herpesviruses: Biology, Therapy, and Immunoprophylaxis*. Vol. 3 Comparative Virion Structures of Human Herpesviruses, Edited by Campadelli-Fiume G Arvin A, Mocarski E, Moore PS, Roizman B, Whitley R, Yamanishi K. Cambridge: Cambridge University Press, 2007.

Liu X, Fitzgerald K, Kurt-Jones E, Finberg R, Knipe D.M. “Herpesvirus tegument protein activates NF-kappaB signaling through the TRAF6 adaptor protein.” *Proc Natl Acad Sci* 105 (2008): 11335–11339

Liu F, Roizman B. "The Herpes Simplex Virus 1 Gene Encoding a Protease Also Contains within Its Coding Domain the Gene Encoding the More Abundant Substratej." *J Virology* 78, (1991): 12668–12671.

Lomakin IB, Kolupaeva VG, Marintchev A, Wagner G, Pestova TV. "Position of Eukaryotic Initiation Factor Eif1 on the 40s Ribosomal Subunit Determined by Directed Hydroxyl Radical Probing." *Genes Dev* 17, (2003): 2786-2797.

Long MC, Leong V, Schaffer PA, Spencer CA, Rice SA. "ICP22 and the Ul13 Protein Kinase Are Both Required for Herpes Simplex Virus-Induced Modification of the Large Subunit of RNA Polymerase II." *J Virology* 73, (1999): 5593-5604.

Loret S, Guay G, Lippe R. "Comprehensive Characterization of Extracellular Herpes Simplex Virus Type 1 Virions." *J Virology* 82, (2008): 8605–8618.

Lynch DP. "Oral Viral Infections." *Clin Dermat* 18, (2000): 619-628.

Maag D, Algire MA, Lorsch JR. "Communication between Eukaryotic Translation Initiation Factors 5 and 1a within the Ribosomal Pre-Initiation Complex Plays a Role in Start Site Selection." *J Mol Biol* 356, (2006): 724-737.

Maag D, Fekete CA, Gryczynski Z, Lorsch, JR. "A Conformational Change in the Eukaryotic Translation Preinitiation Complex and Release of Eif1 Signal Recognition of the Start Codon." *Mol Cell* 17, (2005): 265-275.

Mahiet C, Ergani A, Huot N, Alende N, Azough A, Salvaire F, Bensimon A, Conseiller E, Wain-Hobson S, Labetoulle M, Barradeau S. " Structural Variability of HSV-1 Genomes " *J Virology*, (2012).

Makhov AM, Lee SS, Lehman IR, Griffith JD. "Origin-Specific Unwinding of Herpes Simplex Virus 1 DNA by the Viral Ul9 and ICP8 Proteins: Visualization of a Specific Preunwinding Complex." *Proc Natl Acad Sci* 100, (2003): 898–903.

Malik P, Tabarraei A, Kehlenbach RH, Korfali N, Iwasawa R, Graham SV, Schirmer EC. "Herpes Simplex Virus ICP27 Protein Directly Interacts with the Nuclear Pore Complex through Nup62, Inhibiting Host Nucleocytoplasmic Transport Pathways." *J Biol Chem* 287, (2012): 12277-12292.

Marintchev A, Kolupaeva VG, Pestova TV, Wagner G "Mapping the Binding Interface between Human Eukaryotic Initiation Factors 1a and 5b: A New Interaction between Old Partners." *Proc Natl Acad Sci* 100, (2003): 1535-1540.

Marsden HS, Cross AM, Francis GJ, Patel AH, MacEachran K, Murphy M, McVey G, Haydon D, Abbotts A, Stow ND. "The Herpes Simplex Virus Type 1 Ul8 Protein Influences the Intracellular Localization of the Ul52 but Not the ICP8 or Pol Replication Proteins in Virus-Infected Cells." *J Gen Virol* 77, (1996): 2241–2249.

Mears WE, Rice SA. "The Herpes Simplex Virus Immediate-Early Protein ICP27 Shuttles between Nucleus and Cytoplasm." *Virology* 242, (1998): 128-137.

Meckes DG, Marsh JA, Wills JW. "Complex Mechanisms for the Packaging of the Ul16 Tegument Protein into Herpes Simplex Virus." *Virology* 398, (2010): 208–213

Memedula S, Belmont AS. "Sequential Recruitment of Hat and Swi/Snf Components to Condensed Chromatin by Vp16 " *Curr Biol* 13, (2003): 241-246.

Mettenleite TC, Klupp BG, Granzow H "Herpesvirus Assembly: An Update." *Virus Res* 143, (2009): 222-234.

Metzler DW, Wilcox KW. "Isolation of Herpes Simplex Virus Regulatory Protein ICP4 as a Homodimeric Complex." *J Virology* 55, (1985): 329-337.

Montgomery RL, Warner MS, Lum BJ, et al. "Herpes Simplex Virus- 1 Entry into Cells Mediated by a Novelmember of the Tnf/Ngf Receptor Family." *Cell* 87, (1996): 427- 436.

Mou F, Wills E, Baines JD. "Phosphorylation of the Ul31 Protein of Herpes Simplex Virus 1 by the Us3-Encoded Kinase Regulates Localization of the Nuclear Envelopment Complex and Egress of Nucleocapsids." *J Virology* 83, (2009): 5181–5191

Munger J, Chee AV, Roizman B. "The U(S)3 Protein Kinase Blocks Apoptosis Induced by the D120 Mutant of Herpes Simplex Virus 1 at a Pre-

mitochondrial Stage." *J Virology* 75, (2001): 5491–5497.

Newcomb WW, et al. "Structure of the Herpes Simplex Virus Capsid Molecular Composition of the Pentons and the Triplexes." *Mol Biol* 232, (1993): 499-511.

Newcomb WW, et al. "The Ul6 Gene Product Forms the Portal for Entry of DNA into the Herpes Simplex Virus Capsid." *J Virology* 75, (2001): 10923-10932.

Newcomb WW, et al. "Assembly of the Herpes Simplex Virus Capsid: Identification of Soluble Scaffold-Portal Complexes and Their Role in Formation of Portal-Containing Capsids." *Virology* 77, (2003): 9862-9871.

Nicola AV, McEvoy AM, and Straus SE. “Roles for endocytosis and low pH in herpes simplex virus entry into HeLa and Chinese hamster ovary cells”. *J Virology* 77, (2003): 5324–5332.

O’Donnell CD, Tiwari V, Oh MJ, et al. "A Role for Heparan Sulfate 3 O Sulfotransferase Isoform 2 in Herpes Simplex Virus Type 1 Entry and Spread." *Virology* 346, no. 2 (2006): 452-459.

Ohana B, Lipson M, Vered N, Srugo I, Ahdut M, Morag A. "Novel Approach for Specific Detection of Herpes Simplex Virus Type 1 and 2 Antibodies and Immunoglobulin G and M Antibodies." *Clin Diagn Lab Immunol* 7, (2000): 904-908.

Olsen DS, et al. "Domains of Eif1a That Mediate Binding to Eif2, Eif3 and Eif5b and Promote Ternary Complex Recruitment in Vivo." *EMBO J* 22, (2003): 193-204.

Oroskar AA, Read GS. "A Mutant of Herpes Simplex Virus Type 1 Exhibits Increased Stability of Immediate-Early (Alpha) MRNAs." *J Virology* 61, (1987): 604-606.

Page HG, Read GS. "The Virion Host Shutoff Endonuclease (Ul41) of Herpes Simplex Virus Interacts with the Cellular Cap-Binding Complex Eif4f." *J Virology*, (1987).

Paladino P, Collins SE, Mossman KL. "Cellular Localization of the Herpes Simplex Virus ICP0 Protein Dictates Its Ability to Block Irf3-Mediated Innate Immune Responses." *PLoS ONE* 5, (2010): 10428-10428.

Panagiotidis CA, Lium EK, Silverstein SJ. "Physical and Functional Interactions between Herpes Simplex Virus Immediate-Early Proteins ICP4 and ICP27." *J Virology* 71, (1997): 1547–1557.

Pasieka TJ, Lu B, Crosby SD, Wylie KM, Morrison LA, Alexander DE, Menachery VD, Leib DA. "Herpes Simplex Virus Virion Host Shutoff Attenuates Establishment of the Antiviral State." *J Virology* 82, (2008): 5527-5535.

Passmore LA, et al. . "The Eukaryotic Translation Initiation Factors Eif1 and Eif1a Induce an Open Conformation of the 40s Ribosome." *Mol Cell* 26, (2007): 41-50.

Paulin FE, Campbell LE, O'Brien K, Loughlin J, Proud CG. "Eukaryotic Translation Initiation Factor 5 (Eif5) Acts as a Classical Gtpase-Activator Protein." *Curr Biol* 11, (2001): 55-59.

Pelham HR. “Speculations on the functions of the major heat shock and glucose-regulated proteins.” *Cell* 46 (1986)**:**959-961.

Pelletier J, Sonenberg N. "Internal Initiation of Translation of Eukaryotic MRNA Directed by a Sequence Derived from Poliovirus RNA." *Nature* 334, (1988): 320-325.

Pereira L, Wolff MH, Fenwick M, Roizman B "Regulation of Herpesvirus Macromolecular Synthesis. V. Properties of Alpha Polypeptides Made in HSV-1 and HSV-2 Infected Cells." *Virology* 77, (1997): 733-749.

Perez-Parada J, Saffran HA, Smiley JR. "RNA Degradation Induced by the Herpes Simplex Virus Vhs Protein Proceeds 5′ to 3′ in Vitro." *J Virology* 78, no. 23 (2004): 13391-13394.

Pestova TV, Borukhov SI, Hellen CUT. "Eukaryotic Ribosomes Require Initiation Factors 1 and 1a to Locate Initiation Codons." *Nature* 394, (1998): 854-859.

Pestova TV, Hellen CU, Shatsky IN. "Canonical Eukaryotic Initiation Factors Determine Initiation of Translation by Internal Ribosomal Entry." *Mol Cell Biol* 16, (1996): 6859-6869.

Pestova TV, Kolupaeva VG. "The Roles of Individual Eukaryotic Translation Initiation Factors in Ribosomal Scanning and Initiation Codon Selection." *Genes Dev* 16, (2002): 2906-2922.

Pestova TV, Lorsch JR, Hellen CUT. *Translational Control in Biology and Medicine* Edited by Sonenberg N Mathews MB, Hershey JWB. New York, NY: Cold Spring Harbor Laboratory Press, 2007.

Pestova TV, Shatsky IN, Hellen CUT. "Functional Dissection of Eukaryotic Initiation Factor 4f: The 4a Subunit and the Central Domain of the 4g

Subunit Are Sufficient to Mediate Internal Entry of 43s Preinitiation Complexes." *Mol Cell Biol* 16, (1996): 6870-6878.

Pestova TV, Shatsky IN, Fletcher SP, Jackson RJ, Hellen CUT. "A Prokaryotic-Like Mode of Cytoplasmic Eukaryotic Ribosome Binding to the Initiation Codon During Internal Translation Initiation of Hepatitis C and Classical Swine Fever Virus Rnas." *Genes Dev* 12, (1998): 67-83.

Pisarev AV, et al. "Specific Functional Interactions of Nucleotides at Key -3 and +4 Positions Flanking the Initiation Codon with Components of the Mammalian 48s Translation Initiation Complex." *Genes Dev* 20, (2006): 624-636.

Read GS, Bradley BM, Knight K. "Isolation of a Herpes Simplex Virus Type 1 Mutant with a Deletion in the Virion Host Shutoff Gene and Identification of Multiple Forms of the Vhs (Ul41) Polypeptides." *J Virology* 67, (1993): 7149-7160.

Read GS, Frenkel N. "Herpes Simplex Virus Mutants Defective in the Virion-Associated Shutoff of Host Polypeptides Synthesis and Exhibiting Abnormal Synthesis of A (Immediate-Early) Viral Polypeptides." *J Virology* 46, (1983): 498-512.

Read GS, Karr BM, Knight K. "Isolation of a Herpes Simplex Virus Type 1 Mutant with a Deletion in the Virion Host Shutoff Gene and Identification of Multiple Forms of the Vhs (Ul41) Polypeptide." *J Virology* 67, (1993): 7149-7160.

Reynolds AE, et al. "Ul31 and Ul34 Proteins of Herpes Simplex Virus Type 1 Form a Complex That Accumulates at the Nuclear Rim and Is Required for Envelopment of Nucleocapsids." *J Virology* 75, (2001): 8803-8817.

Reynolds AE, Wills EG, Roller RJ, Ryckman BJ, Baines JD. "Ultrastructural Localization of the Herpes Simplex Virus Type 1 Ul31, Ul34, and Us3 Proteins Suggests Specific Roles in Primary Envelopment and Egress of Nucleocapsids." *J Virology* 76, (2002): 8939–8952

Rice SA, Long MC, Lam V, Spence CA. "RNA Polymerase Ii Is Aberrantly Phosphorylated and Localized to Viral Replication Compartments Following Herpes Simplex Virus Infection." *J Virology* 68, (1994): 988-1001.

Rice SA, Long MC, Lam V, Schaffer PA, Spencer CA. "Herpes Simplex Virus Immediate-Early Protein ICP22 Is Required for Viral Modification of Host RNA Polymerase Ii and Establishment of the Normal Viral Transcription Program." *J Virology* 69, (1995): 5550-5559.

Rogers GW, Richter NJ, Lima WF, Merrick WC. "Modulation of the Helicase Activity of Eif4a by Eif4b, Eif4h, and Eif4f." *J Biol Chem* 276, (2001): 30914-30922

Roizman B, Borman GS, Kamali-Rousta M. "Macromolecular Synthesis in Cells Infected with Herpes Simplex Virus." *Nature* 206, (1965): 1375-1375.

Roizman B, Sears AE. *Fields Virology* Herpes Simplex Viruses and Their Replication, Edited by D. M. Knipe B. N. Fields, and P. M. Howley Philadelphia, Pa: Lippincott-Raven 1996.

Roizmann B, Desrosiers RC, Fleckenstein B, Lopez C, Minson AC, Studdert MJ. "The Family Herpesviridae: an update." *Arch Virology* 123, no. 3-4 (1992): 425-449.

Saffran HA, Read GS, Smiley JR. "Evidence for Translational Regulation by the Herpes Simplex Virus Virion Host Shutoff Protein." *J Virology* 84, (2010): 6041-6049.

Samady L, Costigliola E, MacCormac L, McGrath Y, Cleverley S, Lilley CE, Smith J, Latchman DS, Chain B, Coffin RS. "Deletion of the Virion Host Shutoff Protein (Vhs) from Herpes Simplex Virus (HSV) Relieves the Viral Block to Dendritic Cell Activation: Potential of Vhs− HSV Vectors for Dendritic Cell-Mediated Immunotherapy." *J Virology* 77, (2003): 3768-3776.

Sandri-Goldin RM. "ICP27 Mediates HSV RNA Export by Shuttling through a Leucine-Rich Nuclear Export Signal and Binding Viral Intronless RNAs through an Rgg Motif." *Genes Dev* 12, (1998): 868-879.

Sandri-Goldin RM. "ICP27 Mediates Herpes Simplex Virus RNA Export by Shuttling through a Leucine-Rich Nuclear Export Signal and Binding Viral Intronless Rnas through an Rgg Motif " *Genes Dev* 12, (1998): 868-879.

Sandri-Goldin RM. "Interactions between a Herpes Simplex Virus Regulatory Protein and Cellular MRNA Processing Pathways." *Methods* 16, (1998): 95-104.

Sarnow P. “Translation of glucose-regulated protein 78/immunoglobulin heavy-chain binding protein mRNA is increased in poliovirus-infected cells at a time when cap-dependent translation of cellular mRNAs is inhibited.” *Proc Natl Acad Sci U S A*. 86(1989): 5795–5799.

Schneider R, et al. "New Ways of Initiating Translation in Eukaryotes " *Mol Cell Biol* 21, (2001): 8238-8246.

Schuler M, et al. "Structure of the Ribosome-Bound Cricket Paralysis Virus IRES RNA." *Nature Struct Mol Biol* 13, (2006): 1092-1096.

Sciabica KS, Dai QJ, Sandri-Goldin RM. "ICP27 Interacts with Srpk1 to Mediate HSV Splicing Inhibition by Altering Sr Protein Phosphorylation." *EMBO J* 22, (2003): 1608-1619.

Sciortino MT, et al. "The Virion Host Shut-Off Rnase Plays a Key Role in Blocking the Activation of Protein Kinase R in Cells Infected with Herpes Simplex Virus 1." *J Virology* 87, no. 6 (2013): 3271-3276.

Sciubba JJ. "Herpes Simplex and Aphthous Ulcerations: Presentation, Diagnosis and Management—an Update." *Gen Dent* 53, (2003): 510-516.

Shatsky IN, Dmitriev SE, Terenin IM and Andreev DE. “Cap- and IRES-Independent Scanning Mechanism of Translation Initiation as an Alternative to the Concept of Cellular IRESs.” *Mol. Cells* 30 (2010):285-293.

Shieh M, WuDunn D, Montgomery R, et al. . "Cell Surface Receptors for Herpes Simplex Virus Are Heparan Sulfate Proteoglycans." *J Cell Biol* 116, (1992): 1273-1281.

Shiflet LA, Read GS. "MRNA Decay During Herpes Simplex Virus (HSV) Infections: Mutations That Affect Translation of an MRNA Influence the Sites at Which It Is Cleaved by the HSV Virion Host Shutoff (Vhs) Protei." *J Virology* 87, no. 1 (2013): 94-109.

Shukla D, Liu J, Blaiklock P, et al. "A Novel Role for 3- O- Sulfated Heparan Sulfate in Herpes Simplex Virus 1 Entry." *Cell* 99, (1999): 13-22.

Siridechadilok B, Fraser CS, Hall RJ, Doudna JA, Nogales E. "Structural Roles for Human Translation Factor Eif3 in Initiation of Protein Synthesis." *Science* 310, (2005): 1513-1515.

Smibert CA, Smiley JR. "Differential Regulation of Endogenous and Transduced B-Globin Genes During Infection of Erythroid Cells with a Herpes Simplex Virus Type 1 Recombinant." *J Virology* 64, (1990): 3882-3894.

Smiley JR. "Herpes Simplex Virus Virion Host Shutoff Protein: Immune Evasion Mediated by a Viral RNase? ." *J Virology* 78, (2004): 1063-1068.

Smith AE, Helenius A. "How Viruses Enter Animal Cells." *Science* 304, (2004): 237-242.

Smith CA, Bates P, Rivera-Gonzalez R, Gu B, DeLuca NA "ICP4, the Major

Transcriptional Regulatory Protein of Herpes Simplex Virus Type 1, Forms a Tripartite Complex with TATA-Binding Protein and TfIIb." *J Virology* 67, (1993): 4676–4687.

Smith-Donald BA, Durand LO, Roizman B. "Role of Cellular Phosphatase Cdc25c in Herpes Simplex Virus 1 Replication." *J Virology* 82, no. 9 (2008): 4527-4532.

Sodeik B, Ebersold MW, Helenius A. "Microtubule-Mediated Transport of Incoming Herpes Simplex Virus 1 Capsids to the Nucleus." *J Cell Biol* 136, no. 5 (1997): 1007-1021.

Spear P. "Entry of alphaherpesviruses into cells." *Semin Virol* 4, (1993): 167–180.

Spear PG, Eisenbergr J, Cohen G. "Three Classes of Cell Surface Receptors for Alphaherpesvirus Entry." *Virology* 275, (2000): 1-8.

Spencer CA, Dahmus ME, Rice SA. "Repression of Host RNA Polymerase Ii Transcription by Herpes Simplex Virus Type 1." *J Virology* 71, (1997): 2031-2040.

Spencer JV, Newcomb WW, Thomsen DR, Homa FL, Brown JC. "Assembly of the Herpes Simplex Virus Capsid: vhs expression plasmid Triplexes Bind to the Nascent Capsid." *J Virology* 72, (1998): 3944–3951.

Stampfer SD, Heldwein EE. "Stuck in the middle: structural insights into the role of the gH/gL heterodimer in herpesvirus entry." *Curr Opin Virol* 3, (2013): 13-19

Steffy KR, Weir JP. "Mutational Analysis of Two Herpes Simplex Virus Type 1 Late Promoters." *J Virology* 65, (1991): 6454-6460.

Stengel G, Kuchta RD. "Coordinated Leading and Lagging Strand DNA Synthesis by Using the Herpes Simplex Virus 1 Replication Complex and Minicircle DNA Templates." *J Virology* 85, (2011): 957–967.

Steven AC, Spear PG. *Structural Biology of Viruses.* Herpesvirus Capsid Assembly and Envelopment, Edited by Burnett RM Chiu W, Garcea RL. New York: Oxford University Press, 1997.

Steven AC, Spear PG. *Structural Biology of Viruses* Herpesvirus Capsid Assembly and Envelopment Edited by Burnett RM Chiu W, Garcea R. Oxford: Oxford University Press 1997.

Strom T, Frenkel N. "Effects of Herpes Simplex Virus on MRNA Stability." *J*

Virology 61, (1987): 2198-2207.

Sturm RA, Das G, Herr W. "The Ubiquitous Octamer-Binding Protein Oct-1 Contains a Pou Domain with a Homeo Box Subdomain." *Genes Dev* 2, (1988): 1582–1599.

Suzutani T, Nagamine M, Shibaki T, Ogasawara M, Yoshida I, Daikoku T, Nishiyama Y, Azuma M "The Role of the Ul41 Gene of Herpes Simplex Virus Type 1 in Evasion of Non-Specific Host Defence Mechanisms During Primary Infection." *J Gen Virol* 81, (2000): 1763-1771.

Svitkina TM, Bulanova EA, Chaga OY, Vignjevic DM, Kojima S, Vasiliev JM, and Borisy GG. "Mechanism of Filopodia Initiation by Reorganization of a Dendritic Network." *J Cell Biol* 160, (2003): 401-421.

Svitkin YV, Maslova SV and Agol VI. "The genomes of attenuated and virulent poliovirus strains differ in their in vitro translation efficiencies". *Virology* 147 (1985):243–252

Sydiskis RJ, Roizman B. "Polysomes and Protein Synthesis in Cells Infected with a DNA Virus." *Science* 153, (1966): 76-78.

Sydiskis RJ, Roizman B. "The Disaggregation of Host Polyribosomes in Productive and Abortive Infection with Herpes Simplex Virus." *Virology* 32, (1968): 678-686.

Taddeo B, Sciortino MT, Zhang W, Roizman B. "Interaction of Herpes Simplex Virus Rnase with Vp16 and Vp22 Is Required for the Accumulation of the Protein but Not for Accumulation of mRNA." *Proc Natl Acad Sci* 104, no. 29 (2007): 12163-12168.

Taddeo B, Zhang W, Roizman B. "The Herpes Simplex Virus Host Shutoff Rnase Degrades Cellular and Viral mRNAs Made before Infection but Not Viral MRNA Made after Infection." *J Virology* 87, no. 8 (2013): 4516-4522.

Trono D, Andino R, Baltimore D. "An RNA sequence of hundreds of nucleotides at the 5' end of poliovirus RNA is involved in allowing viral protein synthesis." J. Virol. 62 (1988):2291–2299.

Trgovcich J, Johnson D, Roizman B. "Cell Surface Major Histocompatibility Complex Class Ii Proteins Are Regulated by the Products of the Γ134.5 and Ul41 Genes of Herpes Simplex Virus 1." *J Virology* 76, (2002): 6974-6986.

Trus BL, et al. "The Herpes Simplex Virus Procapsid: Structure, Conformational Changes Upon Maturation, and Roles of the Triplex Proteins Vp19c and

Vp23 in Assembly." *J Mol Biol* 263, (1996): 447-462.

Trus BL, et al. "Structure and Polymorphism of the Ul6 Portal Protein of Herpes Simplex Virus Type 1j." *J Virology* 78, (2004): 12668-12671.

Turner A, Bruun B, Minson T, et al. "Glycoproteins Gb, Gd, and Ghgl of Herpes Simplex Virus Type 1 Are Necessary and Sufficient to Mediate Membrane Fusion in a Cos Celltransfection System." *J Virology* 72, (1998): 873-875.

Turner R, Shehab Z, Osborne K, Hendley JO. "Shedding and Survival of Herpes Simplex Virus from “Fever Blisters”." *Pediatrics*, no. 70 (1982): 547-549.

Unbehaun A, Borukhov SI, Hellen CUT, Pestova TV. "Release of Initiation Factors from 48s Complexes During Ribosomal Subunit Joining and the Link between Establishment of Codon-Anticodon Base-Pairing and Hydrolysis of Eif2-Bound Gtp." *Genes Dev* 18, (2004): 3078-3093.

Van Der Velden A, Kaminski A, Jackson RJ and Belsham GJ. “Defective point mutants of the encephalomyocarditis virus internal ribosome entry site can be complemented in trans.” *Virology* 214 (1995):82-90.

Van Eden ME, Byrd MP, Sherrill KW, Lloyd RE "Demonstrating Internal Ribosome Entry Sites in Eukaryotic MRNAs Using Stringent RNA Test Procedures." *RNA* 10, (2004): 720-730.

Vignali M, Steger DJ, Neely KE., Workman JL. "Distribution of Acetylated Histones Resulting from Gal4-Vp16 Recruitment of Saga and Nua4 Complexes." *EMBO J* 19, (2000): 2629–2640.

Vittone V, Diefenbach E, Triffett D, Douglas MW, Cunningham AL, Diefenbach RJ "Determination of Interactions between Tegument Proteins of Herpes Simplex Virus Type 1." *J Virology* 79, (2005): 9566–9571.

Vogel JL, Kristie TM. "The Novel Coactivator C1 (Hcf) Coordinates Multiprotein Enhancer Formation and Mediates Transcription Activation by Gabp." *EMBO J* 19, (2000): 683–690.

Volpon L, Osborne MJ, Topisirovic I, Siddiqui N, Borden KL. "Cap-Free Structure of Eif4e Suggests a Basis for Conformational Regulation by Its Ligands." *EMBO J* 25, (2006): 5138-5149.

Wagner EK, Guzowski JF, Singh J. "Transcription of the Herpes Simplex Virus Genome During Productive and Latent Infection " *Prog Nucleic Acid Res Mol Biol* 51, (1995): 123-165.

Wagner EK, Petroski MD, Pande NT, Lieu PT, Rice M. "Analysis of Factors

Influencing Kinetics of Herpes Simplex Virus Transcription Utilizing Recombinant Virus." *Methods* 16, (1998): 105-116.

Ward S, Weller S *Alphaherpesviruses: Molecular Virology* HSV-1 DNA Replication Edited by Weller SK. Norfolk, UK: Caister Academic, 2011.

Ward S, Weller S. *Alphaherpesviruses: Molecular Virology* HSV-1 DNA Replication. Norfolk, UK: Caister Academic, 2011.

Whitbeck JC, Connolly SA, Willis SH, et al. "Localization of the Gd- Binding Region of the Human Herpessimplex Virus Receptor, HVEA." *J Virology* 75, (2001): 171- 180.

Whitley RJ, Roizman B. "Herpes Simplex Virus Infections." *Lancet*, (2001): 1513-1518.

Wilson JE, Pestova TV, Hellen CUT, Sarnow P. "Initiation of Protein Synthesis from the a Site of the Ribosome." *Cell* 102, (2000): 511-520.

Wisner TW, et al. "Herpesvirus gB-Induced Fusion between the Virion Envelope and Outer Nuclear Membrane During Virus Egress Is Regulated by the Viral Us3 Kinase." *J Virology* 83, (2009): 3115-3126.

Wolfstein A, et al. "The Inner Tegument Promotes Herpes Simplex Virus Capsid Motility Along Microtubules in Vitro." *Traffic* 7, (2006): 227-237.

Yao F, Schaffer PA. "Physical Interaction between the Herpes Simplex Virus Type 1 Immediate-Early Regulatory Proteins ICP0 and ICP4." *J Virology* 68, (1994): 8158–8168.

Yang Q and Sarnow, P. “Location of the internal ribosome entry site in the 5′ non-coding region of the immunoglobulin heavy-chain binding protein (BiP) mRNA: evidence for specific RNA-protein interactions.” *Nucl. Acids Res.* 25 (1997): 2800-2807.

York IA, Roop C, Andrews DW, Riddell SR, Graham FL, Johnson DC. “A cytosolic herpes simplex virus protein inhibits antigen presentation to CD8+ T lymphocytes.” *Cell* **77** (1994): 525–535.

Young RM, Wang S-J, Gordan JD, Ji X, Liebhaber SA and Simon MC. “Protein Synthesis, Post-Translational Modification, and Degradation: Hypoxia-mediated Selective mRNA Translation by an Internal Ribosome Entry Site-independent Mechanism”. *J. Biol. Chem.* 283 (2008):16309-16319.

Yu D, Weller SK. "Genetic Analysis of the Ul 15 Gene Locus for the Putative Terminase of Herpes Simplex Virus Type 1." *Virology* 243, (1998): 32-44.

Zelus BD, Stewart RS, Ross J. "The Virion Host Shutoff Protein of Herpes Simplex Virus Type 1: Messenger Ribonucleolytic Activity in Vitro." *J Virology* 70, (1996): 2411-2419.

Zhou C, Knipe DM. "Association of Herpes Simplex Virus Type 1 ICP8 and ICP27 Proteins with Cellular RNA Polymerase Ii Holoenzyme." *J Virology* 76, (2002): 5893-5904.

Zhou ZH, He J, Jakana J, Tatman JD, Rixon FJ, Chiu W. "Assembly of Vp26 in Herpes Simplex Virus-1 Inferred from Structures of Wild-Type and Recombinant Capsids." *Nat Struct Biol* 2, (1995): 1026–1030.

Zhou ZH, Macnab SJ, Jakana J, et al. "Identification of the Sites of Interaction between the Scaffold and Outer Shell in Herpes Simplex Virus-1 Capsids by Difference Electron Imaging." *Proc Natl Acad Sci* 96, (1998): 2778-2783.